EFFECTS OF METHANOL FUEL SUBSTITUTION ON MULTI-DAY AIR POLLUTION EPISODES

Final Report

Contract No. A3-125-32

California Air Resources Board

Principal Investigator

William P. L. Carter

Program Manager

Roger Atkinson

Research Staff

William D. Long
Li Li N. Parker
Margaret C. Dodd

Statewide Air Pollution Research Center
University of California
Riverside, CA 92521

September 1986

ARB-86:meth86

ABSTRACT

A series of indoor and outdoor environmental chamber experiments were conducted to investigate the effects on ambient air quality of widespread conversion of motor vehicles to methanol fuel. Three organic surrogates were compared in 2- to 3-day NO_x-air irradiations: a base case mixture representing present emissions into the California South Coast Air Basin; a mixture in which 33% (by carbon) of the base mix was substituted by methanol; and a mixture in which 33% of the base mix was substituted by a 90% methanol, 10% formaldehyde mix. The organic/NO_x ratio was varied from 3 to 15.

Substitution by methanol alone resulted in reduced day 1 ozone and PAN formation in all experiments, with the ozone benefit being less on day 2. However, if 10% formaldehyde is co-emitted with methanol, no clear-cut ozone benefit from methanol substitution was observed, though PAN is still reduced. Methanol substitution resulted in increased formaldehyde levels, even if formaldehyde is not co-emitted, though the increase was usually less than 50%. The magnitudes of the substitution effects, especially for ozone and PAN, were found to be highly dependent on meteorological conditions and the organic/NO_x ratio.

TABLE OF CONTENTS

		Page
Abstract		ii
Acknowledgments		v
List of Figures		vii
List of Tables		ix
Glossary		xi
I.	PROJECT SUMMARY	I-1
	A. Introduction and Statement of the Problem	I-1
	B. Objectives	I-2
	C. Methods of Approach	I-2
	D. Summary of Results and Conclusions	I-4
	E. Recommendations for Future Research	I-13
II.	INTRODUCTION AND BACKGROUND	II-1
III.	EXPERIMENTAL	III-1
	A. Indoor Chamber Experiments	III-1
	1. Chamber	III-1
	2. Experimental Procedures	III-1
	B. Outdoor Chamber Irradiations	III-5
	1. Chamber and Facility	III-5
	2. Experimental Procedures	III-8
	C. Analytical Techniques	III-10
	1. Gas Chromatographic Analyses	III-10
	2. Formaldehyde	III-14
	3. Continuous Monitoring Instruments	III-16
	4. Light Intensity	III-18
IV.	RESULTS	IV-1
	A. Control and Characterization Runs	IV-18
	1. NO_x-Air Irradiations	IV-19
	2. n-Butane-NO_x-Air Irradiations	IV-24
	3. Acetaldehyde-Air Irradiations	IV-26
	4. Ozone Conditionings and Dark Decay Determinations	IV-28
	5. Propene-NO_x-Air Irradiations	IV-29
	6. Other Control Experiments	IV-31
	7. Side Equivalency Tests	IV-32

TABLE OF CONTENTS
(Concluded)

		Page
	8. Characterization of the Light Source in the Indoor Chamber	IV-33
	9. Light Source Characterization for the Outdoor Chamber Experiments	IV-34
B.	Surrogate-NO_x-Air Runs	IV-38
	1. Indoor Chamber Experiments	IV-40
	2. Outdoor Chamber Experiments	IV-49
C.	Results of Model Simulations	IV-77
V.	CONCLUSIONS	V-1
VI.	REFERENCES	VI-1

APPENDIX A

Plots of Results of Chamber Experiments and Model Simulations

APPENDIX B

Chemical Mechanism and Parameters Used in Model Simulations

APPENDIX C

Computer Tape Containing Results of the Chamber Experiments

ACKNOWLEDGMENTS

Stimulating discussions and valuable exchanges of technical information, for which we express appreciation, took place at various times during this program with the following members of the California Air Resources Board: Dr. John Holmes, Dr. Jack Suder, and Mr. Tom Cackette. Helpful discussions with Mr. Michael McCormack of the California Energy Commission, Dr. Joe Norbeck of Ford Motor Co., Dr. Katherine Wilson, consultant to the California Energy Commission, Mr. John White of John White Associates, and Dr. James N. Pitts, Jr. of SAPRC are also gratefully acknowledged.

Mr. William D. Long, Ms. Lili N. Parker and Ms. Margaret C. Dodd were primarily responsible for carrying out the experimental work. Assistance in carrying out the experiments was also provided by Ms. Sara M. Aschmann and Mr. Phillip C. Pelzel. Assistance in the processing of the data obtained in these experiments was provided by Ms. Joanne Lohnes and Ms. Minn P. Poe, and the following student helpers: Monica Murata, Brett McMillan, Fran Tepper, and Scott Harris. Ms. Minn P. Poe and Ms. Susan E. Heffron were primarily responsible for the preparation of the plots in Appendix A to this report. Assistance in preparation of this report was provided by Ms. Christy J. LaClaire and Ms. Bonnie L. Perez. Finally we wish to acknowledge Dr. Arthur M. Winer, Assistant Director of SAPRC, for helpful discussions, for organizing and conducting the workshops held at UCR concerning this program, and for his assistance in the preparation of this final report.

This report was submitted in fulfillment of Contract No. A3-125-32 by the Statewide Air Pollution Research Center, University of California, Riverside, under the sponsorship of the California Air Resources Board. Work was completed as of April 8, 1986.

The statements and conclusions in this report are those of the contractor and not necessarily those of the California Air Resources Board. The mention of commercial products, their source or their use in connection with material reported herein is not to be construed as either an actual or implied endorsement of such products.

LIST OF FIGURES

Figure Number	Title	Page
I-1	Time-concentration profiles for ozone for NO_x-surrogate-air irradiations carried out in the 6,400-liter all-Teflon chamber	I-6
I-2	Time-concentration profiles for replicate base-case surrogate- and the methanol + 10% formaldehyde substitution surrogate-NO_x-air irradiations carried out under differing temperature and lighting conditions in the 50,000-liter outdoor all-Teflon chamber	I-7
III-1	SAPRC all-Teflon indoor chamber with associated analytical instruments	III-2
III-2	SAPRC outdoor Teflon chamber shown in dual-mode configuration	III-6
IV-1	Distribution plot for the ratio of the calculated to experimental k_1 values from the OTC surrogate-NO_x-air irradiations carried out in 1983 and 1985	IV-36
IV-2	Plots of ratios of the calculated to experimental k_1 values against the consine of the solar zenith angle from the OTC-surrogate-NO_x-air irradiations carried out in 1983 and 1985	IV-37
IV-3	Matrix of multi-day surrogate-NO_x-air experiments carried out in the indoor Teflon chamber	IV-41
IV-4	Plots of ozone, PAN, and formaldehyde data for all indoor chamber runs with nominal ROG/NO_x ratios of 15:1	IV-43
IV-5	Plots of ozone, PAN, and formaldehyde data for all indoor chamber runs with nominal ROG/NO_x ratios of 6:1	IV-44
IV-6	Plots of ozone, PAN, and formaldehyde data for all indoor chamber runs with nominal ROG/NO_x ratios of 3:1	IV-45
IV-7	Matrix of multi-day surrogate-NO_x-air experiments carried out in the outdoor Teflon chamber	IV-51
IV-8	Plots of day 1 and day 2 ozone, PAN, and formaldehyde yields against average temperature for the base case, surrogate-NO_x-air irradiations carried out at the 10:1 nominal ROG/NO_x ratio in the outdoor chamber	IV-56

LIST OF FIGURES
(concluded)

Figure Number	Title	Page
IV-9	Plots of day 1 and day 2 ozone, PAN, and formaldehyde yields against average UV radiation intensity for the base case surrogate-NO_x-air irradiations carried out at the 10:1 nominal ROG/NO_x ratio in the outdoor chamber	IV-57
IV-10	Plots of day 1 and day 2 ozone, PAN, and formaldehyde yields against average temperature for the methanol + formaldehyde substitution surrogate-NO_x-air irradiations carried out at the 10:1 nominal ROG/NO_x ratio in the outdoor chamber	IV-58
IV-11	Plots of day 1 and day 2 ozone, PAN, and formaldehyde yields against average UV radiation intensity for the methanol + formaldehyde substitution surrogate-NO_x-air irradiations carried out at the 10:1 nominal ROG/NO_x ratio in the outdoor chamber	IV-59
IV-12	Plots of day 1 and day 2 ozone, PAN, and formaldehyde yields against average temperature for the blank substitution surrogate-NO_x-air irradiations carried out at the 10:1 nominal ROG/NO_x ratio, and for the base case surrogate-NO_x-air irradiations carried out 7:1 nominal ROG/NO_x ratio in the outdoor chamber	IV-60
IV-13	Plots of day 1 and day 2 ozone, PAN, and formaldehyde yields against average UV radiation intensity for the blank substitution surrogate-NO_x-air irradiations carried out at the 10:1 nominal ROG/NO_x ratio, and for the base case surrogate-NO_x-air irradiations carried out 7:1 nominal ROG/NO_x ratio in the outdoor chamber	IV-61
IV-14	Comparison of ozone yields observed in the simultaneous irradiation of the various pairs of surrogate mixtures carried out in the divided outdoor chamber	IV-63
IV-15	Comparison of PAN yields observed in the simultaneous irradiation of the various pairs of surrogate mixtures carried out in the divided outdoor chamber	IV-68
IV-16	Comparison of formaldehyde yields observed in the simultaneous irradiation of the various pairs of surrogate mixtures carried out in the divided outdoor chamber	IV-72

LIST OF TABLES

Table Number	Title	Page
I-1	Nominal Compositions of Organic Surrogates Employed in the Environmental Chamber Experiments	I-4
I-2	Numbers of Each Type of Surrogate-NO_x-Air Irradiation Carried Out in the 6400-Liter Indoor All-Teflon Chamber	I-5
I-3	Surrogate Pairs Simultaneously Irradiated in the 50,000-Liter Outdoor All-Teflon Chamber Experiments	I-5
I-4	Comparison of the Experimental Ozone Yields (in pphm) Observed for the Base Case vs Methanol + Formaldehyde Substitution Surrogates	I-9
I-5	Comparison of the Experimental Ozone Yields (in pphm) Observed from the Base Case vs Methanol Only Substitution Surrogates	I-9
I-6	Comparison of the Experimental PAN Yields (in ppb) from the Base Case vs Methanol + Formaldehyde Substitution Surrogates	I-10
I-7	Comparison of the Experimental PAN Yields (in ppb) from the Base Case vs Methanol-Only Substitution Surrogates	I-10
I-8	Comparison of the Experimentally Observed Day 1 Formaldehyde Yields (in pphm) from the Various Surrogates	I-11
II-1	Nominal Compositions of Organic Surrogates Employed in the Environmental Chamber Experiments	II-5
IV-1	Chronological Summary of Indoor Chamber Experiments	IV-2
IV-2	Chronological Summary of Outdoor Chamber Experiments	IV-8
IV-3	Conditions and Results of the Tracer-NO_x-Air Irradiations Carried Out in the Indoor Teflon Chamber	IV-23
IV-4	Conditions and Results of the Tracer-NO_x-Air Irradiations Carried Out in the Outdoor Teflon Chamber	IV-24

LIST OF TABLES
(concluded)

Table Number	Title	Page
IV-5	Conditions and Selected Experimental and Model Calculation Results for the n-Butane-NO_x-Air Experiments Carried Out in the Outdoor Chamber	IV-25
IV-6	Results of the Acetaldehyde-Air Irradiations Carried Out in the Outdoor Chamber	IV-28
IV-7	Conditions and Experimental and Calculated Maximum Ozone and Formaldehyde Yields in the Propene-NO_x-Air Irradiations Carried Out in the Outdoor Chamber	IV-30
IV-8	Results of NO_2 Actinometry Experiments Carried Our in the Indoor Teflon Chamber	IV-33
IV-9	Conditions and Selected Results of the Multi-Day Surrogate-NO_x-Air Irradiations Carried Out in the Indoor Teflon Chamber	IV-42
IV-10	Conditions and Selected Results of the Surrogate-NO_x-Air Runs Carried Out in the Outdoor Teflon Chamber	IV-52
IV-11	Averages of the Day 1 and Day 2 Formaldehyde Yields Observed in the Outdoor Chamber Irradiations of the Various Surrogate-NO_x-Air Mixtures	IV-76
IV-12	Comparison of Experimental and Calculated Maximum Yields of Ozone, Formaldehyde, and PAN for the Surrogate-NO_x-Air Irradiations Carried Out in the Indoor Chamber	IV-79
IV-13	Comparison of Experimental and Calculated Maximum Yields of Ozone, Formaldehyde, and PAN for the Surrogate-NO_x-Air Irradiations Carried out in the Outdoor Chamber	IV-80
IV-14	Comparison of Experimental and Calculated Percentage Differences in Daily Maximum Ozone, PAN, and Formaldehyde Yields	IV-84

GLOSSARY

ARB	California Air Resources Board
"B"	Base case surrogate, designed to represent current emissions of reactive organics into the California South Coast Air Basin
"BL"	"Blank substitution" surrogate, consisting of the base case surrogate reduced by ~33%
CSCAB	California South Coast Air Basin
ECD	Electron capture detector (for gas chromatographs)
EKMA	"Empirical Kinetic Modeling Approach," a technique for estimating control strategies for ozone
EPA	U. S. Environmental Protection Agency
FID	Flame ionization detector (for gas chromatographs)
GC	Gas chromatograph, used to monitor organics
HC	Hydrocarbon
ITC	Indoor Teflon Chamber
"M"	"Methanol substitution" surrogate, consisting of the base case surrogate with ~33% replaced by methanol
"MF"	"Methanol + formaldehyde" substitution surrogate, consisting of the base case surrogate with 33% replaced by a 90% methanol + 10% formaldehyde mixture
NMRC	Non-methane reactive carbon - same as ROG
NO_x	$NO + NO_2$
OTC	Outdoor Teflon Chamber
PAN	Peroxyacetyl nitrate
ppb	Parts-per-billion
ppm	Parts-per-million
ppmC	Parts-per-million Carbon
PST	Pacific standard time
RH	Relative humidity

GLOSSARY OF TERMS
(concluded)

ROG	Reactive organic gases
SAI	Systems Applications, Inc.
SAPRC	Statewide Air Pollution Research Center at the University of California in Riverside
TSR	Total solar radiometer or light intensity as measured by a total solar radiometer
UCR	University of California, Riverside
UNC	University of North Carolina
UV	Ultraviolet light intensity as measured by an ultraviolet radiometer
W	Watt

I. PROJECT SUMMARY

A. Introduction and Statement of the Problem

During the past few years attention has focused on the use of methanol as an alternative fuel, especially for motor vehicles, because of its ready availability from domestic sources. Indeed, an extensive conversion of motor vehicles from gasoline to methanol fuel is currently under consideration in California, and the initial test fleet programs carried out to date indicate that a large scale conversion of motor vehicles to methanol is feasible. However, since mobile source emissions contribute approximately 50% of the total reactive organic (ROG) emissions into the California South Coast Air Basin (CSCAB), it is obvious that any large scale conversion to methanol fuels could have a highly significant effect of the CSCAB air quality.

The presently available data suggest that the emissions from methanol fueled vehicles are comparable, on a mass basis, to those from gasoline powered vehicles. However, the chemical composition of these emissions are quite different, with methanol fueled vehicle emissions being comprised of methanol (from vaporization and tail pipe emissions) and formaldehyde (a product of incomplete combustion from tail pipe emissions). Thus an extensive conversion of motor vehicles from gasoline to methanol fuel will result in the substitution of the ROG emitted from gasoline powered by an approximately equal amount of methanol and formaldehyde.

To date, however, only a few studies have been carried out to address the issue of the air quality impacts arising from a large scale conversion to methanol fuel, and these have only considered the effects on single-day air pollution episodes. These earlier computer modeling and environmental chamber studies all concluded that, with respect to ozone formation, conversion to methanol fuel would be beneficial for single day air pollution scenarios. However, questions have been raised concerning the effects of conversion from gasoline to methanol on air quality in the CSCAB under multi-day air pollution episodes (the conditions most conducive to highly elevated ozone and other secondary pollutant levels) and concerning the role of the co-emitted formaldehyde in negating any beneficial effects of methanol substitution.

B. Objectives

The principal objective of this program was to carry out a series of multi-day environmental chamber irradiations to examine the issue of the effects of conversion to methanol fuel on air quality under multi-day conditions. A second objective was to provide a data base for testing the chemical mechanisms to be incorporated into urban airshed computer models utilized in the assessment of methanol substitution strategies.

C. Methods of Approach

In order to address the objectives of this program, a total of 81 environmental chamber experiments were carried out in two different chambers, one a 6,400-liter indoor chamber and the other a 50,000-liter outdoor chamber. The experiments consisted of 14 multi-day indoor chamber irradiations, 21 multi-day outdoor chamber irradiations in the dual mode (corresponding to 42 irradiations of distinct mixtures) and a variety of associated chamber characterization runs. Experiments were conducted in both indoor and outdoor chambers because each type of chamber has a set of relatively complementary advantages and disadvantages. Thus the indoor chamber has much more controlled conditions leading to much greater reproducibility and the outdoor chamber has natural sunlight radiation with a diurnally varying intensity and a wider variety of experimental conditions.

To investigate the effects of methanol substitution on air quality, the following organic surrogate-NO_x-air mixtures were irradiated: (1) a "base-case" surrogate designed to represent present emissions of reactive organics into the CSCAB; (2) a "methanol + formaldehyde" substitution mixture in which one-third of the base case surrogate mixture was replaced with 90% methanol + 10% formaldehyde; (3) a "methanol only" substitution mixture in which one-third of the base case surrogate mixture was replaced with methanol; and (4) a "blank" substitution mixture in which the base case surrogate was reduced by one-third. These experiments were conducted at three different organic-to-NO_x ratios in the indoor chamber, and four in the outdoor chamber. The mixtures were irradiated for two to four days.

For the indoor chamber experiments, at least one experiment was carried out for each of the four surrogate mixtures at each of the three organic-to-NO_x ratios. For the outdoor chamber irradiations, most experiments consisted of simultaneous irradiations of two different surrogate mixtures (for example, base case vs methanol + formaldehyde substitution, or blank substitution vs methanol-only substitution, etc.) at the same organic-to-NO_x ratio. In general, more than one irradiation of a given mixture at a given organic-to-NO_x ratio was carried out to allow the reactivities of more than one combination of mixtures to be compared. Furthermore, the outdoor chamber experiments were carried out under a variety of temperature and lighting conditions, allowing the influence of these parameters on the effects of methanol substitution to be assessed.

The compositions of the organic surrogates employed in this program are summarized in Table I-1. The "base case" hydrocarbon surrogate was designed by Systems Applications, Inc. (SAI) and has been employed in several previous studies. The methanol + formaldehyde surrogate composition of 90% methanol + 10% formaldehyde is also the same as that employed in the University of Santa Clara and SAI studies, and is based on the assumption that exhaust and evaporative emissions from methanol-fueled vehicles are approximately equal, with the exhaust containing ~20% formaldehyde. In order to assess the importance of this assumed formaldehyde content in the emissions, experiments were also carried out assuming negligible formaldehyde emissions from methanol-fueled vehicles. In addition, the blank substitution experiments were carried out for control purposes and to provide data concerning how methanol substitution compares with totally eliminating emissions from an equal number of vehicles.

The experimental procedures and analytical techniques employed in this study are similar to those employed in our previous EPA-funded study aimed at providing data to test models for multi-day effects (Carter et al. 1985), and are discussed in Section III of this report. The experiments were conducted by initially injecting all of the reactants into the chamber, and then irradiating the mixtures for two to four days (with natural sunlight for the outdoor chamber runs, or 12 hours of blacklight irradiation alternating with 12 hours of darkness for the indoor runs), until NO_x was consumed and no further O_3 formation occurred. This

Table I-1. Nominal Compositions of Organic Surrogates Employed in the Environmental Chamber Experiments

Component	Carbon Percent			
	Base Case	Methanol + Formaldehyde Substitution	Methanol Substitution	Blank Substitution
Base Case Surrogate				
n-Butane	15	10	10	10
n-Pentane	20	13	13	13
iso-Octane	15	10	10	10
Ethene	6	4	4	4
Propene	6	4	4	4
Isobutene[a]	16	11	11	11
Toluene	11	7	7	7
m-Xylene	11	7	7	7
Methanol Surrogates				
Methanol	0	30	33	0
Formaldehyde	0	3	0	0

[a]Used to represent formaldehyde in the base case surrogate, since isobutene rapidly reacts to form formaldehyde.

procedure allowed the maximum ozone formation potential for each surrogate-NO_x-air mixture to be determined.

D. Summary of Results and Conclusions

The initial ROG and NO_x concentrations used in these environmental chamber runs, together with the number of irradiations carried out at each of these ROG/NO_x ratios, are given in Tables I-2 and I-3 for the indoor and outdoor chambers, respectively. Typical ozone time-concentration profiles obtained from NO_x-air irradiations of selected surrogate mixtures in these two chambers are shown in Figures I-1 and I-2. Figure I-1 shows that the ozone yield on the different days of irradiation are a function of both the particular surrogate irradiated and the initial ROG/NO_x ratio. The day-to-day reproducibility of irradiations conducted in this chamber

Table I-2. Numbers of Each Type of Surrogate-NO_x-Air Irradiation Carried Out in the 6400-Liter Indoor All-Teflon Chamber

Case	ROG/NO_x = 15	ROG/NO_x = 6	ROG/NO_x = 3
Base Case	2	1	1
MF Substitution	1	2	1
M Substitution	1	1	1
Blank Substitution	1	1	1

Table I-3. Surrogate Pairs Simultaneously Irradiated in the 50,000-Liter Outdoor All-Teflon Chamber Experiments

Pair of Cases	Number of Runs at Each ROG/NO_x Ratio			
	(5:1)	(7:1)	(10:1)	(13:1)
Base vs MF	2	2	3	1
Base vs M	1	1	2	1
Base vs Blank		1	1	
MF vs M		2	1	
MF vs Blank			1	
M vs Blank		1		

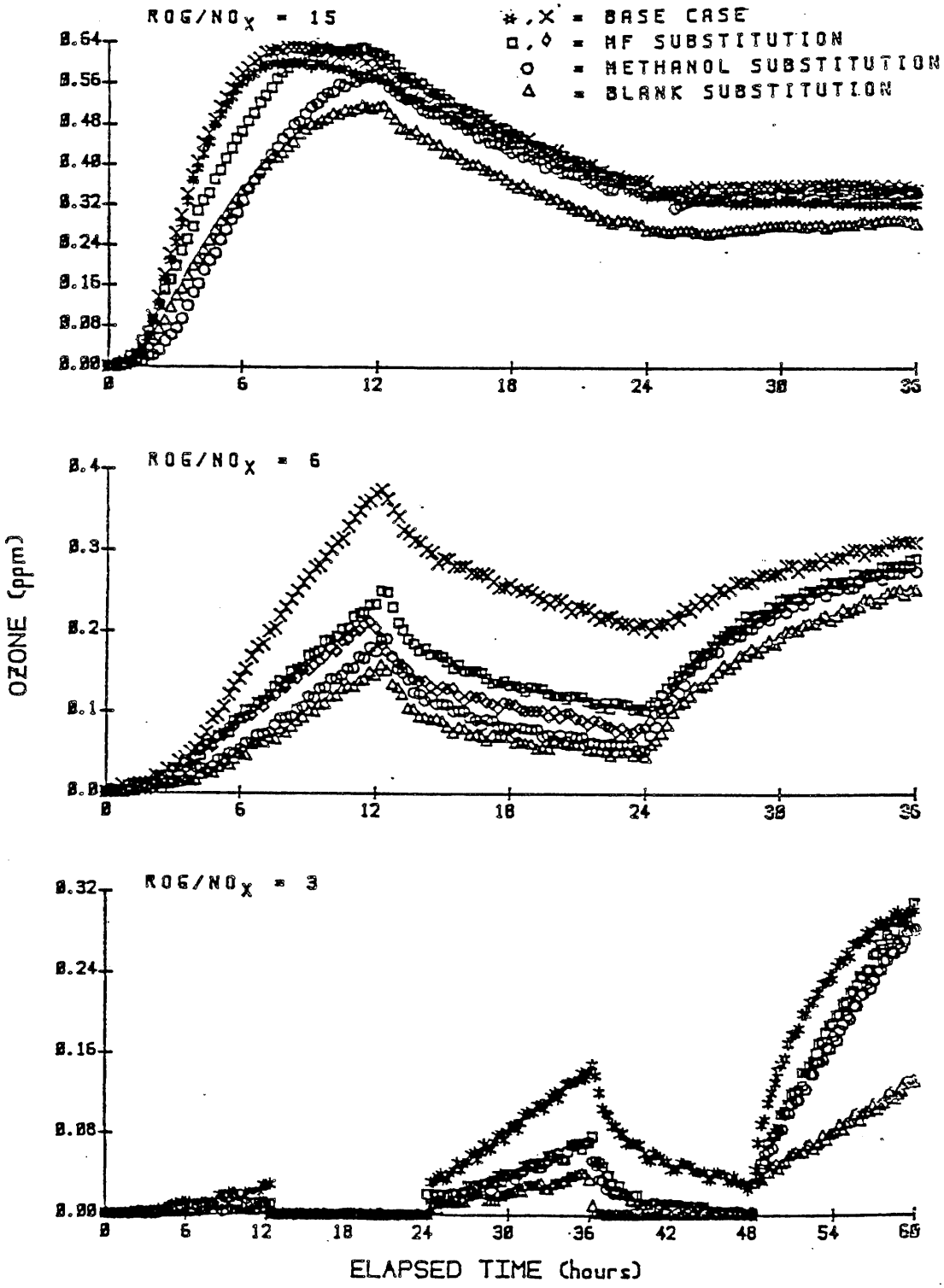

Figure I-1. Time-concentration profiles for ozone for NO_x-surrogate-air irradiations carried out in the 6,400-liter all-Teflon chamber.

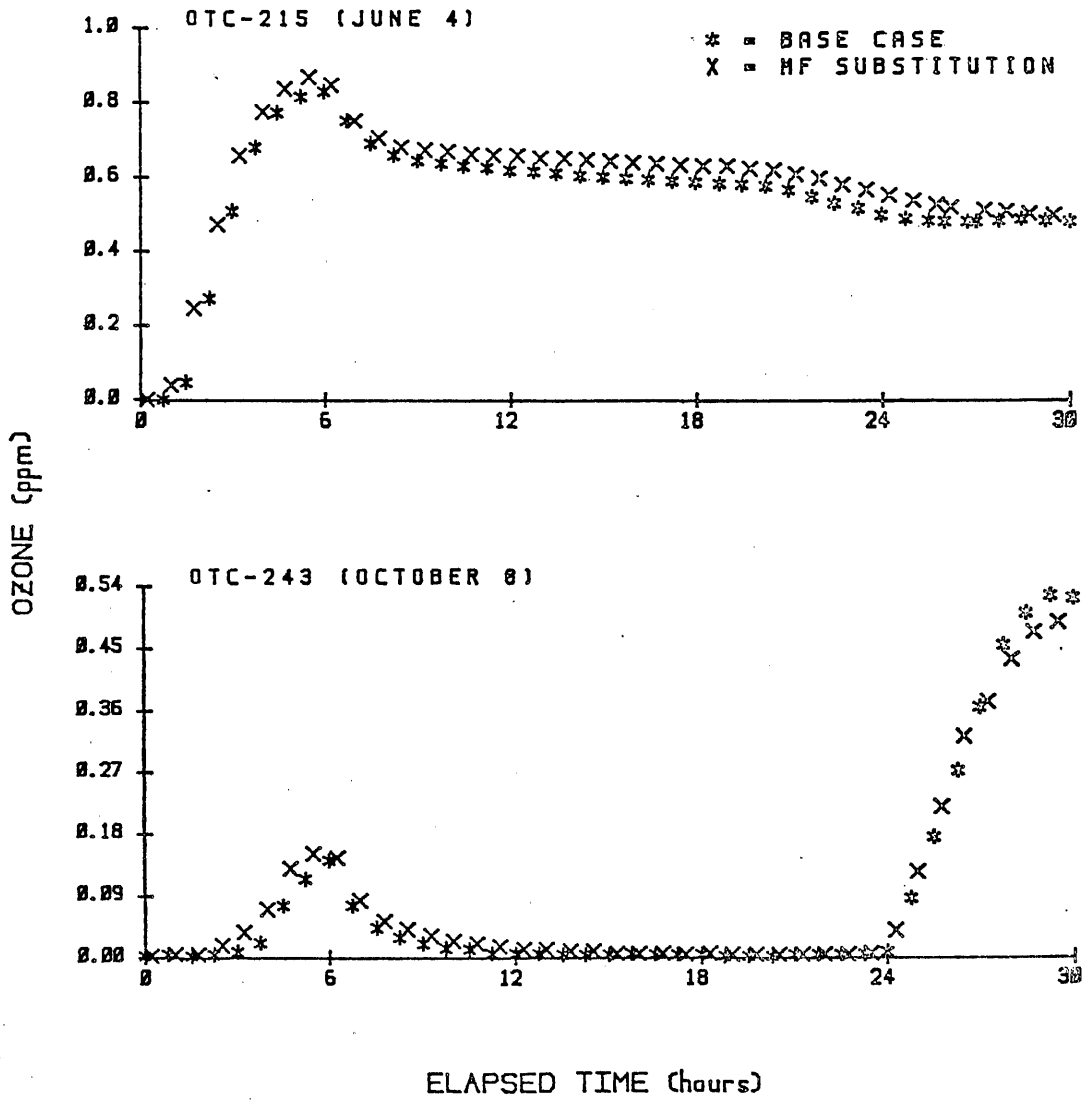

Figure I-2. Time-concentration profiles for replicate base-case surrogate- and the methanol + 10% formaldehyde substitution surrogate-NO_x-air irradiations carried out under differing temperature and lighting conditions in the 50,000-liter outdoor all-Teflon chamber.

are also evident from this figure. In contrast, Figure I-2 shows that in the 50,000-liter outdoor chamber there was a large variability in the data obtained due to variations in, for example, the temperature and light intensity. This inherent day-to-day variability in the results of the outdoor chamber experiments was the reason for conducting all of the NO_x-surrogate-air irradiations under dual mode conditions, thus allowing direct comparisons between the different surrogates to be made.

The results of the environmental chamber experiments are summarized in Tables I-4 through I-8, in which the ozone, peroxyacetyl nitrate (PAN) and formaldehyde yields observed from the surrogate mixtures at the various ROG/NO_x ratios investigated are compared.

The results of our experiments indicate that the benefits of methanol substitution on the atmospheric levels of ozone will depend critically on the amount of formaldehyde co-emitted with methanol. If little or no formaldehyde is emitted from methanol-fueled vehicles, then methanol substitution can result in a reduction in atmospheric ozone levels, although the amount of reduction depends on such factors as the ROG/NO_x ratio, temperature and lighting conditions, and the number of days of irradiation in the multi-day experiments. However, if significant quantities of formaldehyde are co-emitted with methanol, then our experiments indicate that the benefits of substitution on ozone levels will be significantly less, if not eliminated entirely. In particular, if the base case surrogate employed in this study is reasonably representative of current ROG emissions into the CSCAB, then these data indicate that the formaldehyde content in emissions from methanol-fueled vehicles must be less than 10% in order to achieve a reduction in ambient ozone levels (assuming no significant changes in the total amounts of ROG or NO_x emitted).

The results of these experiments also indicate that the reductions in ozone from methanol substitution decrease with increasing ROG/NO_x ratios, and also with the number of days the pollutants are irradiated. In particular, although methanol substitution (with no added formaldehyde) resulted in reduced day 1 ozone levels at the low or moderate ROG/NO_x ratios, little or no improvement in final ozone levels was observed at the highest ROG/NO_x ratios, or after two or three days of irradiation at lower ROG/NO_x ratios. The benefits of methanol substitution on ozone yields at

Table I-4. Comparison of the Experimental Ozone Yields (in pphm) Observed for the Base Case vs Methanol + Formaldehyde Substitution Surrogates

Chamber	ROG/NO_x	Day 1			Day 2		
		Base	MF	% diff.	Base	MF	% diff.
Outdoor	13:1	67	67	0%	48	47	-2%
"	10:1	83	87	+5%	49	55	+12%
"	"	35	33	-6%	23	25	+9%
"	"	14	15	+7%	53	49	-8%
"	7:1	33	24	-27%	39	33	-15%
"	"	6	8		41	43	+5%
"	5:1	25	30	+20%	44	40	-9%
"	"	5	11				
Indoor	15:1	62	63	0%	36	36	0%
"	6:1	38	23	-39%	31	29	-6%
"	3:1	3	1		15	8	

Table I-5. Comparison of the Experimental Ozone Yields (in pphm) Observed from the Base Case vs Methanol Only Substitution Surrogates

Chamber	ROG/NO_x	Day 1			Day 2		
		Base	M	% diff.	Base	M	% diff.
Outdoor	13:1	81	78	-4%	53	49	-8%
"	10:1	83	48	-42%	-	37	0%
"	"	81	76	-6%	50	44	-12%
"	7:1	64	18	-72%	34	35	+3%
"	5:1	22	3	-86%	33	11	-67%
Indoor	15:1	62	58	-6%	36	35	-3%
"	6:1	38	19	-50%	31	28	-10%
"	3:1	3	1		15	7	-53%

Table I-6. Comparison of the Experimental PAN Yields (in ppb) from the Base Case vs Methanol + Formaldehyde Substitution Surrogates

Chamber	ROG/NO_x	Day 1			Day 2		
		Base	MF	% diff.	Base	MF	% diff.
Outdoor	13:1	64	47	-27%	13	11	-15%
"	10:1	125	123	-2%	17	10	-41%
"	"	65	45	-31%	83	62	-25%
"	"	21	21	0%	50	37	-26%
"	7:1	50	36	-28%	26	25	-4%
"	"	12	13	+8%	51	50	-2%
"	5:1	34	25	-26%	25	17	-32%
"	"	1	1				
Indoor	3:1	2	0		15	4	

Table I-7. Comparison of the Experimental PAN Yields (in ppb) from the Base Case vs Methanol-Only Substitution Surrogates

Chamber	ROG/NO_x	Day 1			Day 2		
		Base	M	% diff.	Base	M	% diff.
Outdoor	13:1	62	46	-26%	3	3	
"	10:1	121	68	-44%	-	11	
"	"	64	46	-28%	10	10	0%
"	7:1	38	20	-47%	18	26	+44%
"	5:1	29	1	-97%	33	12	-64%
Indoor	15:1	134	97	-28%	36	46	+28%
"	3:1	2	0		15	5	-67%

Table I-8. Comparison of the Experimentally Observed Day 1 Formaldehyde Yields (in pphm) from the Various Surrogates

Chamber	ROG/NO_x	Day 1 HCHO Max (pphm)				% Change from Base		
		Base	MF	M	Blank	MF	M	Blank
Outdoor	13:1	23	23	27		0	+17	
"	10:1	22	24	26	15	+9	+18	-32
"	7:1	15	16	12	7	+7	-20	-53
"	5:1	7	10	6		+43	-14	
Indoor	15:1	14[a]	22	15	11	+57	+7	-21
"	6:1	5	11	8	3	+120	+60	-40

[a]Average of 21 pphm for ITC-865 and 7 pphm for ITC-891.

the lower ROG/NO_x ratios and with limited irradiation times can be attributed to the fact that substitution of the base case organics by methanol reduces the rate of ozone formation, the main factor in determining how much ozone is formed under those particular conditions. At higher ROG/NO_x ratios, or if the irradiation proceeds for a sufficiently long period of time, then the amount of ozone formed is not determined by the rate of ozone formation, but rather by the maximum ozone forming potential of the ROG and NO_x mixture employed. The fact that methanol substitution does not reduce the maximum ozone yields under conditions of high ROG/NO_x ratios or of long irradiation times shows that the ultimate ozone forming potential of methanol is very similar to that of the base case surrogate mixture employed in this study. However, provided that formaldehyde co-emissions are kept sufficiently low (i.e., much less than 10%), these data do not indicate any conditions where methanol substitution will have significant adverse impacts on ozone levels; such substitution would either be beneficial or have no net effect, depending on the conditions.

The experiments carried out in this program further indicate that methanol substitution will have a beneficial effect on PAN levels under essentially all conditions, although the exact magnitude of the improvement will vary considerably with the atmospheric conditions. In contrast

with the results for effects on ozone, the improvement in PAN levels caused by substitution does not appear to be significantly affected by formaldehyde co-emissions, nor by the number of days of irradiation in multi-day episodes. This clear-cut benefit of methanol or even methanol + formaldehyde substitution on PAN levels is not unexpected, since PAN is formed only from the reactions of the components of the base case surrogate, and not from methanol or formaldehyde.

However, since formaldehyde is expected to be co-emitted with methanol, and is also its major atmospheric photooxidation product, this is one aspect of air quality where methanol substitution is expected to have an adverse impact. The worst impacts in this regard are expected to be the possibility of unacceptably high levels of formaldehyde in the immediate vicinity of methanol vehicles under poor mixing conditions (such as garages, tunnels, street-canyons, etc.). Our experiments were not designed to address this aspect of methanol substitution. However, methanol substitution is also expected to have an impact on formaldehyde levels in the bulk atmosphere away from the immediate emission sources, and the data obtained in this program provide useful information in this regard.

The results of these experiments indicate that methanol substitution will tend to increase atmospheric formaldehyde levels, but that the increases are relatively moderate compared to the amounts of formaldehyde already formed in the photochemical reactions of the base case organics.

The data obtained in this program were used to test a recently-developed detailed photochemical mechanism (Carter et al. 1986). The model gave reasonably good fits to the results of most of the experiments carried out in this program, and also correctly predicted the observed effects of substitution. However, the detailed chemical mechanism employed is too large to be used in current airshed models, and the development of a suitably condensed mechanism, which is also consistent with the results of these experiments, is required.

E. Recommendations for Future Research

The present experimental program has provided a data base which shows that for a sufficiently small amount of formaldehyde co-emitted along with the methanol emissions, widespread conversion of gasoline powered vehicles to methanol will be beneficial in terms of ambient atmospheric ozone and PAN levels. However, any reductions in the ozone concentrations will be highly dependent on the duration of multi-day episodes and on other atmospheric conditions. In fact, it is clear that the present experimental data can only provide a qualitative assessment of the benefits in air quality resulting from a large scale conversion to methanol. To obtain a quantitative estimate of the effects on air quality of such a fuel conversion strategy, a full scale computer modeling study will be necessary, employing the most up-to-date emission inventory for present and future ROG and NO_x emissions and the best chemical mechanism available. In particular, it is necessary not only that any such airshed computer modeling study incorporate the latest test data concerning emissions from methanol fueled vehicles of methanol, formaldehyde and NOx, but also that it incorporate an appropriate representation of the reactivity of the organic emissions from conventionally fueled vehicles and other ROG sources.

The environmental chamber data obtained in this program and discussed in this report should prove useful for the testing and refinement of the chemical mechanisms for urban emissions with and without inclusion of methanol.

II. INTRODUCTION AND BACKGROUND

During the last few years, much attention has focused on the use of methanol as an alternative motor vehicle fuel. Methanol is now available at competitive cost from renewable, and vast, domestic sources (CEC 1982) and yields acceptable performance and fuel economy when used in suitably modified motor vehicles (see, for example, the Proceedings of the 5th International Alcohol Fuel Technology Symposium, Auckland, New Zealand, May 13-18, 1982). Furthermore, on the basis of air quality and other considerations, the use of neat methanol fuel appears to be more appealing than alcohol-fuel blends ("gasohol"), another alternative fuel which has been extensively studied (Brinkman 1979, CEC 1981).

For these reasons, an extensive conversion of motor vehicles from gasoline to methanol fuels is currently under active consideration, particularly in the State of California. For instance, Senate Bill 620 appropriated $10 million to investigate this topic and to carry out an alcohol fuel fleet test program (CEC 1981, 1982). The results of this program have indicated that large scale conversion of motor vehicles to methanol fuel is feasible, and that it will probably begin by conversion of large automobile fleets (CEC 1981, 1982). Interest in conversion to methanol fuels in California is not restricted solely to the state government; for example, since 1979 the Bank of America has been converting its fleet to methanol, with the ultimate goal of 100% conversion (De Lorenzo 1982). Thus the initial stages of conversion of California's motor vehicles to methanol fuel is already underway, albeit on a minor scale.

Since mobile source emissions constitute approximately 50% of the total reactive organic emissions into the California South Coast Air Basin (CSCAB), it is obvious that any significant change in the composition of vehicular fuels could have an impact on emissions into the CSCAB, and thus affect the resulting air quality. While emissions of reactive organics from motor vehicles powered by methanol appear to be comparable in mass to emissions from gasoline powered vehicles, their chemical composition, consisting primarily of methanol from evaporative emissions and methanol plus formaldehyde from exhaust emissions (Pullman 1979), are obviously quite different. Thus an extensive conversion of motor vehicles in the

CSCAB could result in a substitution of up to 50% of the reactive organic gases presently emitted into the basin by methanol and formaldehyde.

Despite its potential importance, there have been relatively few studies to date concerning the impact of a large-scale conversion to methanol fuel would have on air quality in the CSCAB. Preliminary calculations concerning the effects of methanol substitution on one-day air pollution episodes have been carried out at Caltech (O'Toole et al. 1983) and by Systems Applications, Inc. (SAI) (Whitten and Hogo 1983). The results of both of these studies indicate that methanol substitution will be beneficial by reducing peak ozone levels. In addition, the Caltech calculations indicate that substitution will also result in reduced levels of PAN, a secondary pollutant formed from gasoline constituents, but not from methanol or formaldehyde. These predictions are consistent with the environmental chamber studies carried out at the University of Santa Clara, from which it was determined that replacing 33% of a multi-component "urban surrogate" mixture with a 90% methanol + 10% formaldehyde mixture, designed to represent both evaporative and exhaust emissions from methanol-fueled vehicles, resulted in reduced peak ozone levels in single day irradiations (Pefley et al. 1984).

However, these studies have not unambiguously established that methanol substitution will be beneficial under all conditions. For example, methanol substitution is expected to result in increased atmospheric levels of formaldehyde, both from direct emissions and from atmospheric formation, and hence may result in a degradation in this aspect of air quality. The previous computer model calculations also indicate that the degree of improvement in predicted peak ozone levels depends on the assumed formaldehyde content of the emissions from methanol-fueled vehicles, with the calculated ozone benefit being reduced as the formaldehyde content of the exhaust emissions increases. However, the effects on air quality of varying formaldehyde emissions from methanol-fueled vehicles has not been experimentally tested, and these computer model predictions have not as yet been validated. In addition, the previous modeling and experimental studies have not assessed the effects of methanol substitution under multi-day pollution episode conditions. This is a potentially important consideration, since the worst air pollution episodes in the CSCAB tend to be multi-day in nature. Compared with most

of the gasoline constituents which it would replace, methanol reacts relatively slowly in the atmosphere, and hence is expected to persist in the atmosphere longer, leading to higher levels of organics from previous day emissions. These unreacted organics may then result in progressively higher reactivities on subsequent days in multi-day episodes.

This report describes the results of a series of environmental chamber experiments carried out to provide further data needed to assess the atmospheric impacts of methanol fuel substitution, particularly with regard to multi-day effects and the effects of varying formaldehyde emissions from methanol-fueled vehicles. A total of 81 experiments were carried out, including 20 multi-day irradiations of organic surrogate-NO_x-air mixtures in the SAPRC 30,000- to 45,000-liter outdoor chamber (OTC) operating in dual mode, 14 multi-day irradiations of surrogate-NO_x-air mixtures in the SAPRC 6400-liter indoor Teflon chamber (ITC), with most of the remainder being associated control and characterization runs in the ITC or OTC.

Experiments were carried out in two chambers because each type of chamber has its own set of complementary advantages and limitations. Outdoor chamber experiments have the advantages of natural lighting conditions and diurnally varying light intensity, and a relatively large surface to volume ratio, while the indoor chamber experiments have the advantages of more controlled experimental conditions, such as temperature, light intensity, etc., yielding results which tend to be more reproducible. In addition, the use of data from more than one type of chamber allows for a more comprehensive testing of photochemical models.

The following representative organic mixtures were employed in the multi-day organic surrogate-NO_x-air irradiations carried out in this program: (1) a "base-case" surrogate designed to represent present emissions of reactive organics into the CSCAB; (2) a "methanol + formaldehyde" substitution mixture in which one-third of the base case surrogate mixture was replaced with 90% methanol + 10% formaldehyde; (3) a "methanol only" substitution mixture in which one-third of the base case surrogate mixture was replaced with methanol; and (4) a "blank" substitution mixture in which the base case surrogate was reduced by one-third. These experiments were carried out at three different organic to NO_x ratios, and the mixtures were irradiated for two to four days.

For the indoor chamber experiments, at least one experiment was carried out for each of the four surrogate mixtures at each of the three organic-to-NO_x ratios. For the outdoor chamber irradiations, most experiments consisted of simultaneous irradiations of two different surrogate mixtures (for example, base case vs methanol + formaldehyde substitution, or blank substitution vs methanol-only substitution, etc.) at the same organic-to-NO_x ratio. In general, more than one irradiation of a given mixture at a given organic-to-NO_x ratio was carried out to allow the reactivities of more than one combination of mixtures to be compared. Furthermore, the outdoor chamber experiments were carried out under a variety of temperature and lighting conditions, allowing the influence of these parameters on the effects of methanol substitution to be assessed.

The compositions of the organic surrogates employed in this program are summarized in Table II-1. The "base case" hydrocarbon surrogate was designed by SAI and has been employed in the single-day methanol-substitution chamber study carried out at the University of Santa Clara (Pefley et al. 1984), in a previous chamber study of multi-day effects carried out at SAPRC (Carter et al. 1985), and in the methanol-substitution airshed calculations carried out by SAI (Whitten and Hogo 1983). This surrogate mixture was used in this program to allow a direct comparison of our results with those of the previous studies. The methanol + formaldehyde surrogate composition of 90% methanol + 10% formaldehyde is also the same as that employed in the University of Santa Clara and SAI studies, and is based on the assumption that exhaust and evaporative emissions from methanol-fueled vehicles are approximately equal, with the exhaust containing ~20% formaldehyde. In order to assess the importance of this assumed formaldehyde content in the emissions, experiments were also carried out assuming negligible formaldehyde emissions from methanol-fueled vehicles. In addition, the blank substitution experiments were carried out for control purposes and to provide data concerning how methanol substitution compares with totally eliminating emissions from an equal number of vehicles.

The experimental procedures and analytical techniques employed in this study are similar to those employed in our previous EPA-funded study aimed at providing data to test models for multi-day effects (Carter et

Table II-1. Nominal Compositions of Organic Surrogates Employed in the Environmental Chamber Experiments

Component	Carbon Percent			
	Base Case	Methanol + Formaldehyde Substitution	Methanol Substitution	Blank Substitution
Base Case Surrogate				
n-Butane	15	10	10	10
n-Pentane	20	13	13	13
iso-Octane	15	10	10	10
Ethene	6	4	4	4
Propene	6	4	4	4
Isobutene[a]	16	11	11	11
Toluene	11	7	7	7
m-Xylene	11	7	7	7
Methanol Surrogates				
Methanol	0	30	33	0
Formaldehyde	0	3	0	0

[a]Used to represent formaldehyde in the base case surrogate, since isobutene rapidly reacts to form formaldehyde.

al. 1985), and are discussed in Section III of this report. The experiments were conducted by initially injecting all of the reactants into the chamber, and then irradiating the mixtures for two to four days (with natural sunlight for the outdoor chamber runs, or 12 hours of blacklight irradiation alternating with 12 hours of darkness for the indoor runs), until NO_x was consumed and no further O_3 formation occurred. This procedure allowed the maximum ozone formation potential for each surrogate-NO_x-air mixture to be determined.

The results of the multi-day surrogate-NO_x-air runs and the associated characterization experiments are discussed in Section IV of this report. These data allow us to directly assess the relative reactivity of the base case, methanol substitution, methanol + formaldehyde substitution, and blank substitution surrogates at a variety of organic-to-NO_x ratios and (for the outdoor chamber runs) temperature and lighting

conditions. In addition, these experiments are useful for testing chemical mechanisms designed to be incorporated into airshed models to test specific methanol substitution scenarios for the CSCAB and other airsheds. Although a computer modeling study was beyond the scope of this experimental program under U.S. EPA funding, we have recently developed and extensively tested an updated detailed chemical mechanism (Carter et al. 1986), and the results of selected experiments carried out in this program are compared with the predictions of this model. This comparison of the experimental data with the results of computer model simulations provides not only a test of the model, but also provides a uniform method to check the quality and consistency of the experimental data.

This report contains three appendices. Appendix A contains plots of the measured concentrations of the major species monitored in the surrogate-NO_x-air experiments and the propene-NO_x-air, n-butane-NO_x-air, formaldehyde-NO_x-air, and methanol-NO_x-air control runs carried out in this program. Model simulations were carried out for most of these runs, and the results of these model simulations are also given in the plots in Appendix A for those runs. A listing of the chemical mechanism and chamber-dependent parameters employed in the model calculations is given in Appendix B, though Carter et al. (1986) should be consulted for more detailed documentation of this mechanism. The detailed data tabulations and associated comments for all of the experiments carried out in this program are available on computer tape, and the format of these data distributed on tape is given in Appendix C to this report. Copies of this tape are available from SAPRC for the cost of duplication.

III. EXPERIMENTAL

A. Indoor Chamber Experiments

1. Chamber

The ~6400-liter SAPRC indoor Teflon chamber employed for all of the indoor chamber experiments for this program is shown schematically in Figure III-1. The chamber consisted of a reaction bag which was constructed of 2-mil thick FEP Teflon panels heat-sealed together using a double-lap seam and externally reinforced with Mylar tape. The reaction bag was fitted inside an aluminum frame of dimensions of 8 ft x 8 ft x 4 ft. One edge was hinged to allow the bag to collapse to less than one-fifth of its maximum volume (see Figure III-1).

The light source for this indoor Teflon chamber consisted of two diametrically opposed banks of 40 Sylvania 40-W BL blacklamps backed by arrays of Alzak-coated reflectors. The light intensity could be controlled by switching on or off sets of lights as previously described (Darnall et al. 1981), although for all the indoor runs reported here, the light intensity was held constant at 70% of its maximum. The intensity and spectral characteristics of this light source are discussed in Section IV-A-8 and by Carter et al. (1984, 1985, 1986).

Pure dry air for these experiments was provided by an air purification system which has been described in detail previously (Doyle et al. 1977). In this system, ambient air was drawn through Purafil beds (to remove NO_x), compressed by a liquid (water) ring compressor to 100 psig, and passed successively through a heatless dryer, a Hopcalite tower (to remove CO) and a second heatless dryer packed with activated coconut charcoal. The latter acts as a pressure-swing adsorption unit and routinely reduced the hydrocarbon levels (as measured in the chamber) to ~800 ppb methane, <5 ppb of C_2 hydrocarbons and propane and <1 ppb of all higher hydrocarbons.

2. Experimental Procedures

Before each experiment, the chamber was flushed with purified air for at least three hours with the lights on and then for at least two hours with the lights off. For the final flush purified air humidified to ~50% relative humidity (RH) was employed. Prior to any reactant injections, background samples were analyzed using all of the gas

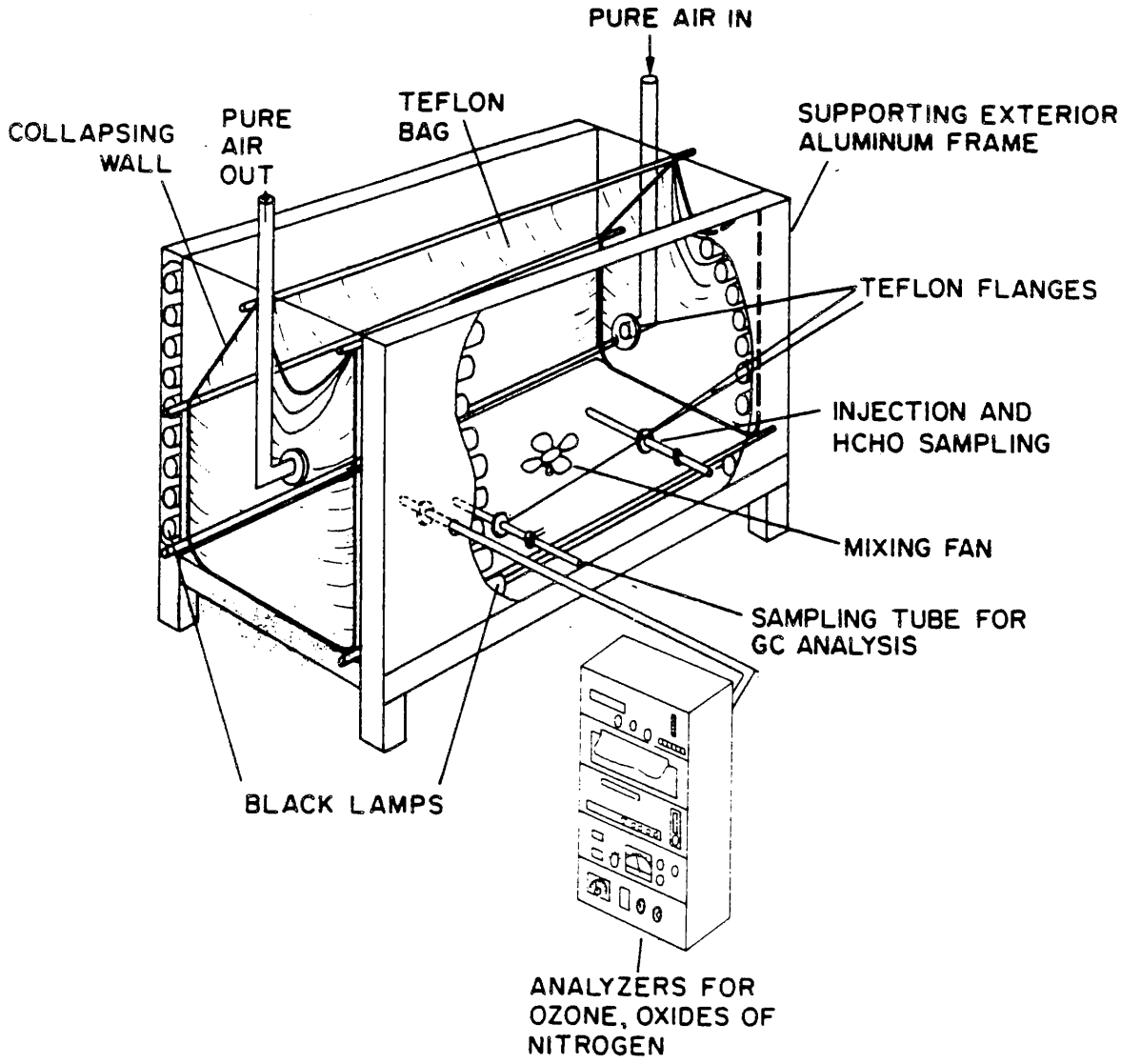

Figure III-1. SAPRC all-Teflon indoor chamber with associated analytical instruments.

chromatographic instruments to be employed during the run. NO, NO_2 and the various surrogate components were then injected individually, as described below. Gas chromatographic (GC) samples were then taken on all instruments prior to the beginning of the irradiations, which, as noted above, were all carried out at 70% of the maximum light intensity.

The reactants were injected into the chamber using several methods, depending on the compound or group of compounds being injected. In the case of NO, the calculated volume of gaseous NO was taken from a cylinder of Matheson, C.P. grade nitric oxide with a 20-mℓ gas-tight, all-glass syringe (with a stainless steel tip), and diluted to 100-mℓ with N_2 using a separate 100-mℓ syringe. The NO_2 was prepared in a similar manner, except that the NO was diluted with an excess of O_2 to yield NO_2. The calculated amounts of other gaseous reactants (e.g., propene for the propene-NO_x-air irradiations, or propene and n-butane in the tracer-NO_x-air runs) were also measured using gas-tight syringes, and diluted to 100-mℓ in a syringe. The contents of these syringes were then injected into the chamber through the Pyrex tube running into the chamber through the injection and formaldehyde sampling port (see Figure III-1), and then flushed into the chamber with N_2.

Compounds which are liquids at room temperature, such as the methanol used in the methanol substitution experiments and the acetaldehyde used in the acetaldehyde-air runs, were injected as follows: The desired amount of the liquid was injected, using a microsyringe, into a 5-liter Pyrex bulb equipped with stopcocks on each end and a port for the injection of the liquid. The port was then closed, and one end of the bulb was attached to the injection port of the chamber and the other to a nitrogen source. The stopcocks were then opened, and the vaporized contents of the bulb were flushed into the chamber for approximately 20 minutes.

The components of the "urban surrogate" used in all the multi-day surrogate-NO_x-air runs were injected using a third technique. Dilute mixtures of these compounds prepared in two separate cylinders which were purchased for this purpose from Scott Environmental Technology, Inc. The first cylinder (Serial no. AAL5874) contained the surrogate components which are gaseous at room temperature, and consisted of 105 ppm ethene, 77.3 ppm propene, 149 ppm isobutene, and 165 ppm n-butane in N_2. The second cylinder (serial no AAL8341) contained the vapors of the surrogate

components which are liquid at room temperature, and consisted of 164 ppm n-pentane, 77.2 ppm isooctane, 74.9 ppm toluene, and 64.3 ppm m-xylene, also in N_2. For each surrogate run, the desired pressures of each cylinder were introduced into evacuated 5-liter bulbs using a vacuum rack (with the pressure being measured using an MKS Baratron capacitance manometer), and then the contents of these bulbs were flushed into the chamber through the injection port.

The formaldehyde in the methanol + formaldehyde substitution experiments and in the formaldehyde-NO_x-air runs was prepared by heating para-formaldehyde in an evacuated vacuum line with a 5-liter bulb attached until the pressure in the bulb corresponded to the desired amount of formaldehyde. The bulb was then closed and detached from the vacuum line, and its contents were flushed into the chamber with N_2 through the injection port. The formaldehyde was prepared on the same day as the start of the run. Separate tests carried out prior to this program where this technique was employed to inject the formaldehyde into the SAPRC evacuable chamber (whose volume is constant and is accurately known) indicated that this technique is a reproducible and reliable method for injecting known amounts of formaldehyde into environmental chambers.

The procedures during the irradiation depended on the type of experiment being conducted. For the "multi-day" surrogate runs, the light intensity was held constant for 12 hours and the lamps were then turned off for 12 hours. GC and formaldehyde samples were taken hourly for at least the initial six hours of each simulated "day," and also immediately prior to turning off the lights. Data from the continuous monitoring instruments were collected every 15 minutes during the entire experiment using an Apple-computer-based data acquisition system similar to that employed in the outdoor experiments. In some experiments NO was injected into the chamber one hour after the resumption of the irradiation on the second or subsequent "days" of the irradiation. The procedures for the various conditioning, characterization and control runs were similar, except that they were generally carried out for shorter periods of time; the details are indicated in the comments for each run which are included with the detailed data tabulations on the computer tape described in Appendix C.

B. Outdoor Chamber Irradiations

1. Chamber and Facility

The outdoor chamber experiments were carried out using the SAPRC outdoor Teflon chamber, shown schematically in Figure III-2. The reaction chamber consisted of a replaceable 30,000- to 45,000-liter bag which was constructed of 2 mil thick FEP Teflon sheets heat-sealed together using a double lap seam and externally reinforced with Mylar tape. Each bag used seven 34-ft x 60-in. Teflon panels. As shown in Figure III-2, there were three Teflon injection or sampling ports on each side of the bag, one for manifold sampling, a second for filling, injecting and formaldehyde sampling and a third for gas chromatographic sampling. Two opposite corners of the bag were not heat-sealed and were used to empty the bag. During the experiments, these were held tightly shut with specially designed metal clamps. A single Teflon reaction chamber was used for all outdoor chambers carried out during this program.

The Teflon chambers were supported by nylon rope running across a 14-ft x 28-ft cast-iron pipe frame held 2.5 feet off the ground to allow air circulation under the chamber. No mechanical stirring devices were used in these experiments. Rather, the reactants were mixed after injection by manual agitation of the sides of the flexible chamber. Wind action on the chamber and temperature gradients within the chamber were sufficient to ensure adequate mixing during an experiment. The chamber was held on the frame with a net connected to the frame by a system of ropes and weights (not shown in Figure III-2). When the chamber contents were not being irradiated, the reaction bag was covered by an opaque, grey tarp attached to a dual framework of steel tubing (see Figure III-2) which could be readily opened (to uncover the chamber) or closed (to cover it). This chamber cover system is different than that employed in our previous outdoor chamber studies (e.g., Carter et al. 1981, 1985), and was constructed as part of this program to facilitate the process of covering and uncovering the chamber, and to avoid use of a framework which casts shadows on the reactor, as was the case with the design previously employed.

The majority of the analytical monitoring instruments employed were housed in an air conditioned 15-ft x 10-ft portable building sited approximately five feet from the chamber. The sample lines were constructed of

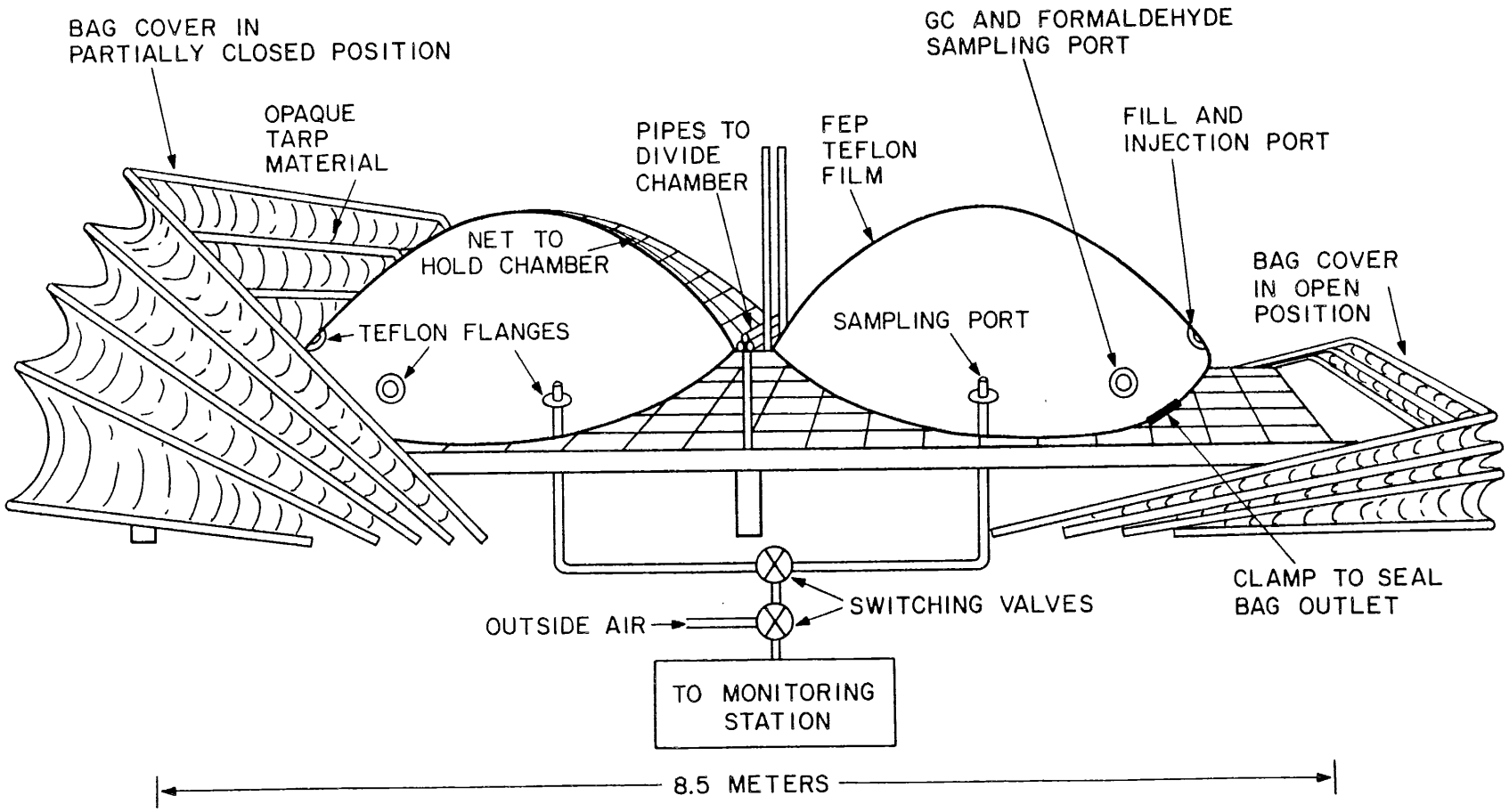

Figure III-2. SAPRC outdoor Teflon chamber shown in dual-mode configuration.

0.5-in. o.d. FEP Teflon tubing, and were connected to the sample ports on each side of the chamber (see Figure III-2). The Teflon tubing from each side of the chamber was attached to an all-Teflon solenoid valve with 0.5-in. orifices, which selected the side from which the sample was taken. This valve was attached, via Teflon tubing, to a similar valve which selected whether the sample was drawn from the Teflon chamber or from ambient air. After these valves, the sample lines led into a glass sampling manifold within the monitoring station to which the continuous analyzers were attached. The total air flow through the manifold was approximately 3.7 ℓ min^{-1}, and the transit time from the chamber to the manifold was approximately five seconds.

The switching valves which selected the source of air into the sampling manifold were controlled by an Apple II microcomputer which was also used to collect the data from the continuous monitoring instruments. For experiments during daylight hours, sampling was carried out on a 45-minute cycle, with samples being drawn for 15 minutes alternately from each side of the chamber and from the ambient air (the latter designated "side 3" on the data sets in the computer data tapes described in Appendix C). During nighttime hours, sampling was carried out on a 90-minute cycle with the valves being switched to draw sample gases from each side of the chamber and the ambient air for 30 minutes each. In some cases, particularly for three-day runs, the chamber contents were not sampled overnight in order to minimize the volume of air withdrawn from the bag and to avoid the bag being excessively deflated by the end of the run. Data were not collected by the computer until 11 minutes (for the 45-minute cycle) or 26 minutes (for the 90 minute cycle) after the valves were switched, and the signals from the instruments were then averaged for four minutes. These data were printed and stored on a diskette for later transfer to a central campus computer for processing.

As shown in Figure III-2, the outdoor chamber could be operated in a dual mode configuration to allow parallel experiments under the same lighting and temperature conditions to be conducted. This division of the entire chamber was carried out by means of three 1.4-in. diameter cast-iron pipes, which were surrounded by foam insulation to protect the Teflon reactor. The chamber is oriented such that these pipes dividing the reaction bag run in a north-south direction, with side 1 (or A), by

convention, always referring to the eastern half of the chamber. The reaction bag was divided by raising the lower pipe and placing it tightly between the upper pipes, and then rotating them by 180 degrees, thus forming the seal. Previous data have shown that this procedure resulted in an exchange rate between the chamber sides of <0.1% per hour (Carter et al. 1981).

Dry (≤5% RH), pure air for filling and flushing the chamber was supplied by an Aadco 737-15 air purification system which could generate an air flow of 250 liter min^{-1}. Background samples from the chamber filled from the output air from the AadCo air purification system indicated negligible contamination by oxides of nitrogen or organics. The data tabulations indicate the dew point depression measured during the experiments, from which the humidity can be calculated.

2. Experimental Procedures

The chamber was filled with dry pure air in the morning immediately before the run began, and to determine background levels samples were analyzed using all of the gas chromatographic instruments prior to injection of the reactants. Following this, and prior to separating the sides, any reactants whose initial concentrations were the same on both sides were injected.

The reactants were prepared and injected into the chamber as described above for the indoor chamber experiments, except as noted below. Instead of being injected directly into the chamber, the contents of the syringes containing the gaseous reactants (e.g., NO, NO_2, propene, or n-butane) were first injected into 5-liter glass bulbs, whose contents were then flushed into the chamber with N_2. The urban surrogate contents from the two cylinders were injected into the chamber by flowing the output from the cylinders at 3 liter min^{-1} for the amount of time required to yield the desired concentration in the chamber. For the outdoor chamber runs up to and including OTC-231, the same cylinders were used in the outdoor chamber experiments as used in the indoor chamber experiments discussed above. For runs after OTC-231, a second cylinder (serial no. AAL8265) containing the liquid surrogate components had to be employed since the first one was depleted; the second liquid surrogate cylinder contained 162 ppm n-pentane, 76.5 ppm isooctane, 74.2 ppm toluene, and 63.7 ppm m-xylene in N_2. The reactants were injected into the chamber

through 0.5-in. (o.d.) FEP Teflon tubes. For most of the multi-day surrogate experiments, the NO and NO_2 were injected into the undivided chamber, and the surrogate components and (where applicable) methanol and formaldehyde were injected into each half of the chamber separately after the bag was divided.

For the ozone conditioning experiments, the ozone was prepared and injected as follows: A 5-liter bulb with vacuum Teflon stopcocks at each end was covered with black tape to avoid photolysis. A Welsbach ozone generator was used to produce a flow of ~1.3% O_3 in O_2. This O_3/O_2 mixture was used to flush the bulb for five minutes after which the stopcocks were closed. The bulb was then attached to the outdoor chamber via a 0.5-in. FEP Teflon tube. The other end of the bulb was attached to a nitrogen supply. Both stopcocks were opened and the ozone was flushed into the chamber for five minutes.

The reactants were thoroughly mixed after injection and before any sampling was begun by manually agitating the sides of the chamber. Following the injection and mixing of the reactants, samples were taken for analysis from both sides, using all instruments. The bag was then uncovered to begin the irradiation; this generally occurred around 0900 Pacific Standard Time (PST) for surrogate-NO_x-air runs, though for some characterization or conditioning runs of shorter duration the irradiations were begun later. For multi-day runs, the chamber was covered in the evening around 1500 PST and uncovered again around 0900 PST on the following day. This was carried out to avoid differential irradiation of the western side of the chamber (side 2) in the evenings and of the eastern side (side 1) in the early mornings. On the final day of the run, the run was usually terminated at 1500 PST or earlier depending on whether the reaction mixture was still exhibiting photochemical reactivity (i.e., ozone formation).

Samples were taken for gas chromatographic analyses at least at hourly intervals during the daylight hours of the experiments with, for dual chamber runs, samples alternating between each side of the chamber. Formaldehyde samples were also taken hourly, but in this case samples were usually taken simultaneously from each side of the chamber in dual chamber runs. No gas chromatographic or formaldehyde data were taken during nighttime hours, other than PAN, which was monitored with a GC with an

automated sampling system (see below). However, as indicated above, data from the continuous analyzers were automatically collected from each side of the chamber once an hour at nighttime and once every 30 minutes during daylight hours.

C. Analytical Techniques

In this section, the analytical procedures employed for each set of compounds or physical parameters monitored in this program are described and their calibration technique and estimated accuracy and precision are discussed. Except as indicated, the same technique and calibration procedure for a given set of compounds or parameters was employed for both the indoor and outdoor chamber experiments.

1. Gas Chromatographic Analyses

Organic reactants and products were monitored using six different gas chromatographic systems, each suitable for a particular set of compounds. Samples for chromatographic analyses were withdrawn from the chamber using 100 mℓ gas-tight, all-glass syringes. The syringes were flushed at least three times with the sample gas before the sample for analysis was taken. A syringe was attached to the sample port of the chamber to withdraw a sample; in the case of the indoor chamber, the sample port was an ~18-in. x 0.25-in. Pyrex tube with a Becton-Dickinson stainless steel lever-lok stopcock manifold. The outdoor chamber had an ~18-in. x 0.25-in. FEP Teflon tube with a similar stopcock attached. Depending on the gas chromatographic analysis system, the contents of the syringe were either (1) flushed through ~2-mℓ stainless steel or ~10-mℓ heated glass loops and subsequently injected onto the column by turning a gas sample valve, or (2) condensed in a trap cooled with liquid argon, and then injected onto the column by simultaneously turning the gas sample valve and heating the loop with boiling water or ice water. The various gas chromatographic systems used, and the compounds they monitored, are briefly described below.

- Oxygenates such as acetaldehyde, acetone and 2-butanone, organic nitrates such as 2- and 3-pentyl nitrates and aromatic hydrocarbons such as toluene and m-xylene were monitored using the "C-600" gas chromatograph (GC). This system consisted of a Varian 1400 GC with a flame ionization detector (FID) and a 10-ft x 0.125-in. stainless steel column packed with

10% Carbowax 600 on C-22 Firebrick (30/60 mesh). The flow through this column was set at 50 mℓ min^{-1} and, as was the case with all of the GC's, the carrier gas was nitrogen. The hydrogen flow was kept at 45 mℓ min^{-1}, and the oxygen, used in the place of air to enhance sensitivity, was set at 250 mℓ min^{-1}. The detector was heated to 200°C, and the column was maintained at 75°C. 100-mℓ samples drawn from the chamber were trapped by pushing the gas sample through a 10-in. x 0.125-in. stainless steel tube packed with glass beads (80 mesh) and immersed in liquid argon. The sample was carried onto the column by then immersing the trap in boiling water and simultaneously actuating the gas sampling valve which was heated to 95°C to prevent adsorption of compounds.

- C_2-C_5 alkanes and alkenes were monitored using the "DMS" GC, which consisted of the electrometer and flame ionization detector from a Varian 1400 GC with a 34.5-ft x 0.125-in. stainless steel column packed with 10% 2,4-dimethylsulfolane on acid washed 60/80 mesh Firebrick. At the end of this column, before the detector, was a 2-ft x 0.125-in. stainless steel "soaker" column packed with 10% Carbowax 600 on Firebrick. The carrier nitrogen flow through these two columns was set at 50 mℓ min^{-1}, as was the hydrogen flow. The oxygen flow was 330 mℓ min^{-1}. The columns were maintained at 0°C and the detector was heated to 115°C. The 100-mℓ gas samples were trapped on a 10-in. x 0.125-in. stainless steel column packed with 10% 2,4-dimethylsulfolane on Firebrick, 60/80 mesh, immersed in liquid argon. The sample was then introduced to the column by simultaneously thawing the trap in ice water and turning the gas sampling valve.

- Methane, ethane, ethene and acetylene were monitored using the "PN" GC which consisted of a Varian 1400 GC with a flame ionization detector and a 5-ft x 0.125-in. stainless steel column packed with Porapak N, 80/100 mesh. The nitrogen carrier flow was set at 80 mℓ min^{-1}, the hydrogen at 60 mℓ min^{-1} and the oxygen at 400 mℓ min^{-1}. The column was maintained at 60°C, while the detector was heated to 130°C. When a sample was to be analyzed for methane, 100-mℓ of the sample was pushed through a 3-mℓ stainless steel loop. The sample in the loop was then transferred onto the column by actuating the gas sampling valve. Sampling for ethene, ethane and acetylene was accomplished by trapping the sample in a 11-in. x 0.125-in. stainless steel column packed with 10% Carbowax 400 on Firebrick, 30/60 mesh, immersed in liquid argon. The sample was thawed by

immersing the trap in ice water and at the same time turning the valve so that the sample was transferred to the column.

- $\geq C_5$ alkanes and alkenes, aromatic hydrocarbons and some oxygenates and alkyl nitrates were monitored by a Hewlett-Packard 5711A gas chromatograph with a flame ionization detector and a 30-m x 0.322-mm fused silica capillary column. This column, manufactured by J&W Scientific, Inc., had a film thickness of 1 μm composed of the bonded, liquid phase DB5. The nitrogen carrier flow was set at 0.6 mℓ min^{-1} and the makeup gas, also nitrogen, was set to 30 mℓ min^{-1}. The hydrogen and oxygen flows were maintained at 30 mℓ min^{-1} and 230 mℓ min^{-1}, respectively. Before a sample was taken, the column oven was cooled to $-90^{o}C$. Sampling was accomplished by flushing 100 mℓ of sample through a dichlorodimethylsilane treated 10.2-mℓ glass loop. The GC gas-sampling valve, which was maintained at $145^{o}C$, was then actuated, and the sample was transferred onto the head of the column (at $-90^{o}C$) over a period of 12 minutes. The column was then heated from -90 to $-50^{o}C$ over a 1.3-minute duration. The temperature program was then started with the column being heated from -50 to $200^{o}C$ at a rate of $8^{o}C$ min^{-1}.

- Methanol was monitored using the "PQS" GC, which consisted of a Varian 1400 GC with a flame ionization detector and a 6-ft x 0.125-in. stainless steel column packed with Porapak QS 100/120 mesh. The carrier flow was set at 50 mℓ min^{-1}, the hydrogen flow at 40 mℓ min^{-1}, and the oxygen flow at 300 mℓ min^{-1}. The detector was heated to $200^{o}C$, and the column was maintained at $110^{o}C$. 100-mℓ samples drawn from the chamber were trapped by pushing the gas sample through a 10-in x 0.125-in. stainless steel tube immersed in liquid argon. For the indoor chamber runs and the outdoor chamber runs up to OTC-234, this tube was packed with glass beads (80 mesh). For runs after OTC-234, the tube was packed with 10% 2,4-dimethylsulfolane on Firebrick (60/80 mesh). The sample was thawed by immersing the trap in boiling water and simultaneously turning the valve so that the sample was transferred to the column.

Methanol proved to be a difficult compound to monitor with the level of precision observed for most of the other organic reactants, and problems were experienced with the methanol analysis in some experiments, resulting in the lack of usable methanol data for those runs. One problem observed was a non-reproducibility of the GC retention times, resulting in

changes in the calibration factor by almost a factor of 3. When the methanol analysis system was operating properly, the resulting methanol data are estimated to have uncertainties of 20-30%.

• Peroxyacetyl nitrate (PAN) was monitored using one of two different Aerograph gas chromatographs with electron capture detectors (ECD). On both instruments the detector was equipped with a standing current control, and since the response was directly influenced by the standing current, it was maintained to within ±2% of a constant value during all experiments and calibrations. The GC used initially for the indoor experiments used a 12-in. x 0.125-in. FEP Teflon column containing 5% Carbowax 400 on Chromosorb G (80/100 mesh) operating at room temperature with a nitrogen carrier flow of 75 mℓ min^{-1}. Later, in order to obtain PAN data during the nighttime, PAN in the indoor chamber was measured with a gas chromatograph with an automated sampling system. This automated gas chromatograph was also used for the outdoor experiments. It had a 24-in. x 0.125-in. FEP Teflon column packed with 5% Carbowax 400 on Chromosorb W (100/120 mesh) operating at room temperature with a nitrogen carrier flow of 36 mℓ min^{-1}. Analyses were carried out by flushing a ~2-mℓ loop with the sample, and then injecting the contents of the loop onto the column.

Calibrations of all GC's were performed at approximately two- to three-month intervals, and, except for the gas chromatographs used to monitor PAN, were carried in the same general manner. First, all gas flows were measured to verify that no changes had occurred that would indicate previous measurements were erroneous. After measuring these flow rates, a calibration mixture was made up using one of two methods. The calibration mixture, composed of known quantities of various compounds, was then injected into the appropriate GC. The elution time and height of each peak was recorded. The height of each peak was multiplied by the attenuation and the response in millivolts was obtained.

For gaseous compounds, two 2000-mℓ flasks, whose volumes had been determined by measuring with water, were flushed with nitrogen for 20 minutes, and then 2 mℓ of each pure gas was injected into the first flask with a 5-mℓ syringe. This flask was allowed to mix for 20 minutes, and then 2 mℓ from this flask was transferred into the second flask. The contents of this second flask were allowed to mix for 20 minutes. This resulted in a concentration of ~1 ppm of the gas in the second flask.

Loop calibrations were performed by connecting this second flask directly to the loop and flushing the loop with the contents of the flask. Trap calibrations were accomplished by diluting a 5-mℓ sample from the second flask with nitrogen in a 100-mℓ syringe, and passing the contents of the syringe through the trap. For a flask containing 1 ppm of the compound, this was equivalent to sampling 100-mℓ of gas containing 50 ppb of the compound.

Calibration of compounds that were liquid in a pure state at room temperature was carried out using an ~50-ℓ all-glass carboy, which was first cleaned by being heated from the inside with a heat gun, then cooled with the heat gun with the heat off until the carboy reached room temperature, and finally flushed with nitrogen for one hour. The carboy was then dosed with 1 μℓ of each pure liquid to be calibrated using a 10-μℓ syringe. These were allowed to mix for one hour prior to any samples being taken. Trap and loop calibrations were both accomplished in the same way. A 1-mℓ sample was taken from the carboy with a 5-mℓ syringe and diluted with 99 mℓ of nitrogen. The samples were injected in the manner described previously. The exact concentration of each compound was calculated knowing the amount of liquid injected and its density.

Calibration samples of PAN were prepared in pressurized cylinders as described previously (Stephens et al. 1975), and the PAN concentration was determined by infrared absorption of the 8.6 μ band [absorption cross-section = 13.9×10^{-4} ppm^{-1} (Stephens and Price 1973)]. The contents of the cylinder were diluted using a flow manifold with calibrated rotometers to yield PAN concentrations in the range 5-50 ppb, and 100-mℓ samples were taken directly from the flow manifold using gas-tight, all-glass syringes.

The expected accuracy and precision of concentration measurements of most of the compounds determined by the above systems were, with the exception of PAN and acetaldehyde, ~5% or better. Due to varying peak widths, acetaldehyde concentrations were precise and accurate to ~20%. Peroxyacetyl nitrate measurements were estimated to have ~10% precision and ~25% accuracy.

2. Formaldehyde

Formaldehyde was monitored using the chromatropic acid technique. Samples for analysis by this technique were obtained by drawing, at 1 liter min^{-1}, 20 liters of air from the chamber through a single bubbler

containing 10 mℓ of doubly distilled water. Samples taken from the outdoor chamber were taken through a 0.5-in. FEP Teflon probe, inserted into the chamber with the tip 18 inches from the chamber wall. The sample probe for the indoor chamber consisted of 0.5-in. Pyrex tube with the internal tip also located 18 inches from the chamber wall. A metal bellows pump at the downstream end of the bubbler with a calibrated flow meter and needle valve was used to pull the sample through the bubbler. The samples were developed by adding 0.10 mℓ of chromatropic acid (4,5-dihydroxy-2,7-naphthalenedisulfonic acid disodium salt) to a 4.0 mℓ aliquot of the sample. The solution was acidified by diluting it to 10.0 mℓ with concentrated sulfuric acid. The chromatropic acid solution was prepared by dissolving 0.10 g of the salt in 10.0 mℓ of doubly distilled water. The developed solutions had a purple color and the absorbances were measured at 580 nm by a Beckman Model 35 spectrophotometer, after zeroing the instrument using a prepared blank. Instrumental drift was also periodically checked during the measurements using the same blank.

Periodic calibrations of the spectrophotometer and flow meters were carried out. The spectrophotometer was calibrated by subjecting a known concentration of formaldehyde salt to the same procedure as outlined above.

The accuracy and precision of this formaldehyde analysis technique depended upon a number of factors, including the calibration of the spectrometer and the efficiency of the bubbler in collecting formaldehyde from the air passing through it. In the past, the accuracy and precision of this technique had been quite variable, ranging from an optimum accuracy and precision of ~30%, to periods of anomalously low readings apparently due to problems with the bubbler, to periods of anomalously high and variable readings apparently due to contamination (see, for example, Pitts et al. 1979). Although attempts had been made to improve the reliability of this technique for routine use, they have been met with variable success.

Examination of formaldehyde data obtained during this program indicated that while most runs appeared to produce usable formaldehyde data, for some runs the formaldehyde data were highly scattered and appeared to be anomalously low. In general, the formaldehyde data from the outdoor chamber runs appear to be of higher quality than those from the indoor chamber; this was observed in our previous indoor and outdoor

chamber study of multi-day effects (Carter et al. 1985), but the reason for this is not known. The quality of the formaldehyde data for specific runs or groups of runs is discussed in conjunction with the discussion of the results of these experiments.

3. Continuous Monitoring Instruments

Ozone, nitrogen oxides, temperature and (for the outdoor runs only) the dew point depression were monitored continuously using the instruments described below. Except as noted, samples for analysis by these systems were taken from the gas sampling manifold described in Section II.B.1 for the outdoor chamber, or directly from a probe inserted ~18 inches into the chamber for the indoor chamber, using Teflon or Pyrex sampling lines.

- Ozone was monitored using a REM Inc. Model 612 chemiluminescence ozone monitor for the outdoor chamber, and by a Dasibi Model 1003AH ozone monitor for the indoor chamber runs. Calibrations were carried out every two months against a Dasibi Model 1003AH ozone monitor transfer standard which in turn was routinely calibrated by the California Air Resources Board. The ozone source was a Monitor Labs Calibrator Model 8500, with four different ozone concentrations, and the dilution gas was Liquid Carbonic Company Medical Air. The analyzer being calibrated was first zeroed using Medical Air, then the calibrator was turned on to produce the highest concentration of ozone, ~0.3 ppm. Both analyzers were allowed to equilibrate before any readings were recorded, and the calibrated voltage on the REM was adjusted if any difference between the output of the two analyzers was recorded. The ozone concentration was then reduced, and the output from both instruments was observed to verify that the response was linear, this being repeated at two lower ozone concentrations. If the response was not linear, then corrective action was taken. Finally, the analyzer being calibrated was again zeroed with Medical Air. The precision and accuracy were both better than 5%.

- Nitric oxide and total oxides of nitrogen (NO_x + organic nitrates) were monitored using a Columbia Scientific Industries Series 1600 (for the outdoor chamber runs) or a Teco Model 14-B (for the indoor chamber runs) chemiluminescence oxides of nitrogen analyzer. Calibrations, using a Monitor Labs, Inc. Model 8500 calibrator as the dilution system, and a National Bureau of Standards cylinder of 97.4 ppm of NO in nitrogen, were

performed bimonthly. The dilution gas was Liquid Carbonic Company Medical Air. The analyzer was first zeroed using Medical Air, then calibrated for NO by diluting NO in Medical Air and measuring the flow of each gas with a bubble flowmeter. The analyzer was allowed to equilibrate at each concentration for 30 minutes. The first concentration used was ~0.30 ppm. The potentiometers in the analyzer were adjusted, if necessary, to match the NO output of the analyzer with the actual concentration. Two lower concentrations were used to verify linearity of the analyzer. The converter efficiency was checked by setting up a NO concentration of about 0.30 ppm, and then reacting this with a lesser concentration of ozone. If the converter was operating properly, the NO_2 would equal the difference in NO. The linearity of the converter was verified by using three different concentrations of ozone. After this procedure was completed, the analyzer was re-zeroed with Medical Air. The accuracy and precision of this instrument in the absence of interfering nitrates (see below) was estimated to be comparable to those for the ozone monitors, i.e., better than 5%.

The analysis of NO_2 and NO_x was complicated by the fact that for such instruments the converters have been shown (Winer et al. 1974) to convert PAN, organic nitrates and HNO_3 to NO, and thus such species yield a positive interference in the NO_2 analysis cycle. (The NO data are unaffected.) Conversion of PAN and organic nitrates has been shown to be essentially quantitative (Winer et al. 1974) for the molybdenum converter employed in the Teco analyzer, but this has not been shown to be the case for the converter employed in the Columbia Scientific Industries instrument, and preliminary data from our laboratories have indicated that the conversion of PAN is not quantitative. It should be noted that organic nitrates are expected to be formed in significant yields from larger alkanes such as the isooctane present in the surrogate mixture, though the nitrates expected to be formed from those compounds could not be monitored due to lack of authentic samples for calibration purposes. Therefore, no correction for this interference on the NO_2 data was attempted.

An additional complication in these analyses concerns the fact that HNO_3, a major NO_x sink in NO_x-organic-air irradiations, can also interfere with NO_2 readings. However, because of the tendency of HNO_3 to be absorbed on the Teflon sampling lines, this interference is non-quantitative

(Pitts et al. 1981). This resulted on occasion in erratic NO_2 readings during the later periods of some multi-day indoor chamber runs, presumably due to HNO_3 saturating the Teflon sampling lines and being transported into the NO_2 converter. Less erratic (and lower) NO_2 readings were obtained when a nylon filter, which quantitatively removes HNO_3 (Joseph and Spicer 1978), was placed in line between the chamber and the NO_x analyzer. However, the nylon filter was not employed in these experiments.

- Temperature was monitored in the outdoor runs using a Doric Model DS 350-T3 digital thermocouple indicator, and in the indoor runs with an Analogic Model AN 2572 Digital thermocouple indicator, in both cases using iron-constantan thermocouples. For the outdoor runs, a thermocouple was installed in each manifold sample port so the air temperature was measured immediately as it flowed out of the chamber (see Section II). For the indoor chamber runs, the thermocouple was installed in a probe inserted into the center of the chamber. This instrument was calibrated periodically using ice water as the source for 0^oC and boiling water as the source for 100^oC. The accuracy was better than 5%, and the precision was better than 1%.

- The dew point depression was monitored in the outdoor runs only, using an EG&G International, Inc., Model 880 dew point hygrometer. This instrument was calibrated periodically against a sling psychrometer. This instrument required a daily to weekly cleaning and maintenance, and often time was not available in the schedule to perform these tasks. Thus the precision of the data from this instrument observed during many of the outdoor runs was not particularly good, and these measurements should probably be considered to be primarily qualitative in nature, and should be considered to be invalid in experiments where they are highly scattered.

4. Light Intensity

Light intensity was monitored continuously for the outdoor chamber runs by a UV radiometer, a total solar radiometer (TSR), and by the quartz tube NO_2 actinometry technique developed by Zafonte et al. (1977). For the indoor chamber runs, where the light intensity was constant, continuous light intensity measurements were not necessary. The light intensity was measured periodically in separate experiments using

the quartz tube NO_2 actinometry technique. This technique and the UV radiometer measurements employed in the outdoor chamber runs are discussed below:

- UV radiation (λ = 290-390 nm) in the outdoor irradiations was monitored continuously using an Eppley radiometer located on the roof of the laboratory adjacent to the chamber. The data from this instrument were collected by the Apple II computer-based data acquisition system, which reported and saved the data as 10-minute averages. The data from this instrument are given in the data sets for these runs only for the period of time during which the chamber was uncovered. The precision of these UV measurements were found to be generally better than 5%. This instrument was calibrated at the factory in February, 1984.

- Total solar radiation (TSR) in the outdoor chamber experiments was monitored using an Eppley Model PSP precision pyranometer which was located next to the UV radiometer discussed above. The data was collected and reported as 10-minute averages for the periods of time when the chamber was uncovered as were the UV radiometer data. This instrument, which was newly acquired at the beginning of this program, was calibrated by the manufacturer. The precision of this instrument is comparable to that of the UV radiometer.

- Measurements of the rate of NO_2 photolysis, k_1, were carried out for both indoor and outdoor chamber runs.

$$NO_2 + h\nu \rightarrow NO + O(^3P) \qquad (1)$$

In both cases, the quartz tube technique of Zafonte et al. (1977) was employed. For the outdoor runs, the data were recorded every 10 minutes at the same time the data from the continuous analyzers were recorded; for the indoor chamber, a single average value was determined from separate actinometry experiments conducted approximately once a month.

In this technique, the reactor cell consisted of a 100-cm segment of 25-mm (nominal) quartz tubing with 0.25-in. o.d. extensions at each end. The inside diameter of this tube was measured at both ends using calipers and had an average value of 21.44 mm. For the outdoor chamber, the first 20.5 cm of the tube was blackened to permit plug flow conditions to be established before photolysis occurred. Likewise, the final 7.0 cm on the

outlet side was blackened to terminate photolysis before sampling began. This left 72.5 cm over which photolysis was allowed to occur. The tube for the indoor chamber was not blackened at either end.

The NO for the actinometry experiments for the outdoor chamber was obtained from a Scott-Marrin, Inc. cylinder mixture of 100 ppm NO_2 in nitrogen. The mixture was further diluted with nitrogen using calibrated flow meters giving a final average concentration in the cell of 1-2 ppm. The nitrogen dioxide for the indoor chamber was obtained from a Scott-Marrin, Inc. tank mixture of 1.5 ppm NO_2 in nitrogen, and was not diluted further. The NO_2 flow entered the reactor cell via 0.25-in. blackened FEP Teflon tubing, attached with a 0.25-in. stainless steel Cajon ultra-torr union. The exhaust from the cell was connected to the sampling line of the NO_x analyzer, and the excess was vented to the atmosphere via a "T". These sample lines were also blackened FEP Teflon tubing, of diameter 0.125-in. for the outdoor chamber and 0.25-in. for the indoor chamber.

Under typical conditions, the gas flow was set to 37 $m\ell\ s^{-1}$. With an exposed cell volume of 262 $m\ell$, a NO_2 residence time of 9.1 sec was established within the cell. This allowed a sufficient buildup of NO which could then be accurately measured.

NO and NO_2 were measured using a chemiluminescence NO-NO_2-NO_x monitor (a Bendix Model 8101-B for the outdoor experiments, and a Teco Model 14-B for the indoor experiments). NO and NO_2 were alternately measured on a 30-sec cycle. The maximum sensitivity for both gases was 5 ppb. During photolysis, NO concentrations generally ranged from 100-150 ppb. Nitrogen dioxide was measured by chemiluminescence after initial reduction to NO. Caution was exercised to ensure efficient operation of the reduction catalyst. The NO_x analyzer was calibrated bimonthly using the same procedure as for the NO_x analyzer (see above) sampling the contents of the chamber.

The precision of these NO_2 actinometry measurements was generally ~5-10%. This technique as used was inherently less precise and less capable of following rapid changes in light intensity than was the UV radiometric measurement technique. The accuracy of the NO_2 actinometry measurements were determined by a number of factors, including the accuracy of the NO_x analyzer, the extent to which plug flow conditions in the tube had been established, and whether the tube was placed in a location in which the

light intensity and spectral distribution accurately reflected that in the chamber. For the outdoor chamber experiments, the location of the quartz tube also needs to be taken into account. For these runs, the quartz tube was located underneath one of the sides of the outdoor chamber and that the light had to pass through both layers of the Teflon bag surface before reaching the tube, which meant that the intensity of the light reaching the tube would be somewhat lower than the intensity of the light within the outdoor chamber. In our previous outdoor chamber program (Carter et al. 1985), the NO_2 actinometry data were also affected by the fact that periodically the shadows the framework used to support the chamber cover would fall on the actinometry tube, resulting in anomalously low readings. The framework used to support the chamber cover was redesigned for this program so it pivots out of the way when the chamber is uncovered and thus does not cast shadows on the reactor (see Figure III-2). Hence the problem of shadows on the actinometry tube was much less serious for these experiments.

IV. RESULTS

A total of 81 environmental chamber experiments were carried out in this program. These included 14 multi-day surrogate-NO_x-air irradiations carried out in the indoor chamber, 20 multi-day surrogate-NO_x-air irradiations carried out in the outdoor chamber in the divided mode (with two different surrogate mixtures being irradiated at the same time), 6 propene-NO_x-air and 3 n-butane-NO_x-air control runs, 18 radical tracer-NO_x-air runs, including 2 with methanol added and 2 with formaldehyde added later in the run, 4 acetaldehyde-air runs, 2 ozone dark decay determinations, 3 side equivalency tests (in the dual outdoor chamber), 6 NO_2 actinometry experiments (in the indoor chamber), and 5 miscellaneous, conditioning, or aborted runs. Chronological listings of all the chamber runs carried out in this program, together with brief summaries of the description, conditions, and major qualitative results of each experiment, are given in Tables IV-1 and IV-2 for the indoor and the outdoor chamber experiments, respectively.

Concentration-time plots for the species measured in the multi-day surrogate-NO_x-air experiments and selected types of control experiments are given in Appendix A to this report. These plots in Appendix A are ordered by run type, for each run for which plots are given, the figure number in Appendix A is given in parentheses underneath the run type in Tables IV-1 and IV-2. Computer model simulations were carried out for most of these runs, and the results of the model calculations are shown along with the experimental results in the plots in Appendix A.

Detailed tabulations of the data from all the runs carried out in this program (except NO_2 actinometry experiments carried out in the indoor chamber) are available on tape in computer-readable format, and a description of the computer data sets containing these data are given in Appendix C. In addition to giving the relevant experimental measurements made during each of the runs, the detailed tabulations given in Appendix B and the computer data sets described in Appendix C indicate which instrument was used for each set of measurements, and includes comments describing the experimental operations, problems or special situations which occurred during the run, and other relevant observations which may affect the interpretation or validity of the data.

Table IV-1. Chronological Summary of Indoor Chamber Experiments, With Qualitative Description of Problems Encountered and Results Obtained

ITC Run No.	Run Type[a] (Data Plots)[b]	Comments, Results and Problems
859	NO_x-Air	Initial NO_x = 0.53 ppm. Results indicated normal chamber radical source, but higher NO oxidation rate than usual, suggesting some background reactive organics.
860	Propene-NO_x-Air Conditioning (A-4)	Initial Propene = 0.99. NO_x = 0.51 ppm. 0.58 ppm O_3 formed. Results in the normal range.
861	NO_x-Air	Initial NO_x = 0.55 ppm. Results indicated normal chamber radical source and background reactive organics.
862	NO_2 Actinometry	NO_2 photolysis rate (k_1) = 0.317 min^{-1}. Within the expected range.
863	NO_x-Air + Methanol (A-12)	Methanol added after a 2-hour tracer-NO_x-air run. Initial NO_x = 0.56 ppm. Results of NO_x-air portion indicated normal background chamber reactivity. Analytical problems for methanol resulted in no valid methanol being obtained. The amount of methanol added is estimated to be approximately 25-35 ppm based on the volume of liquid methanol injected into the chamber. The addition of methanol caused OH radical levels (as measured by the propene and n-butane tracers) to increase by approximately 25% for the first hour after methanol addition, and by approximately a factor of 2 for the second hour. It also caused the NO oxidation rate to increase from 0.06 ppb min^{-1} to approximately 1.6 ppb min^{-1}.
864	NO_x-Air + Formaldehyde (A-10)	0.5 ppm Formaldehyde added after a 2-hour tracer-NO_x-air run. Initial NO_x = 0.54 ppm. The results of NO_x-air portion indicated normal background chamber reactivity. Addition of formaldehyde resulted in the OH radical levels to increase from an average of approximately 6 x 10^5 radicals cm^{-3} for the hour before formaldehyde addition to approximately 4 x 10^6 radicals cm^{-3} for the hour after addition, and caused the NO oxidation rate to increase from 0.1 ppb min^{-1} to 1.7 ppb min^{-1} for the same two periods. These results are in reasonable agreement with model predictions.

(continued)

Table IV-1 (continued) - 2

ITC Run No.	Run Type[a] (Data Plots)[b]	Comments, Results and Problems
865	15-B Surrogate (A-14)	4-Day run with NO added after first hour of days 3 and 4 in order to allow continued ozone to form on those days. Ozone, PAN, and formaldehyde yields for the first two days, prior to NO addition, are given on Table IV-9. Ozone formation occurred only on day 1 and day 3 (after the NO addition), and increases in PAN and formaldehyde concentrations only occurred on day 1. The last PAN measurement on day 1 was taken at t = 6 hours, and the data do not indicate whether higher PAN levels were attained after that time.
866	NO_x-Air	Initial NO_x = 0.51 ppm. Results indicated normal background chamber reactivity.
867	15-MF Surrogate (A-16)	4-Day run with NO added after first hour of days 3 and 4 in order to allow continued ozone to form on those days. Ozone formation occurred only on day 1 and on day 3 after the NO was added. Too much NO added on day 4 for ozone formation to occur. PAN and formaldehyde formation occurred only on day 1. The last PAN measurement on day 1 was taken at t = 6 hours, and the data do not indicate whether higher PAN levels were attained after that time.
868	15-BL Surrogate (A-18)	2-Day run. Initial NO_x high by approx. 25% compared to other HC/NO_x = 17 runs. Capillary GC problems. The highest ozone levels occurred on day 1, but ozone formation also occurred on day 2. Measurable increases in PAN and formaldehyde occurred only on day 1. The last PAN measurement on day 1 was taken at t = 6 hours, but it appears probable that higher PAN levels were formed between then and the start of day 2.
869	NO_2 Actinometry	NO_2 photolysis rate (k_1) = 0.336 min^{-1}. Within the expected range.
870	NO_x-Air	Initial NO_x = 0.35 ppm. Results indicated normal background chamber reactivity.

(continued)

Table IV-1 (continued) - 3

ITC Run No.	Run Type[a] (Data Plots)[b]	Comments, Results and Problems
871	6-B Surrogate (A-19)	2-Day run. Capillary GC problems. Ozone formation occurred on both day 1 and day 2, with day 1 ozone being slightly higher. PAN measurements were made only for the first 6 hours of each day, and the PAN levels at the start of day 2 were higher than at t = 6 hours of day 1, suggesting that the maximum PAN levels occurred between then. No PAN formation occurred on day 2. The formaldehyde data are highly scattered, particularly on day 2.
872	6-MF Surrogate (A-20)	2-Day run. Run ended after only 6-hours irradiation on day 2, instead of after 12 hours, which is the normal procedure for these runs. Capillary GC problems. Slightly more ozone was formed on day 2 than on day 1, but ozone formation was still occurring when the run ended. PAN measurements were made only for the first 6 hours of each day, and the PAN levels at the start of day 2 were higher than at t = 6 hours of day 1, suggesting that the maximum PAN levels occurred between then. No PAN formation occurred on day 2. The formaldehyde levels changed relatively little throughout day 1 and were only slightly lower on day 2.
873	6-BL Surrogate (A-23)	2-Day run. Capillary GC problems. Ozone formation occurred on both days, but the day 2 ozone levels were higher. PAN measurements were made only for the first 6 hours of each day, and the PAN levels at the start of day 2 were higher than at t = 6 hours of day 1, suggesting that the maximum PAN levels occurred between then. A slight increase in PAN levels occurred on day 2. The formaldehyde data are highly scattered, particularly on day 2.
874	6-M Surrogate (A-22)	2-Day run. Capillary GC problems. Ozone formation occurred on both days, but the day 2 ozone levels were higher. This is the first run where PAN measurements were taken using the automated PAN GC instrument, but due to a malfunction, PAN data were not obtained from t = 6.5 on day 1 and the start of day 2,

(continued)

Table IV-1 (continued) - 4

ITC Run No.	Run Type[a] (Data Plots)[b]	Comments, Results and Problems
		and the maximum day 1 PAN levels probably occurred sometime between those times, since the PAN levels at the start of day 2 were higher. The PAN levels changed relatively little on day 2. Formaldehyde increased throughout day 1, and remained essentially constant on day 2.
875	NO_x-Air	Initial NO_x = 0.42 ppm. Results indicated normal background chamber reactivity.
876	NO_2 Actinometry	NO_2 photolysis rate (k_1) = 0.327 min^{-1}. Within the expected range.
877	6-MF Surrogate (A-21)	2-Day run. Capillary GC problems resolved. Ozone formation occurred on both day 1 and day 2, with the day 2 ozone being slightly higher. This is the first run with PAN data available throughout the experiment. PAN increased at an essentially constant rate for 14 hours (2 hours after the lights were turned off on day 1), and declined slowly throughout the remainder of the run. Formaldehyde levels changed relatively little on day 1 and were lower (and more scattered) on day 2.
878	NO_x-Air	Initial NO_x = 0.79 ppm. Results indicated normal background chamber reactivity.
879	Surrogate Attempt	Run aborted at start of day 2 due to acetone contamination in chamber. Data not processed.
880	3-B Surrogate (A-24)	3-Day run. Formaldehyde data appear to be anomalously low and are probably not valid. Only minor ozone formation occurred on day 1, more ozone was formed on day 2 and the most ozone on day 3. No PAN formed on day 1, but roughly equal amounts of PAN formed on day 2 and day 3, with no significant decrease in PAN levels at night.
881	3-MF Surrogate (A-25)	3-Day run. Formaldehyde data may be valid; but data for runs 880 and 881 indicate that they may be unreliable. Essentially no ozone

(continued)

Table IV-1 (continued) - 5

ITC Run No.	Run Type[a] (Data Plots)[b]	Comments, Results and Problems
		formation on day 1 and only minor ozone formation on day 2, but significant ozone formation occurred on day 3. Results similar for PAN. Formaldehyde levels changed relatively little on day 1 and day 2, but appear to be lower on day 3, though the day 2 and day 3 data are scattered.
882	NO_x-Air	Initial NO_x = 0.70 ppm. Results indicated normal background chamber reactivity.
883	NO_2 Actinometry	NO_2 photolysis rate (k_1) = 0.327 min^{-1}. Within the expected range.
884	NO_x-Air	Initial NO_x = 0.68 ppm. Results indicated normal background chamber reactivity.
885	3-BL Surrogate (A-27)	3-Day run. Formaldehyde data appear to be anomalously low and are probably not valid. Essentially no ozone formation occurred on day 1, minor ozone formation occurred on day 2, and the most ozone formed on day 3. Results similar for PAN.
886	3-M Surrogate (A-26)	3-Day run. NO_x analyzer problems encountered after the first few hours of this run, and NO and NO_2 values after t = 2 hours are probably not valid. Essentially no ozone formed on day 1, a little formed on day 2, and the most on day 3. Results for PAN were similar. Formaldehyde levels increased on day 1, were essentially constant on day 2 at the maximum day 1 level, and were lower (and more scattered) on day 3.
887	NO_x-Air + Methanol (A-13)	Approx. 35 ppm methanol added after a 2-hour NO_x-air run. Initial NO_x = 0.30 ppm. Results of NO_x-air portion indicate normal background chamber reactivity. Addition of methanol caused the NO oxidation rate to increase from 0.12 ppb min^{-1} to 1.7 ppb min^{-1} and the calculated OH radical levels to change from approximately 1.5×10^6 radicals cm^{-3} to 1.2×10^6 radicals cm^{-3}, where these values are calculated for the hour before and the hour after methanol addition. 0.19 ppm formaldehyde

(continued)

Table IV-1 (concluded) - 6

ITC Run No.	Run Type[a] (Data Plots)[b]	Comments, Results and Problems
		formed in 2 hours after methanol added. The observed increase in NO oxidation rate and formaldehyde levels are significantly less than expected based on model calculations, but the reason for this is unknown.
888	15-M Surrogate (A-17)	2-Day run. Significant ozone and PAN formation only occurred on the first day. The highest PAN levels occurred at the end of day 1, and decreased after that. The formaldehyde levels increased throughout day 1 and decreased throughout day 2.
889	NO_x-Air	Initial NO_x = 0.36 ppm. Results indicated normal background chamber reactivity.
890	NO_2 Actinometry	NO_2 photolysis rate (k_1) = 0.316 min^{-1}. Within the expected range.
891	15-B Surrogate (A-15)	2-Day run. Significant ozone and PAN formation occurred only on day 1. The highest PAN levels occurred around t = 7.5 hours on day 1, and they decreased after that. The day 1 formaldehyde levels appear to be anomalously low.
892	Acetaldehyde-Air	Run to measure NO_x offgassing rate from chamber. 4-hour run. Initial acetaldehyde = 0.6-0.8 ppm (acetaldehyde data highly scattered). PAN formation rate = approx. 3.5 ppb hour-1, which is within the normal range for this chamber.
893	NO_x-Air	Initial NO_x = 0.37. Results indicated normal background chamber reactivity, though the NO oxidation rate was higher than typical for this series.
894	NO_2 Actinometry	NO_2 photolysis rate (k_1) = 0.336 min^{-1}. Within the expected range.

[a]For multi-day, surrogate-NO_x-air runs, the notation of the form "r-S" is used to designate the nominal (desired) initial conditions, where "r" indicates the approximate nominal "base case" hydrocarbon/NO_x ratios, which was either 3, 6, or 15 for the indoor chamber runs, and "S" indicates the surrogate composition employed, which is either "B" for the base case surrogate, "M" for the 33% methanol substitution surrogate, "MF" for 33% methanol + 10% formaldehyde substitution surrogate, and "BL" for 33% blank substitution surrogate.

[b]The figure number for runs whose data are plotted in Appendix A is given in parentheses under the run type.

Table IV-2. Chronological Summary of Outdoor Chamber Experiments, With Qualitative Description of Problems Encountered and Results Obtained

OTC Run No	Date Started	Run Type[a] (Data Plots)[b]	Comments, Results and Problems
209	5/13/85	Ozone Dark Decay	Daytime ozone decay rate = 1.1 x 10^{-4} min^{-1}. Nighttime decay rate = 0.3 x 10^{-4} min^{-1}. These are within the normal range.
210	5/15	Propene-NO_x-Air, Undivided (A-5)	Initial NO_x = 0.57 ppm, propene = 1.1 ppm. Warm weather, high clouds. final ozone = 0.97 ppm, within the normal range.
211	5/16	n-Butane-NO_x-Air, Undivided (A-1)	Initial NO_x = 0.55 ppm, n-butane = 10.7 ppm. Warm weather, no clouds. No ozone formed. Model simulations of this run indicates a relatively low chamber radical source.
212	5/17	NO_x-Air, Undivided	Initial NO_x = 0.55 ppm. High clouds, moderate temperatures. The results of this run indicated a very low chamber radical source and minimal chamber contamination.
213	5/21	Surrogate-NO_x-Air Conditioning	2-Day run. Initial NO_x = 0.40 ppm, Base case surrogate = approx. 3 ppmC. Undivided chamber run used to condition the reaction bag for the surrogate. Hazy, warm weather on day 1, hazy, cool weather on day 2. 0.6 ppm ozone formed at end of second day.
214	5/23	10-MF-MF (Side Equivalency Test) (A-38)	2-Day run with same surrogate-NO_x-air mixture used on both sides of the chamber. Fair weather. Good side equivalency observed. Day 1 ozone = 0.34 ppm, day 2 ozone = 0.40 ppm, both sides. Problems with sampling system and run documentation. This run not used for model testing.
215	6/4	10-B-MF (A-30)	2-Day run. No usable formaldehyde data due to instrument malfunction. Warm, hazy weather on day 1.

(continued)

Table IV-2 (continued) - 2

OTC Run No	Date Started	Run Type[a] (Data Plots)[b]	Comments, Results and Problems
			O_3 formation occurred only on day 1. Essentially no differences on ozone or PAN on either side.
216	6/6	Formaldehyde-NO_x-Air	This run was carried out to test the formaldehyde injection and analysis procedures. The problem with the formaldehyde was subsequently determined to be due to an instrument malfunction. Initial NO_x = 0.52 ppm, Initial HCHO nominally 0.5 ppm, but exact amount unknown. Divided chamber run, with HCHO injected separately on each side (to test injection procedure). Propene and n-butane tracers present. 84 ppb ozone formed on side 1, 113 ppb formed on side 2.
217	6/11	10-M-B (A-33)	2-Day run. No side 2 data or side 1 GC data on day 2 due to leak, so comparative data available for day 1 only. Maximum day 1 ozone and PAN higher on base case side, but maximum formaldehyde higher on methanol substitution side.
218	6/17	Acetaldehyde-Air, Divided	This run is used to determine the NO_x offgassing rate. No NO_x was injected. The PAN yield was 8 ppb on side 1 and 9 ppb on side 2, indicating low-to-normal NO_x offgassing rates for this chamber.
219	6/20	7-MF-M (A-43)	2-Day run. NO_x apparently injected incorrectly; initial NO_2 was greater than initial NO. Severe leakage on side 1. "MF" side formed more O_3 on day 1; day 2 data, side 1 data are questionable. HCHO at end of day 1 was almost as high on "M" side as "MF", and HCHO same on day 2. This run was not used for model testing.
220	6/24	7-MF-B	Aborted before the start due to rain. Run was repeated the next day.

(continued)

Table IV-2 (continued) - 3

OTC Run No	Date Started	Run Type[a] (Data Plots)[b]	Comments, Results and Problems
221	6/25	7-MF-B (A-40)	2-Day run. Overcast, cool weather on day 1, clear and sunny on day 2. O_3 formation occurred on both day 1 and day 2 for both sides, with day 2 O_3 being higher. Base case formed more O_3 on day 1, but O_3 was the same on day 2 for both sides. Final day 1 HCHO and day 2 HCHO same on both sides. Slightly higher PAN on base case side for day 1 only.
222	7/1	10-M-MF (A-35)	2-Day run. O_3 formation only on day 1, both sides. O_3 formed faster on MF side, but final day 1 O_3 and day 2 levels same on both sides. Final day 1 and day 2 HCHO levels also same, and PAN yields the same.
223	7/8	10-B-BL (A-36)	2-Day run. Problem with methanol data. No TSR data. Warm weather. O_3 formation only on day 1 for both sides. O_3 higher on base case side throughout the run. HCHO slightly higher on base case side.
224	7/10	13-M-B (A-29)	2-Day run. No TSR data. Warm. O_3 formation on day 1 only, with only slightly more O_3 formed on base case side. Day 1 HCHO same on both sides, but day 2 HCHO higher on methanol side.
225	7/15	5-B-MF (A-49)	Aborted on day 1 due to rain. Run was repeated (OTC-228). Run aborted before any O_3 formed. Initial conversion of NO to NO_2 was slightly faster on MF side than on base case side. This run was not used for model testing.
226	7/16	7-B-B (Side Equivalency Test) (A-47)	1-Day run + some data for day 2. GC problems caused early end of run on day 2. No TSR data. Clear weather. Good side equivalency observed. 0.74-0.75 ppm ozone on day 1, 0.47-0.50 ppm ozone maximum on day 2. This run was not used for model testing.

(continued)

Table IV-2 (continued) - 4

OTC Run No	Date Started	Run Type[a] (Data Plots)[b]	Comments, Results and Problems
227	7/24	NO_x-Air, Divided	Initial NO_x = 0.46 ppm. The results indicated a near average chamber radical source and low NO oxidation rate. Similar results observed on both sides.
228	7/29	5-B-MF (A-48)	2-Day run. No kl data. O_3 formation occurred on both day 1 and 2, with day 2 O_3 being higher, both sides. Initial NO to NO_2 conversion slightly faster in MF side, but days 1 and 2 ozone levels similar. MF HCHO higher than base HCHO both days. More PAN formed on base case side.
229	7/31	7-M-BL (A-46)	2-Day run. The amount of "BL" surrogate injected was 6% low due to an error in the written instructions for the run. O_3 formation on both days, but much more on day 2, both sides. Slightly more O_3 formed on "M" side on day 1, but the day 2 O_3 formation rates and final levels were the same on both sides. HCHO levels on the "M" side about a factor of 2 higher than on the "BL" side. Day 1 PAN slightly higher on "M" side.
230	8/5	7-B-BL (A-45)	2-Day run. Day 1 O_3 and formation rate higher on base case side, but on day 2, no O_3 formation occurred on base case side, while on the blank substitution side O_3 formation occurred, resulting in the same final O_3 levels. HCHO slightly higher on base case side. More PAN formed on day 1 on the base case side, but its consumption at night was also faster on that side, resulting in day 2 PAN being higher on the blank substitution side.

(continued)

Table IV-2 (continued) - 5

OTC Run No	Date Started	Run Type[a] (Data Plots)[b]	Comments, Results and Problems
231	8/7	5-X-MF[c] (A-51)	2-Day run. Side 1 was supposed to have the "M" surrogate, but due to an error in the written instructions, 1.78 ppmC base case surrogate, rather than the more appropriate 1.19 ppmC surrogate, was injected. Problems with the methanol analysis resulted in the initial concentrations of methanol being unknown. More ozone and PAN formed on day 2 than on day 1, with day 1 O_3 and PAN being similar on both sides, and side 1 forming slightly more of both on day 2. Similar yields of formaldehyde observed on both sides. This run was not used for model testing.
232	8/12	NO_x-Air, Divided	Initial NO_x = 0.45 ppm (approx.) Cool and overcast weather noted on log book, though average UV and k_1 readings were relatively high. The results indicated a normal chamber radical source and relatively low NO oxidation rate. Similar results obtained on both sides.
233	8/13	Propene-NO_x-Air, Undivided (A-6)	Initial NO_x = 0.46 ppm, propene = 1 ppm (nominal). No initial propene data. Cool and overcast weather initially, though it cleared later. Final O_3 = 0.63 ppm. Results within the normal range.
234	8/14	Acetaldehyde-Air, Divided	Run to determine NO_x offgassing rate. No k_1 data. PAN yields observed indicate NO_x offgassing rates which are typical for this chamber. Somewhat more PAN formed on side 2 than side 1.
235	9/10	NO_x-Air + Formaldehyde, Divided (A-11)	NO_x-air irradiation to measure chamber effects. Formaldehyde added to obtain data to test formaldehyde and light intensity model. Initial NO_x = 56 ppm, formaldehyde added estimated to be 0.9 ppm. Partly cloudy weather. The NO_x-

(continued)

Table IV-2 (continued) - 6

OTC Run No	Date Started	Run Type[a] (Data Plots)[b]	Comments, Results and Problems
			air portion indicated low-normal radical input rates and very low NO oxidation rates. The addition of formaldehyde caused the NO oxidation rate to increase from near-zero on both sides to 6 ppb min^{-1} on side 1 and 5 ppb min^{-1} on side 2. The radical tracer consumption rates also increased significantly after formaldehyde was added.
236	9/11	Propene-NO_x-Air, Undivided (A-7)	Control run. Initial NO_x = 0.53 ppm, propene = 1.2 ppm. Cool, mostly clear weather. 0.86 ppm ozone formed.
237	9/12	10-B-M (A-34)	2-Day run. Some GC problems. Clear weather. O_3 formation occurred only on day 1. O_3 and PAN slightly higher on base case side. Day 1 formaldehyde similar on both sides, but day 2 formaldehyde higher on methanol substitution side.
238	9/16	10-BL-MF (A-37)	2-Day run. No k_1 data. No day 2 HCHO data. Some GC problems. Clear, cool weather on day 1, hazy, partly cloudy on day 2. More day 1 ozone formed on "MF" side, but on day 2, no ozone formation occurred on "MF" side, while O_3 formation on the blank substitution side resulted in the final O_3 levels almost being the same on both sides. Day 1 HCHO on "MF" side almost twice as high as on "BL" side. More PAN formed on day 1 on the "MF" side, but its consumption at night was also faster on that side, resulting in day 2 PAN being higher on the blank substitution side.
239	9/23	7-MF-M (A-44)	2-Day run. Warm, partly cloudy weather on day 1, warm and clear on day 2. More ozone formed on day one than day 2, both sides. Ozone on "MF" side higher on day 1, but ozone on "M"

(continued)

Table IV-2 (continued) - 7

OTC Run No	Date Started	Run Type[a] (Data Plots)[b]	Comments, Results and Problems
			side slightly higher on day 2. Formaldehyde levels higher on "MF" side on day 1, but they were similar on day 2. Similar amounts of PAN formed on each side.
240	9/25	5-M-B (A-50)	3-Day run. Clear weather on day 1, but some drizzle on day 2 and overcast at times on days 2 and 3. O_3 formation occurred on all 3 days; day 1 and day 2 O_3 much higher on base case side, but on day 3, very rapid O_3 formation on "M" side resulted in higher final O_3 for that side. HCHO levels similar on day 1, but higher on the "M" side for days 2 and 3. Day 1 and (especially) day 2 PAN higher on base case side, but day 3 PAN slightly higher on "M" side.
241	10/1	13-B-MF (A-28)	2-Day run. Clear weather, warmer on day 2. O_3 formation on day 1 but not day 2, both sides. O_3 profiles almost identical on both sides, though initial ozone formation was slightly faster on the "MF" side. Similar levels of formaldehyde by the end of day 1 and on day 2. PAN levels higher on base case side.
242	10/3	7-M-B (A-42)	2-Day run. Clear, warm weather on day 1, but cloudy and cool on day 2. Day 1 O_3 much higher on base case side, but on day 2, no O_3 formed on base side, and O_3 formed on "M" side, resulting in similar final O_3 levels. Similar formaldehyde levels on both sides. More PAN formed on day 1 on the base case side, but its consumption at night was also faster on that side, resulting in day 2 PAN being higher on the methanol substitution side.

(continued)

Table IV-2 (continued) - 8

OTC Run No	Date Started	Run Type[a] (Data Plots)[b]	Comments, Results and Problems
243	10/8	10-B-MF (A-32)	2-Day run. Cloudy and cool weather on both days. Ozone levels very similar on both sides, and on both sides, more O_3 was formed on day 2 than day 1. The day 1 ozone formation rate was slightly greater on the "MF" side. The final day 1 formaldehyde levels, and the day 2 formaldehyde levels were also similar on both sides. The day 1 PAN yields were very close on both sides, but the day 2 PAN yield was higher on the base case side.
244	10/11	Propene-NO_x-Air, Undivided (A-8)	Control and conditioning run. Clear, warm weather. Initial NO_x = 0.43 ppm, propene = 1.0 ppm. 0.78 ppm ozone formed. Results in normal range.
245	10/15	NO_x-Air, Divided	Initial NO_x = 0.45 ppm. Clear, warm weather. Side 1 radical input and NO oxidation rates appear to be normal, both these rates were >60% higher on side 2.
246	10/16	n-Butane-NO_x-Air, Divided (A-2)	Control run which is sensitive to chamber effects. Initial NO_x = 0.48 ppm, n-butane = 5.4 ppm. Clear, warm weather. No ozone formed on either side. NO oxidation rate approximately 60% higher on side 2, which is consistent with the higher radical input rate observed for side 2 in the previous run.
247	10/17	Acetaldehyde-Air, Divided	Run to measure NO_x offgassing. Clear, warm weather. PAN formation rate for side 1 is consistent with results of previous acetaldehyde-air runs. PAN formed on side 2 was 33% higher, which is also consistent with the results of the previous runs in that more PAN was also formed on side 2 in those runs.

(continued)

Table IV-2 (continued) - 9

OTC Run No	Date Started	Run Type[a] (Data Plots)[b]	Comments, Results and Problems
248	11/5	7-B-MF (A-41)	2-Day run. Mostly clear, warm weather. A number of instrumental problems, but run is still usable. k_1 data on day 2 appear to be anomalously low. Ozone levels very similar on both sides. Only minor O_3 formation occurred on day 1, major O_3 formation on day 2. Day 1 formaldehyde levels higher on "MF" side, but levels on day 2 were similar. PAN profiles were similar on both sides, with most PAN being formed on day 2.
249	11/7	10-B-MF (A-31)	2-Day run. k_1 Data for both days appear to be anomalously low. Warm and clear on day 1, but cool and overcast on day 2. Some instrumental problems. Ozone levels very similar on both sides. Ozone formation on both days, but more on day 1. Initial O_3 formation slightly faster on "MF" side. Day 1 formaldehyde levels higher on "MF" side, but levels similar on day 2. PAN levels higher on base case side than on the "MF" side.
250	11/21	10-MF-MF (A-39)	2-Day side equivalency test run. Mostly clear weather. Good side equivalency observed. Run not used for model testing.
251	11/25	Propene-NO_x-Air, Undivided (A-9)	Control run. No k_1 data. Initial NO_x = 0.46 ppm, propene = 0.9 ppm. Partly cloudy. 0.47 ppm ozone formed. The relatively low ozone yield compared to the other propene runs is consistent with the lower temperature and light intensity for this run.

(continued)

Table IV-2 (concluded) - 10

OTC Run No	Date Started	Run Type[a] (Data Plots)[b]	Comments, Results and Problems
252	11/26	n-Butane-NO_x-Air, Divided (A-3)	Control run which is sensitive to chamber effects. No k_1 data. Initial NO_x = 0.48 ppm, n-butane = 5.0 ppm. Cool, partly cloudy weather. No ozone formed. NO oxidation rate 33% higher on side 2 than on side 1, and model simulations indicate higher than normal chamber radical source on side 2. Higher reactivity on side 2 consistent with results of characterization runs carried out around this time.
253	11/27	Ozone Dark Decay	0.9 ppm Ozone injected into the chamber. Decay rate for first 12 hours was 0.68 ± 0.03% per hour. This is within the normal range for this chamber.

[a]For multi-day, divided chamber, surrogate-NO_x-air runs, the notation of the form "r-S1-S2" is used to designate the nominal (desired) initial conditions, where "r" indicates the approximate nominal "base case" hydrocarbon/NO_x ratio, which was either 13, 10, 7, or 5 for the outdoor chamber runs, and "S1" and "S2" indicate the surrogate composition employed on sides 1 and 2, respectively. The notations for the surrogate compositions are either "B" for the base case surrogate, "M" for the 33% methanol substitution surrogate, "MF" for 33% methanol + 10% formaldehyde substitution surrogate, and "BL" for 33% blank substitution surrogate.

[b]The figure number for runs whose data are plotted in Appendix A is given in parentheses under the run type.

[c]"X" indicates an incorrect surrogate injection was made.

In the following sections, the results obtained in these experiments are summarized and discussed. The results of the control and characterization runs are discussed in Section IV-A, followed by a discussion of the results of the multi-day surrogate runs in Section IV-B. Where appropriate, the experimental results are compared with results of computer model simulations; the chemical mechanism employed is that recently developed and tested by us under EPA funding (Carter et al.

1986), and is summarized in Appendix B to this report. The results of the model simulations of the multi-day surrogate runs are discussed in Section IV-C.

A. Control and Characterization Runs

Several types of control, conditioning, and characterization runs were carried out in conjunction with the multi-day surrogate experiments to ensure that the data were sufficiently well characterized for use in model testing, and to assure that chamber contamination or other unusual chamber conditions did not exist which may affect the validity of the data. The following types of such experiments were carried out:

- Radical tracer-NO_x-air irradiations, where the tracers consisted of approximately 10 ppb each of propene and n-butane added to monitor radical levels from their relative rates of disappearance, were carried out in both chambers to measure the magnitude of the chamber radical source and to determine whether the chamber was excessively contaminated with reactive organics.

- Acetaldehyde-air irradiations were carried out in both chambers to measure NO_x offgassing rates.

- Propene-NO_x-air runs were carried out in both chambers for both chamber conditioning and for control purposes.

- Several n-butane-NO_x-air runs were carried out in the outdoor chamber. These runs are extremely sensitive to the magnitude of the chamber radical source, and provide an independent means of measuring this parameter.

- Several NO_x-air irradiations with added methanol or added formaldehyde were carried out for the purpose of providing data for testing models for the reactions of those compounds, and for control purposes.

- Several side equivalency tests were carried out in the outdoor chamber to assure that the results of the irradiation of a given mixture is the same in side 1 of the divided chamber as in side 2.

- Ozone dark decay determinations were carried out in both the indoor and the outdoor chambers immediately after the new Teflon bag reactor was installed, and in the outdoor chamber at the end of this program.

- One surrogate-NO_x-air irradiation was carried out in the outdoor chamber, in the undivided mode, for chamber conditioning purposes.

- Several NO_2 actinometry experiments were carried out in the indoor chamber to measure the light intensity.

The purposes, results, and data analysis methods used for these characterization and control runs are discussed below for each type of experiment. Where appropriate, model simulations have been used to determine if the results of the control experiments are consistent with the expectations based upon the results of previous experiments, our understanding of the chemistry involved, and our understanding of relevant chamber effects or light intensity parameters. The model employed is that recently developed and tested by Carter et al. (1986), and is given in Appendix B of this report.

1. NO_x-Air Irradiations

In order to obtain a measurement of the chamber radical source and of offgassing of reactive contaminants, a number of NO_x-air and CO-NO_x-air irradiations were carried out periodically throughout this program. These runs, the purpose of which has been discussed in detail elsewhere (Carter et al. 1982), consisted of irradiations of NO_x-air mixtures (with the NO_x levels representative of those employed in the surrogate-NO_x-air runs), with traces (~10 ppb) of propene and n-butane, for at least two hours. In the absence of chamber radical sources and reactive contaminants, this chemical system is expected to be completely unreactive, and thus it is highly sensitive to these chamber effects.

Radical initiation rates were obtained by equating the initiation rates to termination rates due to the OH + NO_2 reaction [the major termination reaction in this system (Carter et al. 1982)], with the rate of the latter being estimated from the known OH + NO_2 rate constant (Atkinson and Lloyd 1984) and the measured NO_2 and OH radical levels. The OH radical levels were monitored by measuring the relative rates of decay of the two organic tracers (propene and n-butane), which were consumed primarily by reaction with OH radicals:

$$\text{OH + n-butane} \rightarrow \text{products} \qquad \text{(a)}$$

$$\text{OH + propene} \rightarrow \text{products} \qquad \text{(b)}$$

However, propene was also consumed to some extent in this system by reaction with O_3 and with $O(^3P)$ atoms,

$$O_3 + \text{propene} \rightarrow \text{products} \qquad (c)$$

$$O(^3P) + \text{propene} \rightarrow \text{products} \qquad (d)$$

and the appropriate corrections for these additional reactions must be made in the data analysis.

The relevant kinetic differential equations are:

$$d\ln[\text{n-butane}]/dt = -k_a[OH] \qquad (I)$$

$$d\ln[\text{propene}]/dt = -k_b[OH] - k_c[O_3] - k_d[O(^3P)] \qquad (II)$$

where k_a and k_b are the rate constants for the reaction of n-butane and propene with OH radicals, respectively, k_c and k_d are the rate constants for the reaction of propene with O_3 and $O(^3P)$ atoms, respectively, and the O_3 and $O(^3P)$ atom concentrations can be estimated based on the following assumptions: Since $O(^3P)$ atoms are formed primarily from NO_2 photolysis and are consumed primarily by their rapid reaction with O_2, they can, to a very good approximation, be considered to be in photostationary state governed by these two reactions, and thus:

$$[O(^3P)] \simeq \frac{k_1[NO_2]}{k_2[O_2][M]} \qquad (III)$$

where k_1 and k_2 are the rate constants for the photolysis of NO_2 and for the third-order reaction of $O(^3P)$ atoms with O_2 respectively:

$$NO_2 + h\nu \rightarrow NO + O(^3P) \qquad (1)$$

$$O(^3P) + O_2 + M \rightarrow O_3 + M \qquad (2)$$

Similarly, O_3 is also formed by NO_2 photolysis and, under the conditions of our experiments, was consumed primarily by its rapid reaction with NO. Thus it also can be assumed to be in photostationary state, and

$$[O_3] \cong \frac{k_1[NO_2]}{k_3[NO]} \qquad \text{(IV)}$$

where k_3 is the rate constant for the reaction O_3 with NO.

$$NO + O_3 \rightarrow NO_2 + O_2 \qquad (3)$$

Equations (I) through (IV) can be combined and rearranged to yield

$$[OH] = (k_b - k_a)^{-1} \frac{d}{dt} \left(\ln \frac{[\text{n-butane}]}{[\text{propene}]}\right) - k_1 [NO_2]\left(A + \frac{B}{[NO]}\right) \qquad \text{(V)}$$

where

$$A = \frac{k_d}{(k_b - k_a)k_2[O_2][M]}$$

and

$$B = \frac{k_c}{(k_b - k_a)k_3}$$

It can be seen from equation (V) that the correction for consumption of propene by reaction with O_3 and $O(^3P)$ atoms increases with $[NO_2]$ and $[NO_2]/[NO]$, respectively.

The radical flux, R_u, required to fit the data for a given run can be estimated from the fact that the radical initiation and termination rates must balance. Since the only significant radical termination processes in this system are the reactions of OH radicals with NO and NO_2, and since HONO is in photoequilibrium after ~60 min of irradiation (Carter et al. 1982), then

$$R_u = k_4[OH]_{avg}[NO_2]_{avg} \qquad \text{(VI)}$$

where k_4 is the rate constant for the reaction of OH radicals with NO_2,

$$OH + NO_2 \xrightarrow{M} HNO_3 \qquad (4)$$

and $[OH]_{avg}$ and $[NO_2]_{avg}$ (the average OH radical and NO_2 concentrations for t >60 min) are experimentally determined. In general, in these

irradiations the OH radical levels were approximately constant after the first hour of the irradiation.

In the absence of added organics, the NO oxidation rate will reflect the extent of offgassing of reactive contaminants, since these can cause NO oxidation via the following reactions.

$$\text{wall} \rightarrow \text{organic}$$

$$\text{organic} + \text{OH} \xrightarrow{O_2} RO_2$$

$$RO_2 \xrightarrow{NO} \text{products} + \text{OH}$$
$$\downarrow NO_2$$

If no such contamination existed, then the NO oxidation rate would be small, being primarily due to reactions of the propene tracer and the CO present in the matrix air, or the inorganic NO-NO_2 interconversion reactions (Carter et al. 1982). The NO_x-air runs are thus also useful in giving a qualitative measurement of the extent of such contamination.

The results of previous tracer-NO_x-air irradiations carried out in the SAPRC ITC and OTC were discussed by Carter et al. (1982), Pitts et al. (1983), and Carter et al. (1986). For most experiments in these chambers, R_u was found to vary essentially randomly from run-to-run, with no apparent dependence on NO or NO_2 levels, but in general being proportional to light intensity. In order to factor out this proportionality, the quantity k_{RS}, which is defined as

$$k_{RS} = R_u/k_1$$

where k_1 is the NO_2 photolysis rate, is employed. Based on an analysis of the results of previous tracer-NO_x-air experiments, Carter et al. (1986) recommended that for modeling purposes k_{RS} = 0.3 ppb should be assumed for both chambers, though in for individual experiments, it can vary from less than 0.1 ppb up to 0.8 ppb or greater.

The results of the tracer-NO_x-air irradiations carried out in the indoor chamber are given in Table IV-3. Except for run ITC-859, which was carried out before the reactor was completely conditioned, the NO oxidation rates are relatively low and indicate no significant contamination of the chamber by reactive organics. The radical input rate, R_u, varied between 0.04 ppb min^{-1} and 0.14 ppb, with an average value of 0.09 ppb and no apparent dependence on when the experiment was carried out. Since actinometry experiments indicate that k_1 is essentially constant at 0.33 min^{-1} for these experiments (see Section IV-A-8, below), this corresponds to k_{RS} = 0.28 ppb, which is essentially the same as the recommended value of Carter et al. (1986), which was used in all the model simulations of the ITC experiments discussed in this report.

The results of tracer-NO_x-air irradiations carried out in the outdoor chamber are given in Table IV-4. Except for side 2 of run OTC-245, the NO oxidation rates are quite low, and even for run OTC-245B, which appears to have the highest chamber reactivity in terms of radical input rates as

Table IV-3. Conditions and Results of the Tracer-NO_x-Air Irradiations Carried Out in the Indoor Teflon Chamber

	Initial		For Second Hour of Run				
			Avg.	Avg.	Avg.	Radical	-d/dt
ITC Run No.	[NO] (ppm)	[NO_2] (ppm)	T (C)	[NO_2] (ppm)	[OH] (10^6 cm^{-3})	input rate (ppb min^{-1})	[NO] (ppb min^{-1})
859	0.40	0.13	25.8	0.13	1.46	0.12	0.36
861	0.42	0.13	30.7	0.13	0.92	0.08	0.15
863	0.42	0.14	26.1	0.14	0.68	0.06	0.06
864	0.42	0.18	26.3	0.12	0.62	0.05	0.11
866	0.40	0.11	26.9	0.11	1.25	0.09	0.09
870	0.25	0.10	25.4	0.10	1.31	0.09	0.15
875	0.29	0.13	26.2	0.12	1.71	0.14	0.05
878	0.58	0.21	26.3	0.21	0.96	0.13	0.09
882	0.52	0.18	26.5	0.18	0.80	0.09	0.09
884	0.51	0.17	26.3	0.16	1.14	0.12	-0.02
887	0.26	0.04	25.7	0.05	1.45	0.04	0.12
889	0.27	0.09	26.1	0.09	1.32	0.08	0.07
893	0.28	0.09	25.1	0.09	1.51	0.09	0.18

Table IV-4. Conditions and Results of the Tracer-NO_x-Air Irradiations Carried Out in the Outdoor Teflon Chamber

OTC Run No.	Init. NO_x (ppm)	Average[a] T (C)	UV (mw cm^{-2})	k_1[b] (min^{-1})	$[NO_2]$ (ppm)	[OH] (10^6 cm^{-3})	R_u (ppb min^{-1})	k_{RS} (ppb)	-d[NO]/dt (ppb min^{-1})
212	0.55	27.0	4.52	0.45	0.17	0.30	0.03	0.07	0.07
227A	0.46	35.1	4.18	0.38	0.13	0.74	0.06	0.16	0.07
227B	0.46	36.1	4.10	0.38	0.13	1.15	0.10	0.26	0.09
232A	0.44	32.9	4.52	0.38	0.11	0.78	0.06	0.15	0.05
232B	0.47	32.2	4.45	0.37	0.12	0.96	0.08	0.21	0.06
235A	0.56	23.2	2.37	0.16	0.15	0.39	0.04	0.24	~0.02[c]
235B	0.56	22.4	2.54	0.17	0.15	0.21	0.02	0.12	~0.04[c]
245A	0.45	34.5	3.10	0.34	0.15	0.82	0.08	0.23	0.09
245B	0.45	33.6	3.05	0.34	0.16	1.23	0.13	0.37	0.15

[a]Data for first 45-60 minutes of irradiation, and (for run OTC-235) for times after formaldehyde injected not counted in average. Exact periods used to calculate the averages determined by availability of data. For divided chamber runs, averages of temperature, UV radiation and k_1 may be slightly different for the two sides because of slightly different time periods used to calculate the averages.

[b]Average experimental k_1 values multiplied by a factor of 1.2 to correct for the fact that the quartz tube used to measure k_1 is located underneath the chamber. See Section IV-A-9.

[c]Highly approximate. Based on only two data points.

well, the NO oxidation rate is not considered excessively high. The average value of k_{RS}, the normalized chamber radical input rate, is 0.2 ppb, somewhat lower than the value of k_{RS} = 0.3 ppb recommended by Carter et al. (1986) for modeling SAPRC OTC runs. Except as noted, all model simulations of OTC runs discussed in this report employed k_{RS} = 0.2 ppb, consistent with the results of these experiments.

2. n-Butane-NO_x-Air Irradiations

n-Butane-NO_x-air runs are useful for testing models for chamber effects since model simulations of these irradiations are extremely sensitive to the magnitude of the chamber radical source used in the

calculation. Although, as discussed above, the magnitude of the chamber radical source can be derived from an analysis of the results of the tracer-NO_x-air irradiations, it is useful to have a separate check of this parameter. The conditions and results of the three n-butane-NO_x-air runs carried out in the outdoor chamber are given on Table IV-5, and concentration time plots of selected species measured in these runs are given in Figures A-1 through A-3 in Appendix A. Since only low levels of ozone were formed in these experiments, the changes in the quantity ($[O_3]$-[NO]), are tabulated instead. As discussed by Carter et al. (1986) the rate of change of this quantity can be directly related to the levels of peroxy radicals formed in these experiments.

The results of model simulations of these experiments are also given in Table IV-5, and on the concentration-time plots for these runs in Appendix A. Since the results of model simulations of n-butane runs are very sensitive to the assumed chamber radical input rates, calculations were carried out using normalized input rates, k_{RS}, of 0.1 and 0.3 ppb, as well as the default value of 0.2 ppb (derived from the results of the tracer-NO_x-air experiments). It can be seen that the runs OTC-211 and

Table IV-5. Conditions and Selected Experimental and Model Calculation Results for the n-Butane-NO_x-Air Experiments Carried Out in the Outdoor Chamber

OTC Run no.	Avg. T (C)	Avg. UV Rad ($mw\text{-}cm^{-2}$)	Init. n-Butane (ppm)	Init. NO_x (ppm)	Change in ($[O_3]$-[NO]) (ppm) Expt.	Model Calculation[a] (1)	(2)	(3)
211	27.2	4.26	10.7	0.55	0.23	0.29	0.43	0.58
246A	32.9	2.63	5.4	0.48	0.16	0.16	0.27	0.36
246B	32.9	2.63	5.4	0.48	0.25	b	b	b
252A	17.0	1.21	5.0	0.48	0.12	0.06	0.11	0.14
252B	17.0	1.21	5.0	0.47	0.16	b	b	b

[a]Radical input rate varied in model calculations. Codes for calculations: (1) k_{RS} = 0.1 ppb; (2) k_{RS} = 0.2 ppb (standard model); (3) k_{RS} = 0.3 ppb.
[b]Simulations for dual chamber runs apply to irradiations on either side.

OTC-246A are best simulated if k_{RS} = 0.1 ppb is assumed, run OTC-246B is better fit by assuming a normalized radical input value, k_{RS}, of 0.2 ppb, the results of run OTC-253A is better fit by k_{RS} being between 0.2 and 0.3 ppb, and run OTC-253B is better fit with k_{RS} of greater than 0.3 ppb. This variability is consistent with the variability in the radical input rates observed in the tracer-NO_x-air runs, as shown in Table IV-4.

The results of the divided chamber butane-NO_x-air run OTC-246 and 252 indicate a greater radical input rate on side 2 than on side 1 at the time these experiments were carried out. These results are consistent with the results of the tracer-NO_x-air OTC-245, where a higher value of R_u was also observed on side 2. However, this side inequivalency has no apparent impact on results of surrogate-NO_x-air irradiation, as indicated by the surrogate vs surrogate side equivalency test (run OTC-250) carried out between runs OTC-246 and run OTC-252, where good side equivalency was observed (see Table IV-10 in Section IV-B and Figure A-39 in Appendix A). Tracer-NO_x-air irradiations carried out prior to run OTC-245 indicated no significant differences between the sides with regard to radical input rates, with side 1 being slightly more reactive in some runs, and side 2 being slightly more reactive in others.

3. Acetaldehyde-Air Irradiations

The purpose of acetaldehyde-air irradiations is to measure the rate of offgassing of NO_x (NO or NO_2) from the chamber walls upon irradiation. When irradiated in environmental chamber systems, acetaldehyde is consumed either by direct photolysis or by reaction with OH radicals (which are always present during irradiations in environmental chambers), with the latter process giving rise to acetyl peroxy radicals.

$$CH_3CHO + OH \rightarrow CH_3\dot{C}O$$

$$CH_3\dot{C}O + O_2 \xrightarrow{M} CH_3\overset{O}{\overset{\|}{C}}-OO^{\bullet}$$

If any NO_x is present in the system, even at sub-ppb levels, the primary fate of the acetyl peroxy radicals will be reaction with NO or NO_2, with the latter process giving rise to PAN, which is relatively stable in these systems, and whose formation can be readily monitored.

$$CH_3\overset{O}{\overset{\|}{C}}\text{-}OO^{\bullet} + NO \rightarrow CH_3\overset{O}{\overset{\|}{C}}\text{-}O^{\bullet} + NO_2$$

$$CH_3\overset{O}{\overset{\|}{C}}\text{-}OO^{\bullet} + NO_2 \overset{M}{\rightleftharpoons} CH_3\overset{O}{\overset{\|}{C}}\text{-}OONO_2 \quad \text{(PAN)}$$

If measurable ozone is present in the system (as was the case for all of these irradiations except the first), then, since NO reacts rapidly with O_3 forming NO_2, $[NO_2]>>[NO]$ and thus PAN is the dominant product. Of course, PAN formation can only occur if NO_x is present in the system. Furthermore, any NO offgassed from the walls is converted to NO_2 by reaction with O_3 or acetyl peroxy radicals, with the NO_2 yielding PAN by reaction with acetyl peroxy radicals. Thus the PAN formation rate in acetaldehyde-air irradiations can be equated to the NO_x offgassing rate from the chamber walls.

One acetaldehyde-air irradiation was carried out in the indoor chamber near the end of the series of indoor chamber experiments carried out in this program. The PAN formation rate was approximately constant throughout this experiment, with a total of 14 ppb of PAN being formed after 4 hours of irradiation. This corresponds to an average NO_x input rate of 0.06 ppb min^{-1}, approximately a factor of 1.5-2 higher than observed in the acetaldehyde-air irradiations carried out in conjunction with the previous series of multi-day experiments in this chamber (Carter et al. 1985). However, a factor of two variability in this chamber effect is not unexpected, and this value can be considered to be within the normal range for this chamber.

Three acetaldehyde-air irradiations were carried out in the outdoor chamber, one near the beginning of the series of outdoor experiments, one (run OTC-218) after three surrogate irradiations and several conditioning experiments, one (OTC-234) around the middle of the series, and one (OTC-247) near the end. The results of these experiments are summarized in Table IV-6. The PAN formation rates ranged from 0.012 ppb min^{-1} to 0.026 ppb min^{-1}, which is slightly lower than the range of 0.02 to 0.06 ppb min^{-1} observed from the acetaldehyde-air irradiations carried out in conjunction with the previous outdoor multi-day experiments, with the exception of the run carried out with a new reactor, when no PAN formation

Table IV-6. Results of the Acetaldehyde-Air Irradiations Carried Out in the Outdoor Chamber

OTC Run No.	Side	Avg. T (^{o}C)	Avg. UV Rad (mw cm^{-2})	Run Time (hrs)	Final O_3 (ppb)	Final PAN (ppb)	Avg. PAN Form Rate (ppb min^{-1})
218	A	39.1	4.19	5.5	85	8	0.024
	B	38.2	4.14	5.7	88	9	0.026
234	A	34.2	4.12	5.7	56	4	0.012
	B	33.6	4.06	6.0	84	7	0.019
247	A	28.9	2.51	4.0	41	5	0.021
	B	28.0	2.65	3.5	54	8	0.038

was observed (Carter et al. 1985). Thus the results of these experiments indicate that the NO_x offgassing rates for this new series of outdoor chamber experiments is within the normal range for this chamber.

4. Ozone Conditionings and Dark Decay Determinations

In order to characterize the rates of ozone destruction on the walls of these reactors, and to condition new reactors for ozone, ozone conditioning and dark decay determinations were carried out when the Teflon bag reactor in each chamber was new. In addition, an ozone dark decay determination was carried out in the outdoor chamber at the end of the series of outdoor chamber experiments.

In the outdoor chamber, the ozone dark decay rate in the new reactor was 1.1×10^{-4} min^{-1} at daytime temperatures, and 0.3×10^{-4} min^{-1} at night, while the decay rate observed at the end of the experimental program was 0.7×10^{-4} min^{-1} for the first 12 hours. These results indicate no significant dependence of the ozone decay rate on the degree of conditioning of the Teflon reactor, and are within the normal range previously observed in this chamber (Carter et al. 1981, 1985, 1986).

In the indoor chamber, the ozone dark decay rate in the new, unconditioned reactor was 2.2×10^{-4} min^{-1}. This is slightly higher than the range of $(0.7\text{-}2.0) \times 10^{-4}$ min^{-1} observed previously in this chamber (Carter et al. 1981, 1984, 1985, 1986), but can be considered to be within the normal variability.

5. Propene-NO_x-Air Irradiations

Propene-NO_x-air irradiations were carried out in each chamber for both chamber conditioning and control purposes. For both chambers, the newly installed reactor was conditioned by irradiating 1 ppm propene-, 0.5 ppm NO_x-air mixtures. Subsequent propene-NO_x-air runs in the conditioned chamber were carried out as control experiments. Propene runs are useful in this regard because (1) a large number of such runs have been carried out in these and in other chambers, and thus they serve as a type of standard reference experiment, and (2) the chemistry of propene-NO_x-air systems is relatively well characterized, and thus model simulations of such runs can serve as tests of how well the conditions of these experiments are characterized for model testing. If the model calculations cannot successfully simulate the results of these propene runs, then it can be concluded that there is probably some problem with the characterization of the experimental conditions which should be resolved before attempting to use the more complex multi-day surrogate runs for model testing purposes.

One propene-NO_x-air irradiation (ITC-860) was carried out in the indoor chamber after the reactor had been conditioned by a previous propene-NO_x-air irradiation and a NO_x-air experiment. Concentration-time plots for the major species monitored in that run are given in Figure A-4 in Appendix A. Model simulations of this run, using the chemical mechanism and chamber characterization parameters employed by Carter et al. (1986) for this chamber, gave good predictions of the propene consumption rate and predicted 6-hour ozone levels of 0.73 ppm, approximately 25% higher than experimentally observed. This simulation assumed no dilution in this chamber, since in theory the flexible walls of the chamber should allow samples to be withdrawn without dilution occurring. However, the decay rates of n-butane, methanol, and other relatively slowly reacting reactants in the surrogate-NO_x-air experiments, discussed below, indicated that for the ITC runs using this particular reactor the chamber contents were being diluted at a rate of 2.3% $hour^{-1}$. If this is assumed, the model predicts a maximum ozone level of 0.67 ppm, in better agreement with the experimentally observed value. In general, the model tended to overpredict ozone yields in propene runs carried out in SAPRC chambers (Carter et al. 1986), so the result of this experiment can be considered

to be adequately simulated by the model. The results of these simulations are also shown in Figure A-4, where they can be compared with the experimental results.

Four propene-NO_x-air irradiations were carried out in the outdoor chamber, one (run OTC-210) when the reactor was new, and the remainder at various times throughout the series of outdoor experiments. The experimental conditions and observed and calculated maximum ozone and formaldehyde yields for these experiments are summarized on Table IV-7, and concentration-time plots of the major species monitored in these runs are shown in Figures A-5 through A-9 in Appendix A. The results of model simulations of these runs are also shown in Table IV-7 and in the figures in Appendix A. The model tended to overpredict the maximum ozone yields, by ~13% on the average, but this is consistent with the general tendency for this chemical model to overpredict ozone yields for other SAPRC chamber experiments (Carter et al. 1986). The fits of the model to the formaldehyde yields observed in the two experiments in which it was monitored are within the experimental uncertainties of the measurements. The model predictions also give good simulations of the observed propene decay rates and acetaldehyde yields. Thus, the model simulations of these outdoor chamber runs do not indicate any significant problems in the characterization of these runs for use in model testing.

Table IV-7. Conditions and Experimental and Calculated Maximum Ozone and Formaldehyde Yields in the Propene-NO_x-Air Irradiations Carried Out in the Outdoor Chamber

OTC run no.	Avg. T (C)	Avg. UV Rad ($mw\text{-}cm^{-2}$)	Initial Propene (ppm)	Conc. NO_x (ppm)	Maximum O_3 (ppm) Expt.	Maximum O_3 (ppm) Calc.	Maximum HCHO (ppm) Expt.	Maximum HCHO (ppm) Calc.
210	31.8	3.88	1.03	0.57	0.97	0.97	a	0.47
233	28.4	3.65	~1.0[b]	0.46	0.63	0.91	a	0.45
236	26.3	3.80	1.20	0.53	0.85	0.97	0.46	0.54
244	30.0	2.93	1.03	0.43	0.78	0.85	0.59	0.47
251	18.4	1.60	0.90	0.46	0.47	0.46	a	0.42

[a]No data.
[b]Initial concentration data not available. Value given is an estimate.

6. Other Control Experiments

Additional control experiments carried out in this experimental program included one formaldehyde-NO_x-air and one tracer-NO_x-air run with added formaldehyde carried out in the outdoor chamber, and two tracer-NO_x-air runs with added methanol carried out in the indoor chamber. These experiments were carried out to provide data to test the sub-models for the reactions of formaldehyde and methanol independently of the other surrogate components.

Two tracer-NO_x-air irradiations, with approximately 0.5-1 ppm of formaldehyde added after 2 hours of irradiation were carried out in this program, one (ITC-864) in the indoor chamber and the other (OTC-235) in the outdoor chamber. The latter run was a divided chamber run with approximately equal amounts of formaldehyde added on each side. The results of these runs are summarized in the chronological summaries given in Tables IV-1 and IV-2, and concentration-time plots of the major species monitored in these runs are given in Figures A-10 and A-11 of Appendix A for the ITC and the OTC run, respectively. As expected, in both cases the addition of formaldehyde caused a significant increase in the NO oxidation rates and the OH radical levels as determined by Equation (V) in Section IV-A-1 above. The results of the model simulations of these experiments are also shown in Figures A-10 and A-11, where it can be seen that the results of the model simulations are reasonably consistent with the experimental results. Some of the discrepancy between experimental and calculated data can be attributed to uncertainties in the exact amount of formaldehyde which was injected, since for both runs some of the formaldehyde had reacted before the first post-formaldehyde injection formaldehyde samples were taken.

An additional formaldehyde-NO_x-air outdoor chamber run (OTC-216) was carried out to test the formaldehyde injection and analysis technique. As a result of this run and subsequent tests it was determined that there was a problem with the formaldehyde analysis technique, which was subsequently corrected. Because of the lack of valid formaldehyde data, the results of this run are probably of limited utility.

Two tracer-NO_x-air runs were carried out in the indoor chamber with approximately 25-35 ppm of methanol being added after two hours of irradiation. The results of these experiments (runs ITC-863 and ITC-887)

are summarized in the chronological listing of the indoor chamber runs in Table IV-1 and are plotted in Figures A-12 and A-13 in Appendix A. In both cases, as expected, the addition of methanol caused a significant increase in the rate of conversion of NO to NO_2, and the formation of 0.19 ppm of formaldehyde was observed in run ITC-887. (Formaldehyde was not monitored in run ITC-863.) However, model simulations of these runs predicted significantly greater rates of NO to NO_2 conversion and formaldehyde formation than observed experimentally. For example, in run ITC-887, the average NO consumption rate for the first hour after the addition of methanol was calculated from the model to be 3.9 ppb min^{-1}, compared to the experimentally observed rate of 1.7 ppb min^{-1}, and the formaldehyde yield was calculated to be 0.52 ppm, compared to the measured value of 0.19 ppm. This discrepancy is surprising since there are not considered to be any significant uncertainties in our understanding of the atmospheric photooxidation mechanism of methanol (see Atkinson 1986 for a discussion the relevant kinetic and mechanistic data). In addition, as discussed in Section IV-B-3, the model performs reasonably well in simulating the effects of methanol substitution in the surrogate experiments. This discrepancy may be due to characterization problems associated with runs with such high levels of methanol (25-35 ppm, compared with approximately 1 ppm or less in the methanol substitution surrogate experiments), but it clearly represents an uncertainty which has not been resolved, and which requires further investigation.

7. Side Equivalency Tests

An important characteristic of the SAPRC outdoor Teflon chamber is that it can be operated in a dual mode with two different mixtures being irradiated at the same time under the same light intensity and temperature conditions. In order to ensure that the results of irradiations of a given mixture do not depend on the chamber side in which the mixture was irradiated, three side equivalency tests, involving the photolysis of the same surrogate-NO_x-air mixture at the same time in each half of the chamber, were carried out during the series of outdoor chamber experiments. One experiment employed (run OTC-214) the "methanol + formaldehyde" substitution surrogate and was carried out after the reactor was newly conditioned, one (OTC-226) employed the "base case" surrogate and was carried out around the middle of the series of the outdoor runs,

and the last (OTC-250) also employed the "methanol + formaldehyde" substitution surrogate and was the last surrogate experiment carried out in this series.

The results of the side equivalency tests are summarized in Section IV-B-2 in conjunction with the results of the other surrogate runs. In all cases good side equivalency was observed, with maximum day 1 ozone yields agreeing within 10%, 7% and 1% for runs OTC-214, 226, and 250, respectively, and with maximum day 2 ozone agreeing within 1% for run OTC-214 and within 5% for run OTC-250.

8. Characterization of the Light Source in the Indoor Chamber

The light intensity in the indoor chamber experiments was measured by carrying out NO_2 actinometry experiments at various times throughout the series of indoor runs. The results of these experiments are summarized in Table IV-8. It can be seen that there is no significant change in the light intensity in the indoor chamber during the course of these experiments, within the small variation which reflects primarily the precision of the experimental technique employed. The average of the NO_2 photolysis rate observed in these experiments is 0.327 ± 0.009, consistent with overall average of all NO_2 actinometry experiments from ITC-718 through ITC-894 of 0.326 ± 0.013. This overall average NO_2 photolysis rate is assumed in the model simulations of all indoor chamber experiments carried out in this program.

Table IV-8. Results of NO_2 Actinometry Experiments Carried Out in the Indoor Teflon Chamber[a]

ITC Run No.	k_1 (min^{-1})
865	0.317
869	0.336
876	0.327
883	0.327
890	0.316
894	0.337

[a]All runs carried out with light intensity at 70% maximum.

In order to calculate the rates of photolysis reactions when carrying out model simulations of the indoor chamber experiments, it is necessary to know the spectral distribution of the light source as well as the absolute light intensity. Although no measurements of the spectral distribution of the blacklights used in the ITC were carried out during the course of this program, they have been measured on several occasions previously, and were found not to vary significantly with time. The results of a previous measurement of the spectral distribution of the lights for this chamber, which is recommended for use in modeling ITC experiments, is given elsewhere (Carter et al. 1984, 1985, 1986).

9. Light Source Characterization for the Outdoor Chamber Experiments

The light intensity of the outdoor chamber experiments was measured continuously during the periods when the chamber was uncovered using three different techniques. UV radiation intensity and total solar (broadband) radiation intensity were measured using Eppley radiometers, and the NO_2 photolysis rate, k_1, was measured using a quartz tube actinometer. The experimental aspects of these techniques were discussed in Section III-C-4. The results of these measurements are included in the data sets for these experiments, and the averages of the UV radiometer readings obtained during the irradiations are given in the summaries of the conditions and results of the outdoor chamber experiments.

A detailed discussion of how these data are used to derive photolysis rates used in model simulations of outdoor chamber experiments is given by Carter et al. (1986). The method described by Carter et al. (1986) involves use only of the UV radiometer data, and use of these data were preferred over use of the k_1 and the TSR data because (a) most of the outdoor chamber runs modeled by Carter et al. (1986) did not have k_1 data; (b) the UV data tend to be more precise, and more responsive to rapid variations of light intensity, than are the k_1 measurements; and (c) TSR readings respond primarily to the light intensity at wavelengths longer than those which influence most photolysis reactions, and thus their use in deriving photolysis rate constants was considered by Carter et al. (1986) to be less appropriate than UV radiometer readings. The TSR data were obtained in this program to provide further characterization of the light intensity in these experiments, and to allow alternative methods of

analyzing the light intensity data, which may require TSR data, to be employed (e.g., see Jeffries et al. 1982).

Since most of the outdoor chamber experiments carried out in this program have measurements of both UV and k_1 carried out at the same time, the k_1 data can be used to check the technique of Carter et al. (1986) for calculating photolysis rates from the results of the UV measurements. A distribution plot of the ratio of the calculated to the experimentally observed NO_2 photolysis rates is given on Figure IV-1, and a plot of these ratios against the cosine of the solar zenith angle (cos[z]) is shown on Figure IV-2. These figures also show data obtained during outdoor chamber experiments carried out in 1983 under EPA funding, since the same techniques to monitor both UV and k_1 were employed (Carter et al. 1985). It can be seen that the calculated k_1 values are consistently higher than the experimental measurements, with the distribution of most of the calculated/experimental k_1 ratios being centered around a ratio of 1.44, though the distribution is not symmetrical and there are many cases where significantly higher ratios are observed. Figure IV-2 also suggests that the ratio of the calculated to the experimental k_1 values tends to increase, and become more scattered, with increasing zenith angle.

Much of the discrepancy between the experimental k_1 values and the values calculated from the UV data can be attributed to the fact that the NO_2 actinometer is located under the Teflon bag reactor, and thus the sunlight has to pass through the chamber before reaching the actinometer. This is expected to result in some attenuation of the sunlight relative to that reaching the UV radiometer, which is located on a roof nearby. Carter et al. (1985) indicated that the light passing through the chamber to the NO_2 actinometer was suppressed by a factor of 1.2, but the present re-analysis of the data, employing the more sophisticated technique for calculating k_1 from UV radiometer data derived subsequently (Carter et al. 1986), indicates that a suppression factor of 1.44 (or greater) is more appropriate.

Since the light has to pass through two surfaces of the Teflon chamber (the top and the bottom) before reaching the NO_2 actinometer, the suppression factor of 1.44 at the actinometer corresponds to a factor of 1.2 in passing through each wall of the chamber. This suggests that the photolysis rates inside the chamber should be a factor of 1.2 lower than

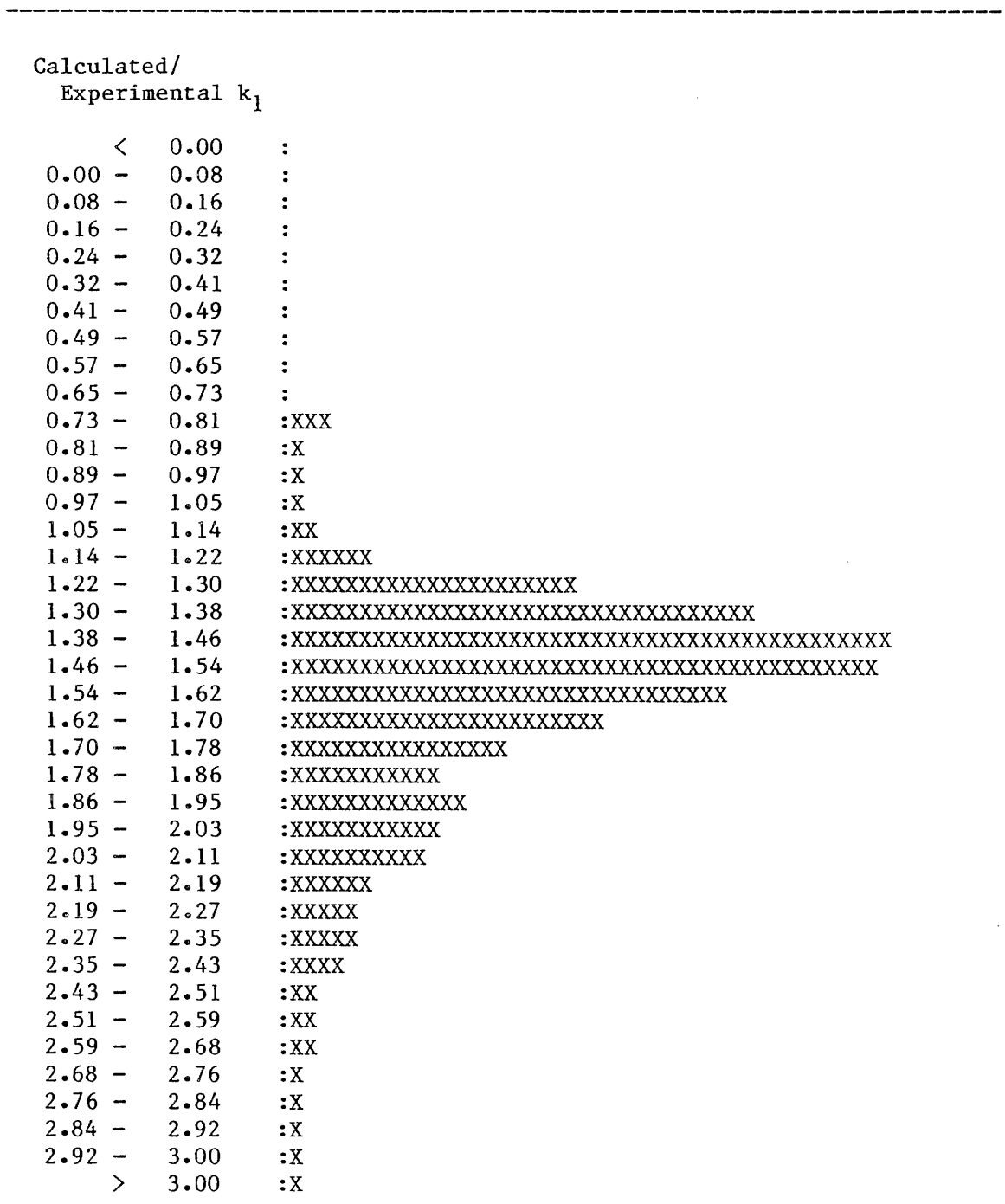

Figure IV-1. Distribution plot for the ratio of the k_1 values calculated from the UV radiometer data, relative to the experimentally measured values for the OTC surrogate-NO_x-air irradiations carried out in 1983 and in 1985.

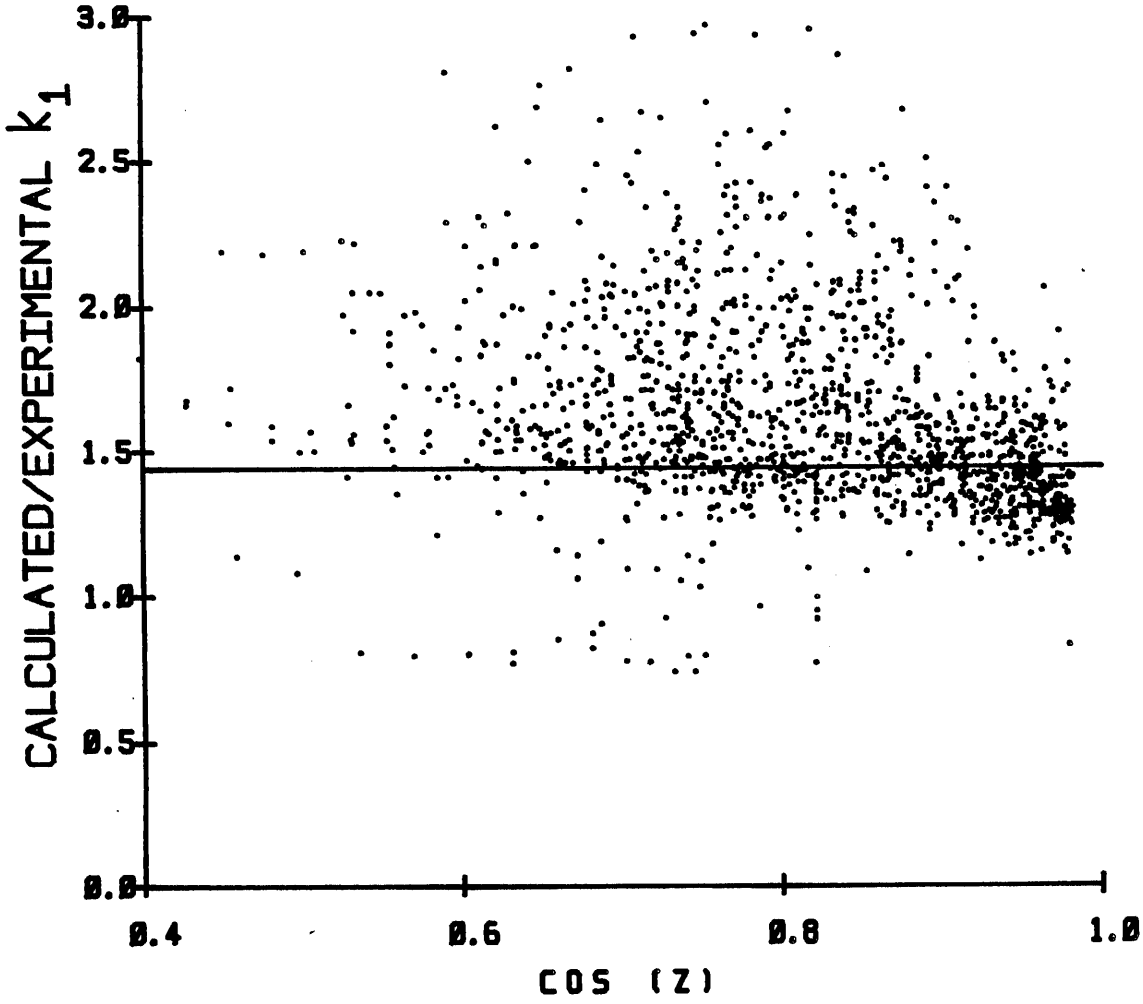

Figure IV-2. Plots of ratios of the calculated to experimental k_1 values against the consine of the solar zenith angle, where the k_1 values were derived from the UV radiometer data as described by Carter et al. (1986), and the data were obtained from the OTC surrogate-NO_x-air irradiations carried out in this program and by Carter et al. (1985) in the Spring and Summer of 1983.

those outside the chamber, calculated based on the UV radiometer data. Thus in all the model simulations of the outdoor chamber experiments discussed in this report, the photolysis rates were reduced by a factor of 1.2 relative to those calculated from the UV radiometer data to be appropriate for the open atmosphere.

The the apparent dependence of the ratios of the calculated to experimental k_1 values on the solar zenith angle, and the cases where the ratios are significantly higher than the distribution centered around 1.44, are more difficult to explain. There are a number of uncertainties involved in the theoretical calculations of the photolysis rates, and these results could reflect these uncertainties. The fact that the light has to pass through the chamber before reaching the NO_2 actinometer may introduce additional zenith angle dependencies which the present analysis does not take into account. Some of the cases where the ratios of calculated to experimental k_1 values were high may have been due to shadows falling on the actinometry tube; this is known to be a problem in the 1983 runs, but is expected to be less of a problem in the runs carried out for this program because of the redesign of the chamber cover framework (see Sections III-B-1 and III-C-4). Thus it is not clear to what extent these effects reflect artifacts in the NO_2 actinometry system employed. However, in view of the fact that model simulations of the OTC propene runs and other control experiments using photolysis rates calculated from the UV data as described by Carter et al. (1986), reduced by a factor of 1.2, gave satisfactory fits to the data in most cases, no attempt was made to further refine our methods for calculating photolysis rates. However, it is clear that further investigations into the most appropriate method to calculate photolysis rates in these outdoor chamber experiments, perhaps taking into account the TSR data as well as the UV and the k_1 measurements, would be useful.

B. Surrogate-NO_x-Air Runs

The main body of experiments carried out in this program were the 35 surrogate-NO_x-air irradiations carried out to elucidate the effects of methanol substitution on single- and multi-day urban air pollution, and to provide data which can be used for chemical mechanism testing. Twenty-one of these experiments consisted of simultaneous irradiations of two

surrogate-NO_x-air mixtures carried out in the divided outdoor chamber, leading to a total of 56 surrogate-NO_x-air mixtures irradiated in this program. Of these, the results of 32 such irradiations are to be useful for model testing, and model simulations of these experiments have been carried out.

As discussed in Section I of this report, both the indoor and outdoor chamber surrogate-NO_x-air runs were carried out at three different hydrocarbon-to-NO_x ratios, with four different "surrogates" to serve as idealized representations of the following emissions scenarios: (1) The "Base Case" surrogate (designated "B" in the summary tables) consisted of an 8-hydrocarbon mixture of representative alkanes, alkenes (including isobutene to represent formaldehyde, which it rapidly forms in NO_x-air irradiations), and aromatics designed by the modelers at SAI (Whitten, private communication) to represent current emissions into the CSCAB. (2) The "Methanol + Formaldehyde" substitution surrogate (designated "MF"), consisted of the base case surrogate with nominally 33% of it replaced by a 90% methanol + 10% formaldehyde mixture, to represent the replacement of 33% of current reactive organic (ROG) emissions with emissions from methanol-fueled vehicles which have relatively high exhaust formaldehyde levels. (3) The "Methanol" substitution surrogate was similar to the "MF" surrogate, except that in this case 33% (nominally) of the base case surrogate was replaced by methanol alone, to represent the replacement of 33% of current emissions with emissions from methanol-fueled vehicles which have negligible exhaust formaldehyde levels. (4) The "Blank" substitution surrogate (designated "BL") consisted of the base case surrogate reduced by 33%, and can be taken to represent reducing total ROG emissions as opposed to substituting the emissions with those from methanol-fueled vehicles. (The "BL" surrogate can also be thought of as representing a scenario where 33% of the ROG emissions are replaced by emissions of compounds which are totally unreactive in the atmosphere.) The substitutions in the "MF" and the "M" surrogates were such that the total level of organics, on a ppmC basis, were the same as in the base case, i.e., the idealized substitution scenarios examined involve no net change in the total amount of ROG emitted. In addition, the idealized scenarios employed in the design of these experiments are based on the assumption that total NO_x emissions will not change, though it should be

pointed out that since experiments were carried out at different ROG/NO_x levels, they can be used to test models which can be used to examine the effects of changing NO_x emissions.

In this section, the results of the multi-day surrogate-NO_x-air irradiations carried out in the indoor chamber are discussed, together with a discussion of the results of the outdoor chamber experiments. Finally, the results of the model simulations of those experiments used for model testing (which constitute all but a few of these runs) are presented and briefly discussed.

1. Indoor Chamber Experiments

A total of 14 multi-day surrogate-NO_x-air irradiations were carried out in the SAPRC indoor Teflon chamber (ITC), one with each of the four surrogates at average ROG/NO_x ratios (excluding "blank" substitution runs) of 15 ± 2, 5.8 ± 0.2, and 3.03 ± 0.01, and two replicate runs at the two highest ROG/NO_x ratios. (The ROG/NO_x ratio of the "blank" substitution experiments were, by design, approximately 33% lower than those in the corresponding "B", "MF", or "M" experiments, but for the purpose of this discussion are treated as they have the same ROG levels as the corresponding runs with which their results are being compared.) The matrix of initial ROG and NO_x levels employed in these experiments is shown in Figure IV-3. It can be seen that the experiments at the two highest ROG/NO_x ratios were carried out at approximately the same NO_x levels, and those at the two lowest ratios were carried out at the same nominal ROG levels. Thus this matrix allows the effects of varying total NO_x or total ROG independently. All of these 14 experiments are considered to be sufficiently well characterized for use in model testing.

The experimental conditions and selected results of these multi-day surrogate-NO_x-air runs are summarized in Table IV-9, and concentration-time plots for the major species monitored in these experiments, together with the results of the model simulations, are given in Appendix A (Figures A-14 through A-27, in the same order in which the runs are listed in Table IV-9. The results of these experiments give information concerning the effects of substitution on the formation of the major secondary pollutants ozone, PAN, and formaldehyde, and these are discussed below.

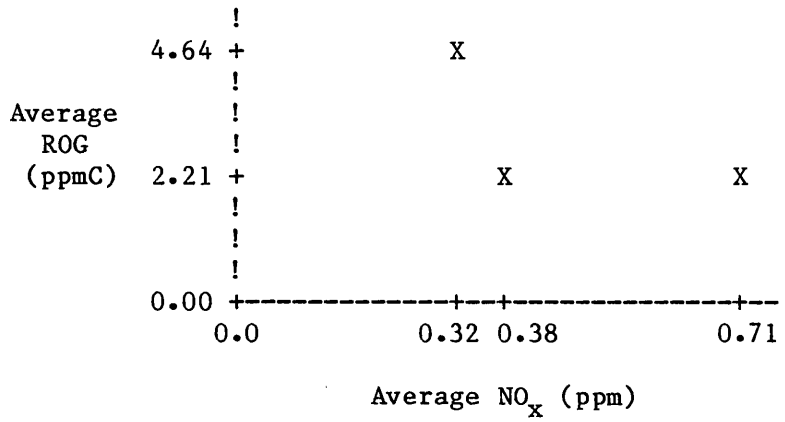

Figure IV-3. Matrix of multi-day surrogate-NO_x-air experiments carried out in the indoor Teflon chamber, showing the average initial NO_x and ROG levels for each group of runs.

Ozone. Concentration-time plots for ozone for all the runs carried out at the same nominal ROG/NO_x ratio are plotted together in Figures IV-4 through IV-6 for the runs at the 15:1, 6:1, and 3:1 ROG/NO_x ratios, respectively. It can be seen that the reactivities with regard to ozone formation in the base case experiments were significantly different at the three ROG/NO_x ratios employed in this study. At the highest ratio, ozone formation occurred on the first day only, and the levels of ozone observed on day 2 reflected only the amounts which were not consumed on the previous night, with no increase in their concentrations being observed. Reasonably good replication of the ozone results of the two base case experiments carried out at the 15:1 ROG/NO_x ratio was observed. At the 6:1 ROG/NO_x ratio, approximately 40% less ozone was formed on the first day of the irradiation than for the 15:1 ROG/NO_x runs. However, on the second day, significant formation of ozone was observed, with the amount of ozone formed on day 2 almost making up for the ozone consumed on the previous night. This resulted in the day 2 levels of ozone in the 6:1 base experiment being almost as high as those in the in the 15:1 runs. At the 3:1 ratio, essentially no ozone was formed on day 1, more was formed on day 2 (though much less than observed in the base case experiments carried out at the higher ratios), and the most was observed on day 3, with the day 3 ozone yield in the 3:1 base case experiment being

Table IV-9. Conditions and Selected Results of the Multi-Day Surrogate-NO_x-Air Irradiations Carried Out in the Indoor Teflon Chamber

ITC Run No.	Run Type[a]	Init. NO_x (ppm)	Init. ROG (ppmC)	Surg. Sub.[b] (% C)	HCHO in MeOH (%)	Maximum Ozone (ppm) Day1	Day2	Day3	Maximum HCHO (ppm) Day1	Day2	Day3	Maximum PAN (ppb) Day1	Day2	Day3
865	15-B	0.28	4.83	-	-	0.63	0.37	-	0.21	0.12	-	>83[c]	36	-
891	15-B	0.32	4.36	-	-	0.60	0.34	-	0.07	0.05	-	134	36	-
867	15-MF	0.28	4.85	39	8	0.63	0.36	-	0.22	0.10	-	>54[c]	23	-
888	15-M	0.33	4.53	36	-	0.58	0.35	-	0.15	0.11	-	97	46	-
868	15-BL	0.38	2.85	39	-	0.52	0.29	-	0.11	0.05	-	>34[c]	19	-
871	6-B	0.38	2.14	-	-	0.38	0.31	-	0.05	0.06	-	>10[c]	22	-
872	6-MF	0.38	2.27	40	10	0.21	0.23[d]	-	0.11	0.09	-	>5[c]	12	-
877	6-MF	0.38	2.28	39	10	0.25	0.29	-	0.11	0.07	-	24	26	-
874	6-M	0.38	2.15	35	-	0.19	0.28	-	0.08	0.08	-	>2[e]	10	-
873	6-BL	0.39	1.40	37	-	0.16	0.26	-	0.03	0.03	-	>2[c]	11	-
880	3-B	0.73	2.20	-	-	0.03	0.15	0.31	0.01[f]	0.01[f]	0.01[f]	2	15	25
881	3-MF	0.73	2.22	36	10	0.01	0.08	0.31	0.09	0.09	0.07	0	4	24
886	3-M	0.73	2.21	36	-	0.01	0.07	0.29	0.07	0.07	0.04	0	5	19
885	3-BL	0.64	1.47	33	-	0.01	0.04	0.13	0.01[f]	0.02[f]	0.01[f]	0	1	8

[a]Notation for run type: Number designates the nominal ROG/NO_x ratio, the symbols "B", "MF", "M", and "BL" refer to the base case, methanol + formaldehyde substitution, methanol substitution, and blank substitution surrogates, respectively.

[b]This column gives the percent of the initial ROG which consists of methanol + formaldehyde (for "MF" surrogates, methanol (for "M" surrogates), or (for "BL" surrogates), the amount the initial ROG has been reduced relative to the averages for the other surrogate runs at the same nominal ROG/NO_x ratio.

[c]Automated chromatograph not employed, so PAN data are available only for the first 6 hours (approximately) of each 12 hour period when the are on. Day 1 PAN maximum probably not attained.

[d]Run ended prematurely, before day 2 ozone maximum reached.

[e]Automated PAN analysis system employed, but PAN data available only for first 6 hours of day 1 because of instrument malfunction. Day 2 PAN data complete.

[f]Formaldehyde measurements judged to be unreliable for this run. Data appear to be highly scattered and are probably anomalously low.

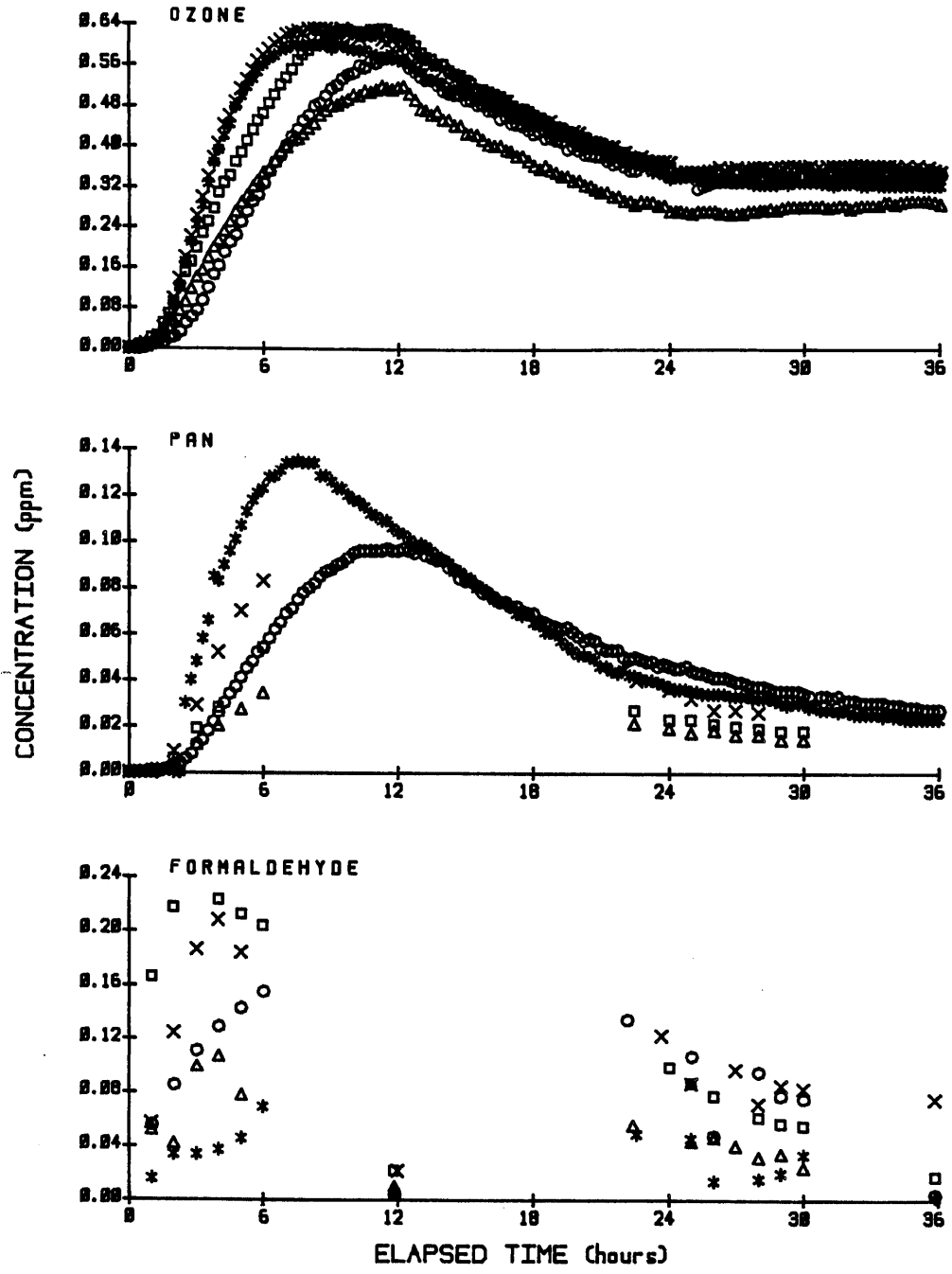

Figure IV-4. Plots of ozone, PAN, and formaldehyde data for all indoor chamber runs with nominal ROG/NO_x ratios of 15:1.

x = ITC-865 (base case)
* = ITC-891 (base case)
□ = ITC-867 (MF substitution)
o = ITC-888 (methanol substitution)
Δ = ITC-868 (blank substitution)

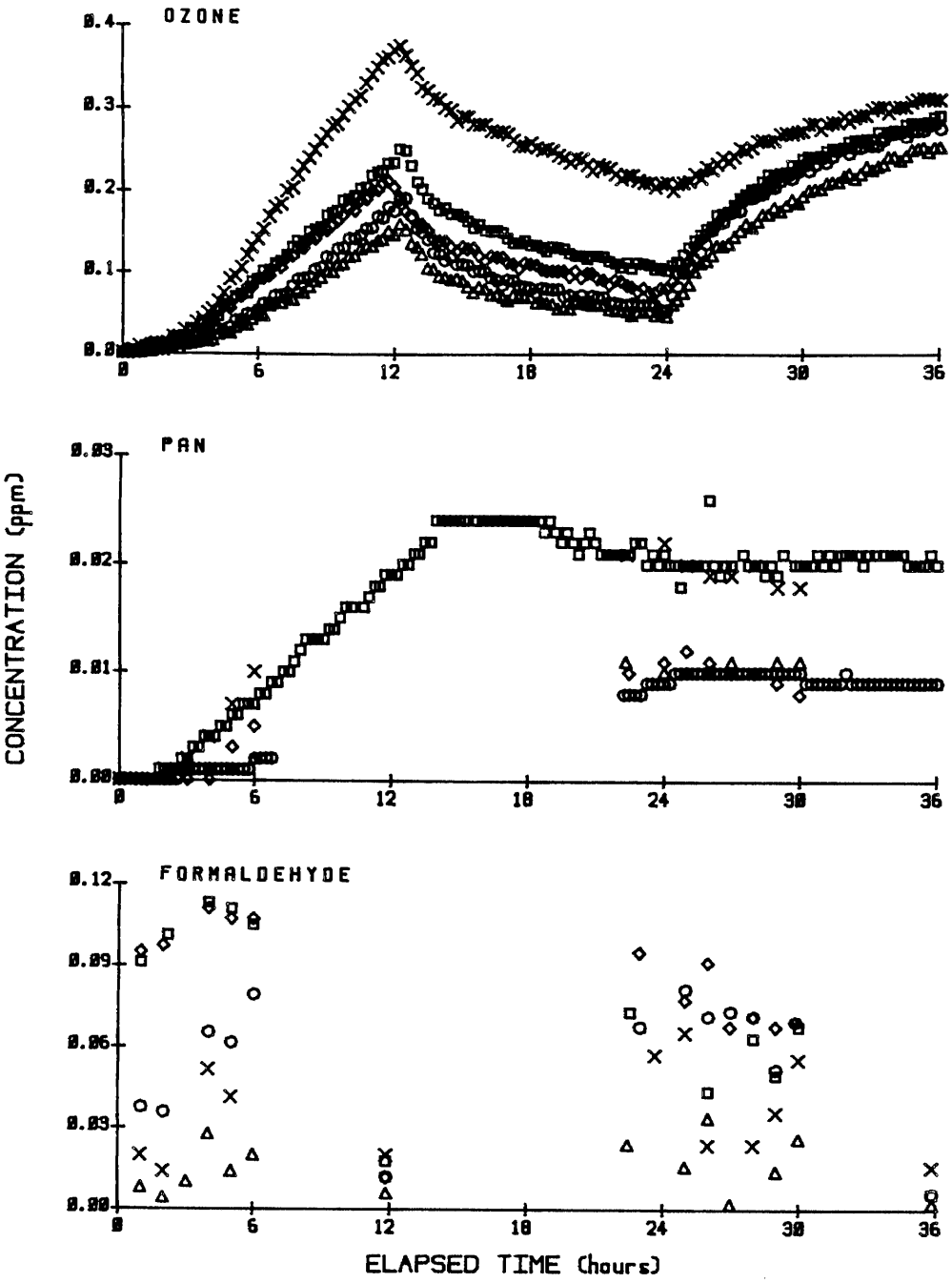

Figure IV-5. Plots of ozone, PAN, and formaldehyde data for all indoor chamber runs with nominal ROG/NO_x ratios of 6:1.

x = ITC-871 (base case)
□ = ITC-877 (MF substitution)
◇ = ITC-872 (MF substitution)
o = ITC-874 (methanol substitution)
Δ = ITC-873 (blank substitution)

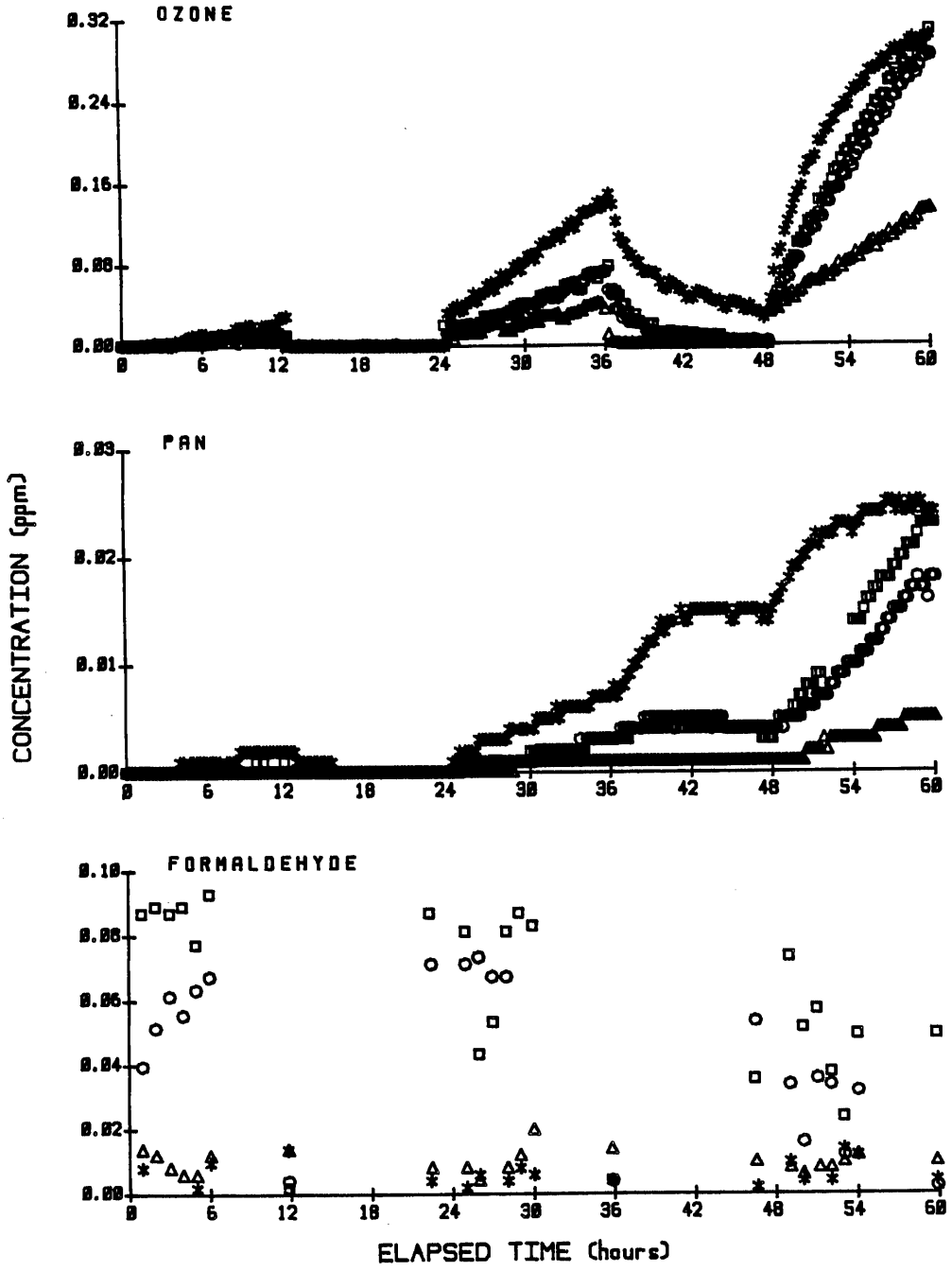

Figure IV-6. Plots of ozone, PAN, and formaldehyde data for all indoor chamber runs with nominal ROG/NO_x ratios of 3:1.

* = ITC-880 (base case)
□ = ITC-881 (MF substitution)
o = ITC-886 (methanol substitution)
Δ = ITC-885 (blank substitution)

essentially the same as the day 2 yield observed in the 6:1 base case experiment.

It can also be seen from Figures IV-4 through IV-6 that the results of these experiments indicate that substitution by methanol + formaldehyde or by methanol alone reduces the initial rate of ozone formation at all ROG/NO_x ratios, though not as much as did blank substitution. As expected, the inclusion of 10% formaldehyde in the methanol substitution mixture significantly increases the ozone formation rate, though not enough to make the mixture more reactive than the base case mixture. In terms of multi-day effects on ozone formation, the results of the substitution experiments were similar to the results of the base case experiments discussed above, with no significant increases in ozone occurring on day 2 for the 15:1 ROG/NO_x runs, but with significant ozone formation occurring on day 2 of the 6:1 runs, and on days 2 and 3 of the 3:1 runs. However, the relative rates of ozone formation on day 2 of the 6:1 ROG/NO_x ratio runs for the different surrogate mixtures was the opposite of that observed on day 1 of those runs, with the day 2 ozone formation rate being the fastest for the blank substitution runs and slowest for the base case runs (though the differences in ozone formation rates were not sufficient to reverse the ordering of the maximum ozone yields). This apparent reversal of reactivity between day 1 and day 2 was observed previously in base case surrogate-NO_x-air (Carter et al. 1985) and fuel-NO_x-air (Carter et al. 1981) irradiations and is affected primarily by the amount of NO_x which has been consumed by reaction with O_3 in the dark between day 1 and day 2, and thus the amount of NO_x remaining on day 2 to allow ozone formation to continue, as opposed to the initial reactivity of the organic mixture employed (Carter et al. 1981, 1985).

Although methanol and "MF" substitution was found to affect the ozone formation rate at all ROG/NO_x ratios in these experiments, the magnitude of the effect on the daily maximum ozone yields depended significantly on the ROG/NO_x ratio. The effect on the maximum ozone yield was the least in the experiments carried out at the highest ROG/NO_x ratio, for which ratio only the blank substitution caused a significant decrease in the daily maximum ozone levels. This can be attributed to fact that the "true" ozone maximum was attained (or almost attained) by the end of day 1 at all of the 15:1 ROG/NO_x ratio runs, and hence the final ozone level was less

strongly affected by the rate at which ozone is formed than if significant ozone formation were still occurring when the lights were turned off.

The greatest effects of methanol or methanol + formaldehyde substitution on the maximum ozone yields were observed in the experiments carried out at the 6:1 ROG/NO_x ratio. Replacing 35-40% of the base case surrogate with the 90% methanol, 10% formaldehyde mixture caused a decrease of 23-43% in the day 1 ozone yield, and replacing the same amount of the surrogate with 100% methanol caused a 49% decrease. However, as indicated above, the day 2 ozone formation rate tended to increase with decreasing reactivity observed on day 1, resulting in the day 2 ozone levels in the surrogate substitution experiments being essentially the same as those in the base case experiments. On the other hand, blank substitution resulted in lower ozone levels on both day 1 and day 2, though the relative amount of ozone reduction caused by decreasing ROG levels was less on day 2 than on day 1, due to the relatively rapid rate of ozone formation on the second day in the blank substitution experiment.

In all of the 3:1 ROG/NO_x surrogate experiments, most of the ozone formation occurred on the third and last day of the irradiations. At this ROG/NO_x ratio, substituting 36% of the base case surrogate with 90% methanol + 10% formaldehyde resulted in almost twice as much ozone being formed on the second day (though the levels in both cases were low), but with essentially the same levels of ozone being formed on the third day. Substitution by methanol alone resulted in lower ozone on both days (though the reduction on day 3 amounted to only 10%). As at the other ROG/NO_x ratios, the greatest reduction in ozone was observed in the blank substitution experiment, with the day 3 ozone being approximately three times less than observed in the base case and in the methanol and "MF" substitution experiments.

PAN. Concentration-time plots for PAN for all the runs carried out at the same nominal ROG/NO_x ratio are plotted together in Figures IV-4 through IV-6 for the runs at the 15:1, 6:1, and 3:1 ROG/NO_x ratios, respectively. As can be seen from the figures and the footnotes to Table IV-9, PAN data are missing for significant periods of time for runs prior to ITC-877, and as a result the maximum day 1 PAN levels are not known for those runs. In addition, PAN was measured by a different instrument for the runs prior to run ITC-874 than employed for run ITC-874 and subsequent

experiments, and the PAN data from the replicate 15:1 base case runs and from the replicate 6:1 "MF" substitution runs, suggest a possible systematic inconsistency between these two instruments. Thus only for runs carried out after ITC-874 are useful PAN data available for assessing the effects of substitution on PAN levels.

Despite these problems, the resulting data indicate that methanol substitution is probably beneficial in terms of reducing PAN yields. At the 15:1 ROG/NO_x ratio, complete PAN data are available for both the base case run and for the methanol + formaldehyde substitution experiment, and (Figure IV-4) the maximum PAN level is approximately 28% less in the "MF" substitution run, a significantly larger difference than the difference in ozone yields in those two runs. At the 6:1 ROG/NO_x ratio (Figure IV-5), complete PAN data are available only for one of the "MF" substitution runs, but the incomplete day 1 PAN data for the other runs indicate lower initial PAN formation rates for the substitution experiments than observed in the base case run. Complete PAN data are available for all the experiments carried out at the 3:1 ROG/NO_x ratio, and the PAN levels in the methanol only and the methanol + formaldehyde substitution runs are significantly lower than those in the base case experiments (especially son on day 2), though they are significantly higher than observed in the blank substitution run. As was the case for ozone, the PAN levels of the methanol substitution experiments at the 3:1 ratio approached those of the base case by the end of the last day of the experiment, but remained significantly higher than those in the blank substitution experiment.

Formaldehyde. Concentration-time plots for formaldehyde for all the runs carried out at the same nominal ROG/NO_x ratio are plotted together in Figures IV-4 through IV-6 for the runs at the 15:1, 6:1, and 3:1 ROG/NO_x ratios, respectively. As indicated in Section III-C-2, the formaldehyde monitoring technique employed in these experiments generally did not yield precise data for formaldehyde levels less than ~100 ppb, and was subject to periods of spuriously low values. For these reasons, care must be employed in using these data for the purpose of assessing the effects of substitution on formaldehyde levels. As indicated in the footnotes to Table IV-8, and from the plots in Figure IV-6, the formaldehyde data for runs ITC-880 and ITC-885 are highly scattered and do not indicate any time dependence, and are unreliable. In addition, as shown in Figure IV-4, the

formaldehyde yields were not well duplicated in the two replicate 15:1 ROG/NO_x base case surrogate experiments (runs ITC-865 and ITC-891), despite fair replication of reaction conditions and good replication of ozone yields. In view of the fact that the chromatropic acid formaldehyde measurement technique as currently employed at SAPRC has a greater tendency to yield anomalously low values as opposed to anomalously high values, together with the fact that it is unreasonable to expect less formaldehyde to be formed in the 15:1 blank substitution run than in the 15:1 base case experiments, it is probable that the low values observed in run ITC-891 are anomalous.

However, the formaldehyde yields in the other pair of replicate runs, the 6:1 ROG/NO_x "MF" surrogate runs OTC-872 and OTC-877, are well replicated despite the fact that the yield is lower than in the "15-B" run ITC-865. In addition, as indicated below, the formaldehyde yields observed in most of the ITC experiments, other than those with obvious problems in the formaldehyde data, are not grossly inconsistent with model predictions. Thus the results of these indoor chamber runs may be useful for at least qualitative assessments of the effects of substitution on formaldehyde yields.

In general, the formaldehyde data obtained in these experiments indicate that the highest formaldehyde levels occurred in the methanol + formaldehyde substitution experiments, as expected since formaldehyde was injected directly into the chamber as a component of the surrogate mixture. However, the differences in the formaldehyde levels in the "MF" experiments compared to the corresponding base case and methanol-only runs at the 15:1 ROG/NO_x ratio, or to the methanol-only substitution runs at the 6:1 and the 3:1 ROG/NO_x ratios, tended to decrease with time on day 1, with the day 2 formaldehyde levels being essentially the same, to within the experimental uncertainty. The scatter and uncertainties in the experimental data do not allow the relative formaldehyde forming potentials of the base surrogate and the methanol-only substitution surrogate to be assessed.

2. Outdoor Chamber Experiments

A total of 24 outdoor chamber experiments were carried out involving surrogate-NO_x-air irradiations, 21 of which were multi-day NO_x-air irradiations of two different surrogate mixtures in the divided

chamber. Nineteen of these latter experiments were carried out for two or more days, and three of these were side equivalency tests involving side equivalency tests of the same surrogate-NO_x-air mixture on the same side of the chamber. Thus, a total of 45 different surrogate-NO_x-air mixtures were irradiated in the outdoor chamber for this program. These experiments consisted of NO_x-air irradiations of the same base case (B), methanol + formaldehyde substitution (MF), methanol-only substitution (MF), and blank substitution (BL) surrogates as employed in the indoor chamber runs, with the dual chamber runs (other than the side equivalency tests) consisting of simultaneous irradiations of two different surrogates at the same initial NO_x levels and nominal ROG/NO_x ratios. Different sets of initial NO_x and ROG levels were employed in the outdoor experiments than in the indoor runs, and the matrix of initial NO_x and ROG levels employed in these runs is shown in Figure IV-7, together with the numbers of different mixtures which were irradiated at each set of initial concentrations. These sets of concentrations correspond to average ROG/NO_x ratios of 13.2 ± 0.8, 9.7 ± 1.1, 6.7 ± 0.7, and 5.5 ± 0.6. Note that the nominal initial concentrations in the "blank substitution" experiments at the 10:1 and the 7:1 ROG/ NO_x ratios are the same as the those for the base case at the 7:1 and 6:1 ratios, respectively, and these experiments were counted as base case runs in determining the number of runs in the different sets of NO_x and ROG levels shown in Figure IV-7.

The initial concentrations, daily averages of the temperature and UV readings, and maximum ozone, PAN, and formaldehyde yields observed in these experiments are summarized in Table IV-10, where the runs are ordered according to the nominal ROG/NO_x ratio employed and the combination of surrogates irradiated. Concentration-time plots of the data from these runs are given in Appendix A (Figures A-28 through A-51), in the same order that the runs are listed in Table IV-10.

A number of replicate irradiations of many of the surrogate-NO_x-air mixtures, particularly at the 10:1 and the 7:1 ROG/NO_x ratios, were carried out to obtain data from irradiations of different pairs of surrogate mixtures under comparable reaction conditions. In addition, the 10:1 ROG/NO_x blank substitution mixture had the same nominal total ROG and NO_x levels as did the 7:1 base case mixture, and similarly for the 7:1 blank substitution and the 5:1 base case mixtures. Since these experiments

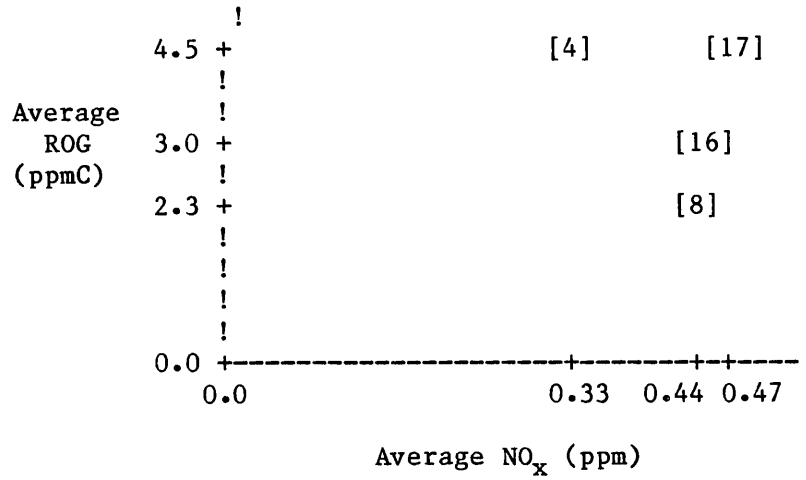

Figure IV-7. Matrix of multi-day surrogate-NO_x-air experiments carried out in the outdoor Teflon chamber, showing the average initial NO_x and ROG levels, and the number of surrogate-NO_x-air mixtures irradiated at each set of initial ROG and NO_x levels.

were carried out over a seven-month period from the beginning of spring to almost the beginning of winter, the replicate irradiations of these and several other mixtures were conducted under a variety of temperature and light intensity conditions. This resulted in a significant variability in the results of these irradiations.

Examples of the variability of the ozone, PAN, and formaldehyde yields observed in the repeated irradiations of similar mixtures, and their dependences on temperature and light intensity, are shown on Figures IV-8 through IV-13. Figures IV-8 and IV-9 show plots of the day 1 and day 2 ozone, PAN and formaldehyde maxima against the average temperature and average light intensity, respectively, for the 10:1 ROG/NO_x base case runs; Figures IV-10 and IV-11 show analogous data for the 10:1 ROG/NO_x methanol + formaldehyde substitution runs; and Figures IV-12 and IV-13 show the data for the 10:1 ROG/NO_x blank substitution/7:1 ROG/NO_x base case runs. It can be seen that in some cases better correlations with temperature are obtained, and in others the data correlate better with light intensity. In general the dependencies on temperature and light intensity are similar, as expected since temperature and light intensity are correlated with each other. These figures show that while in most

Table IV-10. Conditions and Selected Results of the Surrogate-NO_x-Air Runs Carried Out in the Outdoor Teflon Chamber

OTC Run No.	Run Type[b]	Avg. T[a] (°C) Day1	Day2+	Avg. UV Rad[a] (mw cm^{-2}) Day1	Day2+	Init. NO_x (ppm)	Init. NMRC (ppmC)	Surg Sub.[c] (% C)	HCHO in MeOH (%)	Maximum Ozone (ppm) Day1	Day2+	Maximum HCHO (ppm) Day1	Day2+	Maximum PAN (ppb) Day1	Day2+
241A	13-B	32.2	40.0	2.82	2.96	0.32	4.23	–	–	0.67	0.48	0.22	0.21	64	13
241B	13-MF	32.2	40.0	2.82	2.96	0.32	3.86	25	13	0.67	0.47	0.23	0.19	47	11
224A	13-M	38.8	42.4	3.49	3.78	0.33	4.61	35	0	0.78	0.49	0.27	0.19	46	3
224B	13-B	38.8	42.4	3.49	3.78	0.34	4.55	–	–	0.81	0.53	0.23	0.14	62	3
215A	10-B	30.9	37.4	4.02	3.88	0.45	4.80	–	–	0.83	0.49	d	d	125	17
215B	10-MF	30.9	37.4	4.02	3.88	0.44	5.61	32	d	0.87	0.55	d	d	123	10
249A	10-B	30.0	22.7	1.79	1.68	0.48	4.83	–	–	0.35	0.23	0.24	0.21	65	83
249B	10-MF	30.0	22.7	1.79	1.68	0.46	4.90	37	7	0.33	0.25	0.27	0.23	45	62
243A	10-B	21.9	24.6	1.87	2.63	0.47	4.27	–	–	0.14	0.53	0.15	0.18	21	50
243B	10-MF	21.9	24.6	1.87	2.63	0.47	3.77	22	11	0.15	0.49	0.18	0.18	21	37
217A	10-M	36.7	41.6	4.00	4.00	0.50	4.80	40	0	0.48	0.37	d	d	68	–
217B	10-B	36.7	e	4.00	e	0.51	5.00	–	–	0.83	–	d	–	121	–
237A	10-B	37.3	40.3	3.63	3.40	0.52	4.72	–	–	0.81	0.50	0.22	0.19	64	10
237B	10-M	37.3	40.3	3.63	3.40	0.52	4.84	21	–	0.76	0.44	0.26	0.26	46	10
222A	10-M	45.4	47.4	4.93	4.37	0.44	3.76	27	0	0.91	0.58	0.26	0.20	30	2
222B	10-MF	45.4	47.4	4.93	4.37	0.43	3.81	28	14	0.94	0.62	0.25	0.20	31	2
223A	10-B	42.6	40.3	3.29	3.08	0.41	4.43	–	–	0.95	0.62	0.26[f]	0.14	54	3
223B	10-BL	42.6	40.3	3.29	3.08	0.42	3.17	28	–	0.77	0.44	0.20	0.10	33	4
238A	10-BL	31.2	31.7	3.64	3.56	0.51	3.28	22	–	0.41	0.39	0.14	d	47	27
238B	10-MF	31.2	31.7	3.64	3.56	0.50	4.23	–	–	0.70	0.43	0.23	d	53	17

(continued)

Table IV-10 (continued) - 2

OTC Run No.	Run Type[b]	Avg. T[a] (°C) Day1	Day2+	Avg. UV Rad[a] (mw cm^{-2}) Day1	Day2+	Init. NO_x (ppm)	Init. NMRC (ppmC)	Surg Sub.[c] (% C)	HCHO in MeOH (%)	Maximum Ozone (ppm) Day1	Day2+	Maximum HCHO (ppm) Day1	Day2+	Maximum PAN (ppb) Day1	Day2+
214AB	10-MF	38.8	34.7	3.71	3.96	0.45	4.20	-	-	0.35	0.40	d	d	37	42
250A	10-MF	20.8	19.2	1.68	1.50	0.46	4.85	30	10	0.24	0.20	0.28	0.26	34	39
250B	10-MF	20.8	19.2	1.68	1.50	0.46	4.85	30	10	0.24	0.21	0.23	0.21	31	40
221A	7-MF	26.4	44.6	3.38	3.96	0.41	2.81	30	5	0.24	0.39	0.15	0.15	36	25
221B	7-B	26.4	44.6	3.38	3.96	0.42	2.83	-	-	0.33	0.38	0.16	0.13	50	26
248A	7-B	26.0	33.0	1.76	2.13	0.48	3.18	-	-	0.06	0.41	0.13	0.17	12	51
248B	7-MF	26.0	33.0	1.76	2.13	0.46	2.90	24	12	0.08	0.43	0.17	0.17	13	50
242A	7-M	42.3	30.3	3.04	1.88	0.45	2.62	21	-	0.18	0.35	0.12	0.14	20	26
242B	7-B	42.3	30.3	3.04	1.88	0.45	3.51	-	-	0.64	0.34	0.13	0.13	38	18
219A	7-MF	32.9	32.3	4.35	d	0.39	2.46	33	11	0.48	0.28	0.16	0.13	d	14
219B	7-M	32.9	32.3	4.35	d	0.39	2.57	36	0	0.33	0.31	0.13	0.14	d	24
239A	7-MF	37.0	41.1	2.95	3.08	0.49	3.01	20	17	0.34	0.42	0.17	0.13	17	17
239B	7-M	37.0	41.1	2.95	3.08	0.50	3.02	20	-	0.23	0.47	0.13	0.13	17	26
230A	7-B	38.6	41.3	4.17	4.03	0.41	3.44	-	-	0.49	0.31	0.13	0.11	38	4
230B	7-BL	38.6	41.3	4.17	4.03	0.41	2.56	26	-	0.27	0.32	0.08	0.08	24	14
229A	7-M	34.6	36.7	3.93	4.05	0.46	3.20	23	0	0.25	0.54	0.11	0.11	27	19
229B	7-BL	34.6	36.7	3.93	4.05	0.46	2.45	23	0	0.17	0.57	0.06	0.06	23	19
226A	7-B	39.0	e	3.98	e	0.46	2.85	-	-	0.69	-	0.01	-	40	-
226B	7-B	39.0	e	3.98	e	0.46	2.85	-	-	0.74	-	0.02	-	34	-
228A	5-B	36.9	35.8	4.06	4.22	0.41	2.30	-	-	0.25	0.44	0.06	0.02[f]	34	25
228B	5-MF	36.9	35.8	4.06	4.22	0.41	2.39	27	13	0.30	0.40	0.12	0.09[f]	25	17

(continued)

Table IV-10 (concluded) - 3

OTC Run No.	Run Type[b]	Avg. T[a] (°C) Day1	Day2+	Avg. UV Rad[a] (mw cm^{-2}) Day1	Day2+	Init. NO_x (ppm)	Init. NMRC (ppmC)	Surg Sub.[c] (% C)	HCHO in MeOH (%)	Maximum Ozone (ppm) Day1	Day2+	Maximum HCHO (ppm) Day1	Day2+	Maximum PAN (ppb) Day1	Day2+
225A	5-B	30.2	e	1.89	e	0.43	2.12	-	-	0.01	-	0.07	-	1	-
225B	5-MF	30.2	e	1.89	e	0.44	d	d	d	0.01	-	0.08	-	1	-
240A	5-M	37.2	26.9	3.15	1.89	0.50	2.09	24	-	0.03	0.11	0.07	0.09	1	12
			27.8		2.44						0.34		0.09		20
240B	5-B	37.2	26.9	3.15	1.89	0.50	2.23	-	-	0.22	0.33	0.08	0.07	29	33
			27.8		2.44						0.29		0.06		25
231A	5-X[g]	37.1	37.2	3.69	3.81	0.48	d	d	-	0.12	0.45	0.10	0.11	5[h]	19
231B	5-MF	37.1	37.2	3.69	3.81	0.47	d	d	d	0.10	0.39	0.09	0.09	8[h]	13

[a] Averages calculated using measurements made when the chamber was uncovered only.

[b] Run type designation gives nominal hydrocarbon/NO_x ratio, followed by code for surrogate. Surrogate codes used: "B" = base case surrogate; "MF" = methanol + formaldehyde substitution surrogate; "M" = methanol-only substitution surrogate; "BL" = blank substitution surrogate. Note that the nominal hydrocarbon/NO_x ratio is the hydrocarbon/NO_x ratio for the corresponding base case surrogate, not the actual ratio for the blank substitution experiment, which is nominally 33% lower.

[c] Percent surrogate substituted = 100 x (initial methanol + formaldehyde)/(initial total surrogate) for "MF" or "M" substitution runs; = percent surrogate reduced relative to surrogate on other side of chamber for blank ("BL") substitution runs.

[d] Data rejected or no data.

[e] Run aborted on or before day 2.

[f] Anomalously high data point not used to determine maximum.

[g] Does not correspond to any of the standard surrogate mixtures, due to an error in the reactant injections. Consists of the base case surrogate with methanol added.

[h] No nighttime PAN data. PAN maxima occur at night under some conditions.

cases the day 1 ozone yield increases with increasing temperature or light intensity, this was not necessarily the case for the day 2 ozone yields. The PAN yields appear to correlate better with light intensity than with temperature, but in either case the correlations do not appear to be as good for PAN as they are with ozone. This can be attributed to the fact that PAN undergoes decomposition at a rate which increases with temperature (Atkinson and Lloyd 1984), resulting in decreased PAN yields at higher temperatures if other factors were held constant. This is consistent with the observation that for each of these three groups of runs the run carried out at the highest average temperature did not give the highest PAN yields.

In contrast with the results for ozone and PAN, the data shown in Figures IV-8 through IV-13 do not indicate any significant dependence of the formaldehyde yields on either the temperature or the light intensity. No indication of dependencies on either temperature or light intensity was observed for any of the other groups of outdoor chamber runs carried out in this program. Indeed, except for the low formaldehyde data from run OTC-226, shown in Figures IV-12 and IV-13, the results of the irradiations of the similar mixtures give replication of the formaldehyde yields which are within the precision of the analytical technique employed (±30% at these concentrations, as indicated in Section III-C-2), despite the wide variation of temperature and light intensity conditions in these experiments. Thus, if there is any dependence of formaldehyde yields on temperature and light intensity, it is less than the precision of these data.

However, it is clear that the results of these experiments in terms of ozone and PAN yields are significantly dependent on experimental conditions such as temperature and light intensity, and in order to determine the effects of substitution on these aspects of air quality it is necessary to compare results of experiments which were carried out at the same time. This was taken into account in the design of this experimental program, where essentially all of the surrogate-NO_x-air irradiations carried out in the outdoor chamber consisted of simultaneous irradiations of two different surrogates (e.g., base case vs "MF" substitution, "M" substitution vs "MF" substitution, etc.) in the two sides of the chamber. Although it was not possible to carry out

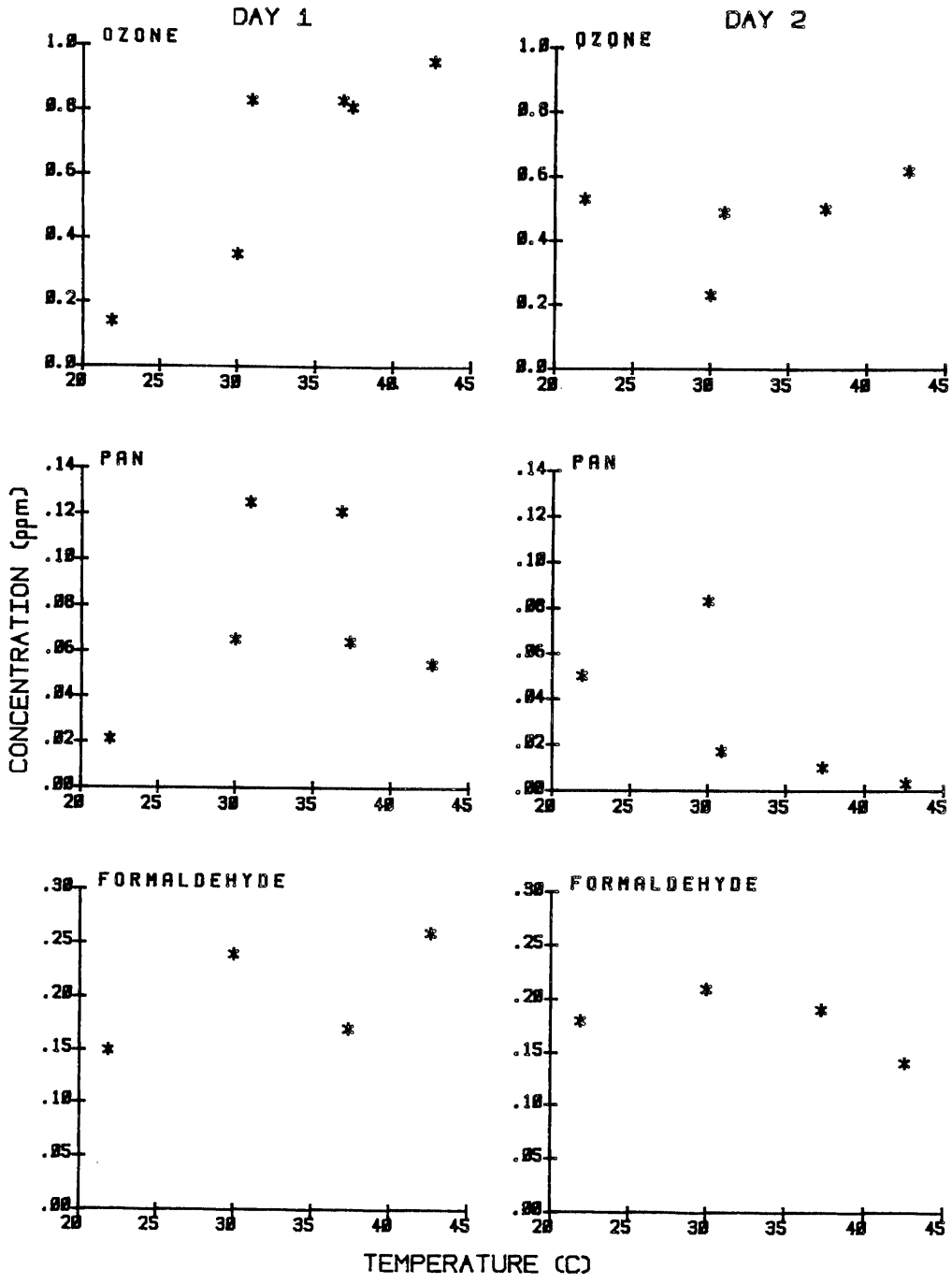

Figure IV-8. Plots of day 1 and day 2 ozone, PAN, and formaldehyde yields against average temperature for the base case, surrogate-NO_x-air irradiations carried out at the 10:1 nominal ROG/NO_x ratio in the outdoor chamber.

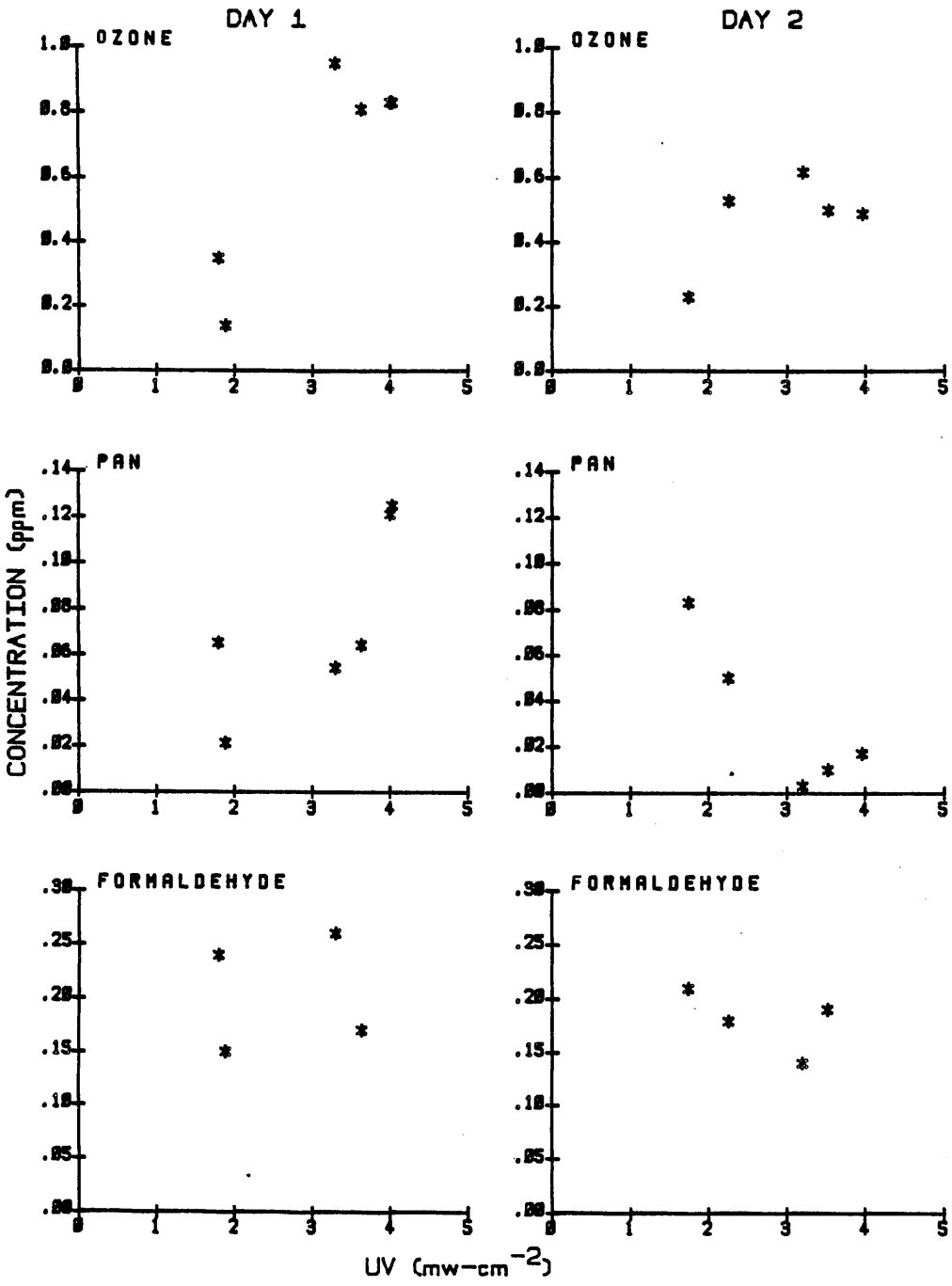

Figure IV-9. Plots of day 1 and day 2 ozone, PAN, and formaldehyde yields against average UV radiation intensity for the base case surrogate-NO_x-air irradiations carried out at the 10:1 nominal ROG/NO_x ratio in the outdoor chamber.

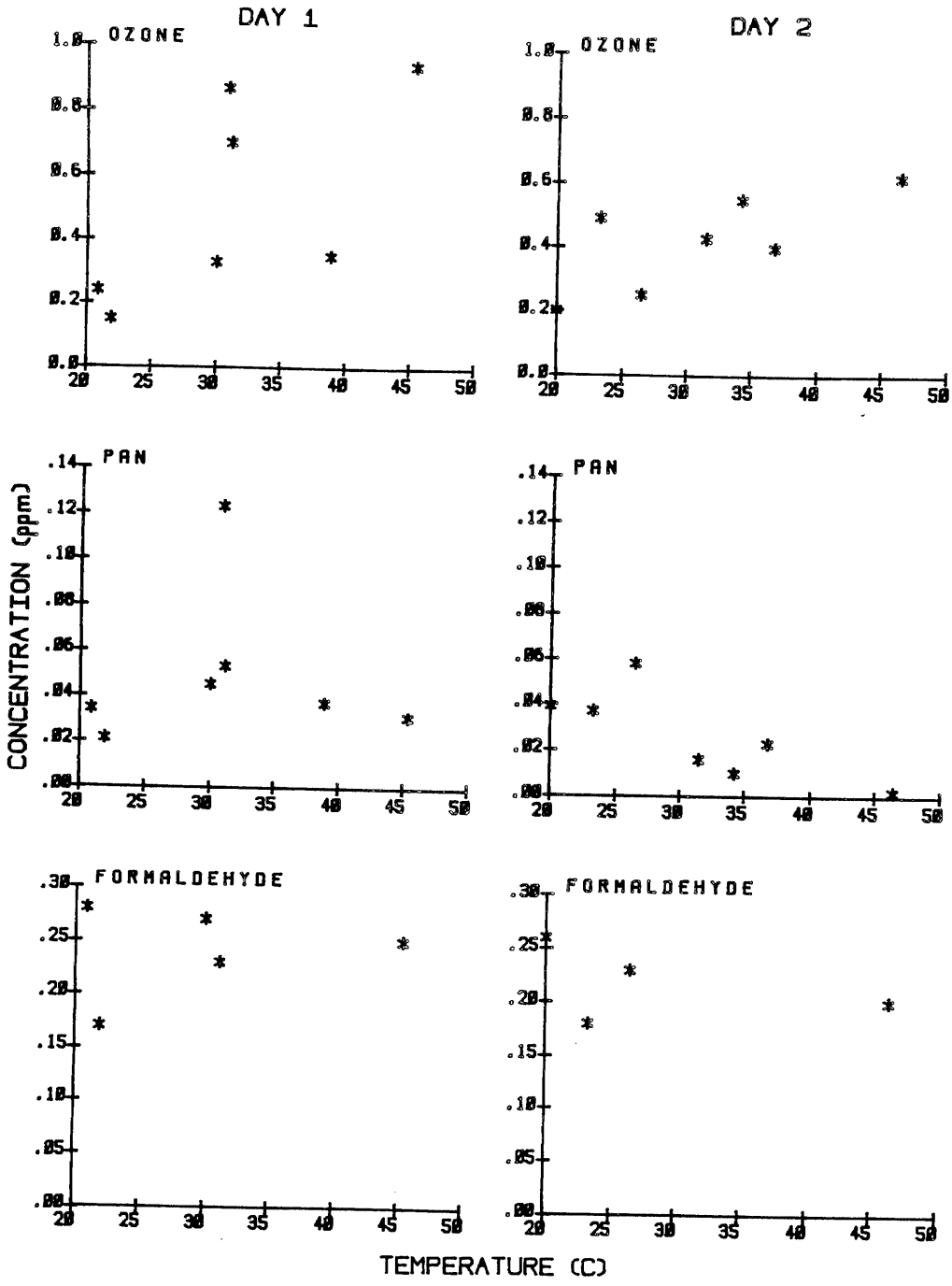

Figure IV-10. Plots of day 1 and day 2 ozone, PAN, and formaldehyde yields against average temperature for the methanol + formaldehyde substitution surrogate-NO_x-air irradiations carried out at the 10:1 nominal ROG/NO_x ratio in the outdoor chamber.

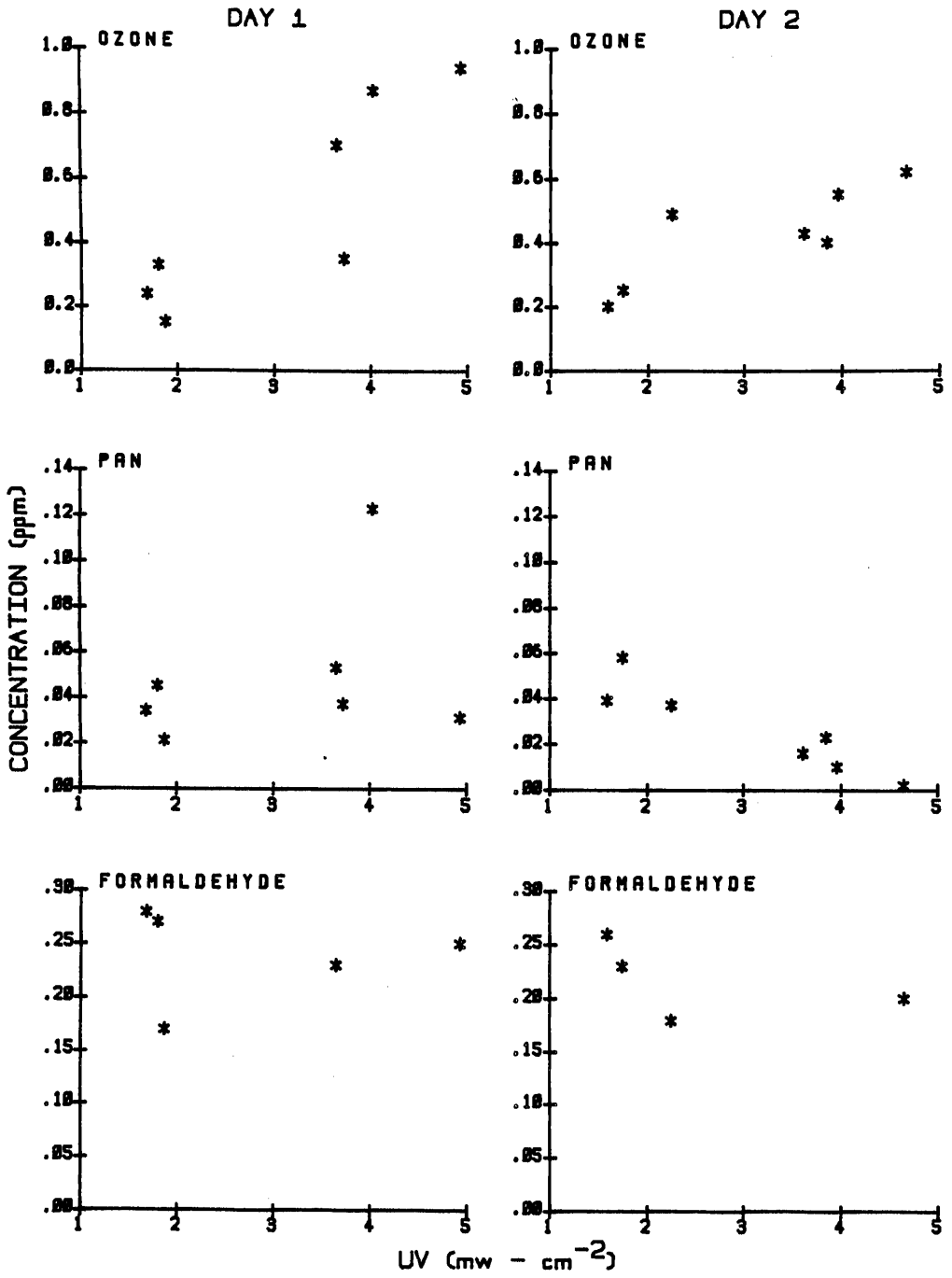

Figure IV-11. Plots of day 1 and day 2 ozone, PAN, and formaldehyde yields against average UV radiation intensity for the methanol + formaldehyde substitution surrogate-NO_x-air irradiations carried out at the 10:1 nominal ROG/NO_x ratio in the outdoor chamber.

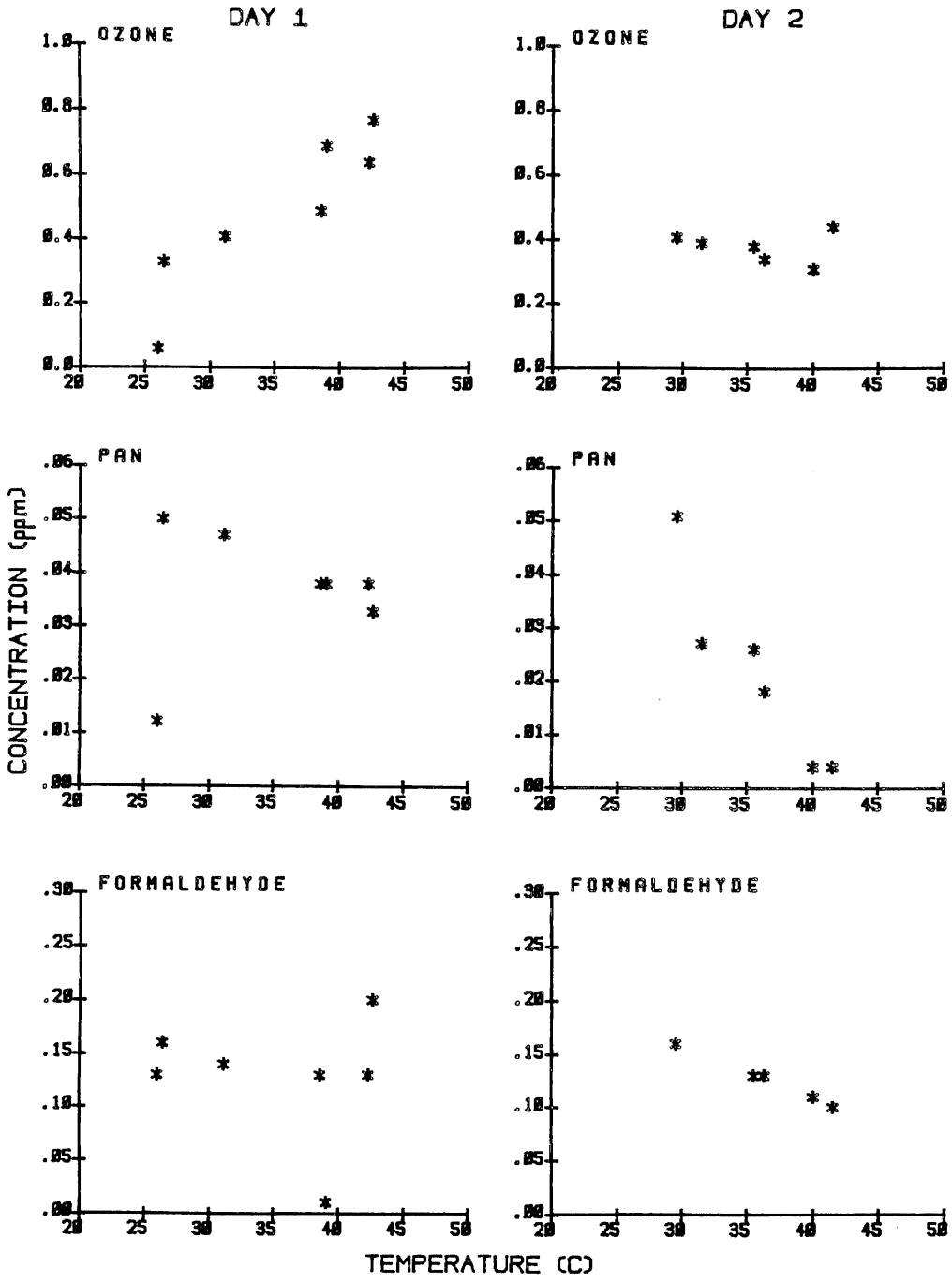

Figure IV-12. Plots of day 1 and day 2 ozone, PAN, and formaldehyde yields against average temperature for the blank substitution surrogate-NO_x-air irradiations carried out at the 10:1 nominal ROG/NO_x ratio, and for the base case surrogate-NO_x-air irradiations carried out 7:1 nominal ROG/NO_x ratio in the outdoor chamber.

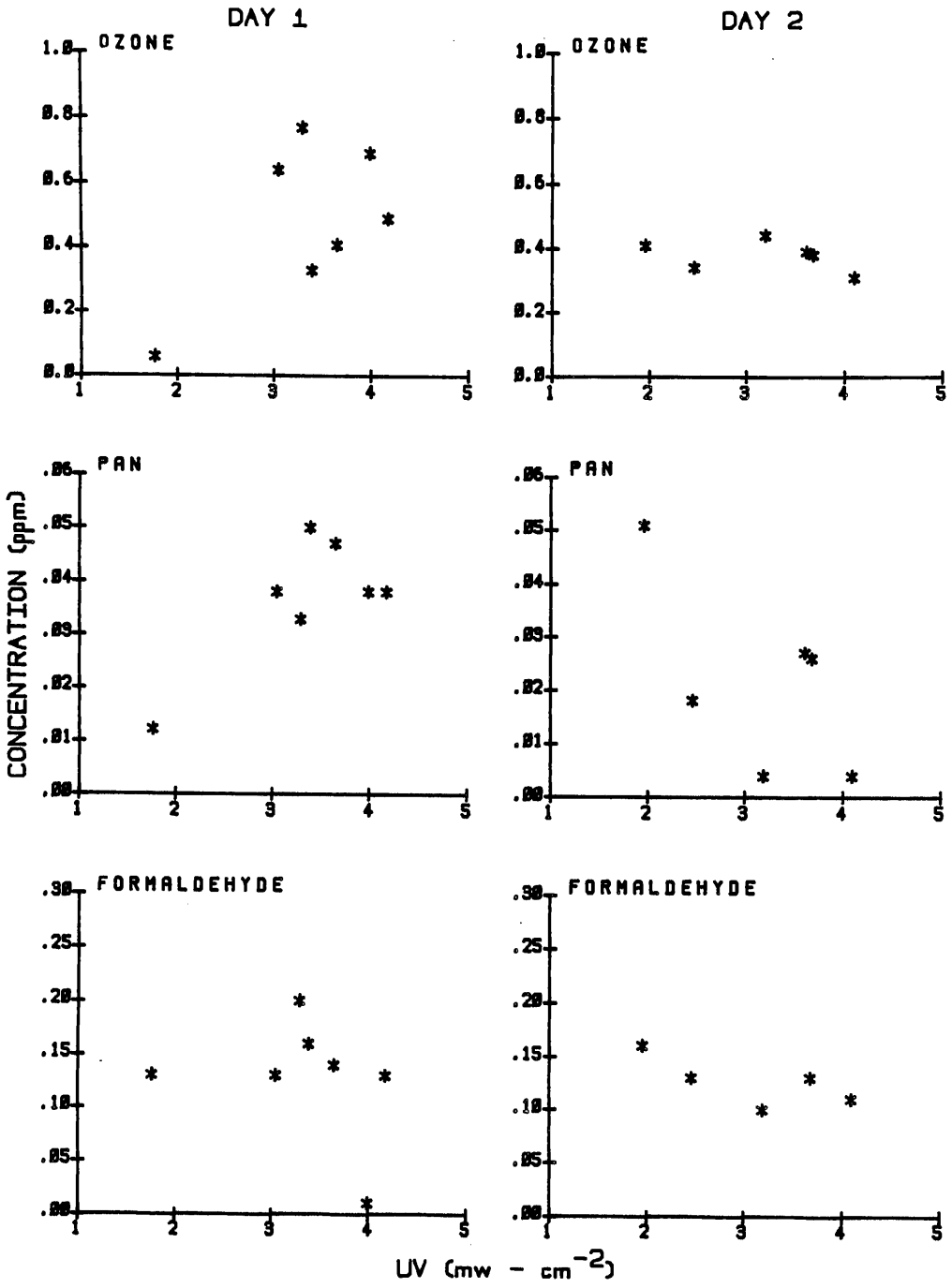

Figure IV-13. Plots of day 1 and day 2 ozone, PAN, and formaldehyde yields against average UV radiation intensity for the blank substitution surrogate-NO_x-air irradiations carried out at the 10:1 nominal ROG/NO_x ratio, and for the base case surrogate-NO_x-air irradiations carried out 7:1 nominal ROG/NO_x ratio in the outdoor chamber.

experiments examining all possible combinations of pairs of surrogates at all four of the ROG/NO_x ratios, all but one of the combinations were examined at the 10:1 and the 7:1 ratios (the exceptions being "M" vs "blank" at the 10:1 ratio, and "MF" vs "blank" at the 7:1 ratio), and the base case was compared with both "MF" and "M" substitution at the 13:1 and the 5:1 ratios. This provides a sufficient data base to allow the relative reactivities of the base case and the various substitution surrogates, and their dependencies on the ROG/NO_x ratios, and (in many cases) on temperature and lighting conditions to be assessed. These relative reactivities are discussed below in terms of the effects of substitution on ozone, PAN, and formaldehyde levels.

Ozone. Figure IV-14 shows the differences in the day 1 and the day 2 ozone yields for each of the different pairs of surrogate mixtures which were simultaneously irradiated. It can be seen that the results of these experiments are consistent with the results of the indoor chamber runs in that methanol-only or blank substitution tended to reduce day 1 ozone yields in irradiations carried out under similar temperature and lighting conditions, but had a smaller effect on the day 2 yields. These data also show, in agreement with the indoor chamber experiments, that blank substitution had a greater effect on reducing ozone than did methanol substitution, and that substitution by methanol alone was more effective in reducing ozone than substitution by the 90% methanol + 10% formaldehyde mixture. The effects of substitution on ozone yields in these experiments tended to be the least at the highest ROG/NO_x ratios, and greatest at the 6 to 7:1 ROG/NO_x ratio. This finding is consistent with the results of the indoor chamber runs, where the effect of substitution (other than blank substitution) on ozone was essentially insignificant at the 13:1 ROG/NO_x ratio, and greatest at the 6:1 ROG/NO_x ratio.

However, the results of the outdoor chamber experiments tend to differ with those for the indoor chamber runs in that in the outdoor runs there does not appear to be any consistent difference in the ozone forming potential between the base case and the methanol + formaldehyde substitution surrogates. In particular, in the indoor chamber runs the "MF" surrogate produced less ozone than did the base case surrogate (at both the 6:1 and the 3:1 ROG/NO_x ratios), while in the outdoor chamber experiments the differences in ozone yields were minor, and showed no consistent

ROG/NO_x Ratio	OTC Run no.	Side	Maximum Ozone (ppm) Day 1		Day 2		Day 3
			Base Case vs MF Substitution				
13:1	241	B	xxxxxxx		xxxxx		
		MF	xxxxxxx	-0%	xxxxx	-2%	
10:1	215	B	xxxxxxxx		xxxxx		
		MF	xxxxxxxxx	+5%	xxxxxx	+12%	
	249	B	xxxx		xx		
		MF	xxx	-6%	xxx	+52%	
	243	B	x		xxxxx		
		MF	x	+7%	xxxxx	-8%	
7:1	221	B	xxx		xxxx		
		MF	xx	-27%	xxxx	+3%	
	248	B	x		xxxx		
		MF	x	+33%	xxxx	+5%	
5:1	228	B	xx		xxxx		
		MF	xxx	+20%	xxxx	-9%	
	225	B	x				
		MF	x				

0.0 0.5 1.0 (ppm) 0.0 0.5 1.0 (ppm) 0.0 0.5 1.0 (ppm)

Figure IV-14. Comparison of ozone yields observed in the simultaneous irradiation of the various pairs of surrogate mixtures carried out in the divided outdoor chamber.

ROG/NO_x Ratio	OTC Run no.	Side	Maximum Ozone (ppm) Day 1		Day 2		Day 3	
			Base Case vs Methanol Substitution					
13:1	224	B	xxxxxxxx		xxxxx			
		M	xxxxxxxx	-4%	xxxxx	-8%		
10:1	217	B	xxxxxxxx		(no data)			
		M	xxxxx	-42%	xxxx			
	237	B	xxxxxxxx		xxxxx			
		M	xxxxxxxx	-6%	xxxx	-12%		
7:1	242	B	xxxxxx		xxx			
		M	xx	-72%	xxxx	+3%		
5:1	240	B	xx		xxx		xxx	
		M	x	-86%	x	-67%	xxx	+17%
			MF Substitution vs Methanol Substitution					
10:1	222	MF	xxxxxxxxxx		xxxxxx			
		M	xxxxxxxxx	-3%	xxxxxx	-6%		
7:1	219	MF	xxxxx		xxx			
		M	xxx	-31%	xxx	+11%		
	239	MF	xxx		xxxx			
		M	xx	-32%	xxxxx	+12%		

0.0 0.5 1.0 (ppm) 0.0 0.5 1.0 (ppm) 0.0 0.5 1.0 (ppm)

Figure IV-14 (continued) - 2

ROG/NO_x Ratio	OTC Run no.	Side	Maximum Ozone (ppm) Day 1		Day 2		Day 3
			Base Case vs Blank Substitution				
10:1	223	B	xxxxxxxxxx		xxxxxx		
		BL	xxxxxxxx	-19%	xxxx	-29%	
7:1	230	B	xxxxx		xxx		
		BL	xxx	-45%	xxx	+3%	
			MF Substitution vs Blank Substitution				
10:1	238	MF	xxxxxxx		xxxx		
		BL	xxxx	-41%	xxxx	-9%	
			Methanol Substitution vs Blank Substitution				
7:1	229	M	xxx		xxxxx		
		BL	xx	-32%	xxxxxx	+6%	

0.0 0.5 1.0 (ppm) 0.0 0.5 1.0 (ppm) 0.0 0.5 1.0 (ppm)

Figure IV-14 (concluded) - 3

pattern. Seven "B" vs "MF" irradiations were carried out (more than any other pair of surrogate mixtures); in five, slightly more ozone was formed on day 1 on the methanol + formaldehyde substitution side; in one, slightly more ozone was formed on day 1 on the base case side. However, the ozone profiles were very similar in all of these runs, and they behaved essentially like side equivalency tests. (Plots of the ozone profiles for these runs are given in Appendix A.) Changing the ROG/NO_x ratio did not have any significant effect on the relative reactivities of these two surrogates. Thus, under the conditions of the outdoor chamber experiments, the inclusion of approximately 10% of formaldehyde in the methanol emissions surrogate was apparently sufficient to make up for the reduced reactivity of methanol relative to the components of the base case surrogate, at least in terms of ozone formation.

The effects of substitution on the day 2 or day 3 ozone levels observed in these dual chamber experiments tended to be more variable than for the day 1 ozone levels. This is because in approximately half the cases the mixture which formed the higher ozone level on day 1 had the lower ozone level on the last day of the irradiation. In addition, runs with relatively large percentage differences in ozone yields between the two sides tended to have lower percentage differences on day 2 (or 3), and runs with relatively small percentage differences in day 1 ozone tended to have somewhat larger differences on day 2. In the case of the base case vs "MF" substitution experiments, the differences in day 2 ozone levels were no more consistent than the differences in the day 1 yields. In the case of the base case vs methanol-only substitution, and the methanol + formaldehyde vs methanol-only substitution experiments, where the side with the base case or the "MF" substitution mixtures, respectively, were consistently the more reactive on day 1, in approximately half the experiments the other mixture formed more ozone on day 2 or day 3. This was also true for the base case vs methanol-only, or "MF" vs blank substitution experiments, where on day 1 the blank substitution side consistently formed less ozone on day 1, but had the higher ozone levels on day 2 in approximately half of the experiments. This contrasts with the results of the indoor chamber experiments, where blank substitution consistently resulted in lower day 2 or day 3 ozone levels than the base case or the methanol or methanol + formaldehyde substitution runs.

The net effect of this reversal of reactivity in terms of ozone formation in many of these multi-day experiments was to decrease the differences in ozone formation potential of the different surrogate employed in multi-day runs as opposed to single day irradiations. The fact that the multi-day effects tended to be more variable in these outdoor chamber experiments than those for the indoor chamber runs discussed above can be attributed to the greater variability in the temperature and light intensity in the outdoor chamber runs, since, as indicated above, these can have a significant effect on ozone formation.

PAN. Figure IV-15 shows the differences in the day 1 and the day 2 PAN yields for each of the different pairs of surrogate mixtures which were simultaneously irradiated. In contrast with the ozone data, the results of these experiments indicate that in almost all cases methanol, and even methanol + formaldehyde, substitution had a beneficial effect on PAN levels, relative to the base case. This was true for the day 2 or day 3 PAN levels as well those on the first day. In the base case vs "MF" substitution runs there were only three experiments with equal or lower day 1 PAN levels on the base case side. However, for all these runs the day 1 PAN levels were relatively low and significantly more PAN was formed on day 2 (with higher PAN yields on the base case side) in the two of those runs for which day 2 data are available. For the base case vs "MF" surrogate runs, the day 1 PAN levels were consistently higher on the base case side, and in only one run (OTC-242) was there a reversal in relative PAN levels on day 2, primarily because between day 1 and day 2 there was a rapid dark decay of PAN on the base case side (see Figure A-42).

In the experiments where "MF" or "M" substitution is compared with blank substitution, i.e., where the levels of the base case surrogate components were the same and the effects of adding methanol or 90% methanol + 10% formaldehyde to the reaction mixtures was examined, the methanol or methanol + formaldehyde caused some increase in PAN relative to the sides where these were not added, but the percentage increases in PAN were significantly less than the percentage increases in ozone. (Thus, in the "10-MF" vs "10-BL" run OTC-238, the difference in day 1 PAN yields was 11%, compared to 41% for day 1 ozone, and in the "7-M" vs "7-BL" run OTC-229, the differences were 15% for PAN and 32% for ozone.) These results indicate that methanol + formaldehyde substitution is much

ROG/NO_x Ratio	OTC Run no.	Side	Maximum PAN (ppb) Day 1		Day 2		Day 3
			Base Case vs MF Substitution				
13:1	241	B	xxxxxx		x		
		MF	xxxxx	-27%	x	-15%	
10:1	215	B	xxxxxxxxxxxxx		xx		
		MF	xxxxxxxxxxxx	-2%	x	-41%	
	249	B	xxxxxxx		xxxxxxxx		
		MF	xxxxx	-31%	xxxxxx	-25%	
	243	B	xx		xxxxx		
		MF	xx	+0%	xxxx	-26%	
7:1	221	B	xxxxx		xxx		
		MF	xxxx	-28%	xxx	-4%	
	248	B	x		xxxxx		
		MF	x	+8%	xxxxx	-2%	
5:1	228	B	xxx		xxx		
		MF	xx	-26%	xx	-32%	
	225	B	x				
		MF	x				

0 50 100 (ppb) 0 50 100 (ppb) 0 50 100 (ppb)

Figure IV-15. Comparison of PAN yields observed in the simultaneous irradiation of the various pairs of surrogate mixtures carried out in the divided outdoor chamber.

ROG/NO_x Ratio	OTC Run no.	Side	Maximum PAN (ppb) Day 1		Day 2		Day 3	
			Base Case vs Methanol Substitution					
13:1	224	B	xxxxxx		x			
		M	xxxxx	-26%	x	+0%		
10:1	217	B	xxxxxxxxxxxx					
		M	xxxxxxx	-44%	x			
	237	B	xxxxxx		x			
		M	xxxx	-28%	x	+0%		
7:1	242	B	xxxx		xx			
		M	xx	-47%	xxx	+44%		
5:1	240	B	xxx		xxx		xxx	
		M	x	-97%	x	-64%	xx	-20%
			MF vs Methanol					
10:1	222	MF	xxx		x			
		M	xxx	-3%	x	+0%		
7:1	219	MF	x		x			
		M	x	+0%	xx	+71%		
	239	MF	xx		xx			
		M	xx	+0%	xxx	+53%		

0 50 100 (ppb) 0 50 100 (ppb) 0 50 100 (ppb)

Figure IV-15 (continued) - 2

ROG/NO_x Ratio	OTC Run no.	Side	Maximum PAN (ppb)					
			Day 1		Day 2		Day 3	
			Base Case vs Blank Substitution					
10:1	223	B	xxxxx		x			
		BL	xxx	-39%	x	+33%		
7:1	230	B	xxxx		x			
		BL	xx	-27%	x	+250%		
			MF Substitution vs Blank Substitution					
10:1	238	MF	xxxxx		xx			
		BL	xxxxx	-11%	xxx	+59%		
			Methanol Substitution vs Blank Substitution					
7:1	229	M	xxx		xx			
		BL	xx	-15%	xx	+0%		
			0 50 100		0 50 100		0 50 100	

Figure IV-15 (concluded) - 3

more effective in reducing PAN levels than in reducing ozone levels under the conditions of these outdoor chamber experiments, and that this is probably the case (though to a much lesser extent) for methanol-only substitution as well.

The results of these experiments suggest that the inclusion of formaldehyde in the methanol surrogate will probably result in some increase of PAN levels, though the methanol vs methanol + formaldehyde substitution runs suggest that the effect of the added formaldehyde on PAN would be much less than the effect on ozone. In particular, in the methanol vs "MF" substitution runs, where more ozone was consistently formed on day 1 on the "MF" substitution side, there were no significant differences in the PAN levels on day 1, and, in two of the three runs, somewhat less PAN on the "MF" side on day 2. However, the base case vs methanol or methanol + formaldehyde substitution experiments suggest that initial addition of formaldehyde may have a tendency to increase PAN levels, since the methanol-only substitution tended to decrease day 1 PAN levels to a greater extent than did methanol + formaldehyde substitution.

Formaldehyde. Figure IV-16 shows the differences in the day 1 and the day 2 formaldehyde yields for each of the different pairs of surrogate mixtures which were simultaneously irradiated. As discussed above, the formaldehyde yields in these outdoor chamber experiments were relatively insensitive to variations in the experimental conditions, and thus a comparison of the averages for runs carried out at different times can provide a useful assessment of the relative formaldehyde forming potential of the different surrogate mixtures employed. Averages of the formaldehyde yields observed in the replicate irradiations of the various surrogate-NO_x-air mixtures are summarized in Table IV-11, and the differences between the average yields for the groups of replicate runs are shown in Figure IV-16, from which they can be seen to be consistent with the differences in the formaldehyde yields observed in the individual runs where the mixtures were irradiated simultaneously.

As expected, the highest formaldehyde levels tended to be in the methanol + formaldehyde experiments, since those are the only runs where formaldehyde was initially present, although at the highest ROG/NO_x ratio the differences appeared to be minor. Although the initial formaldehyde levels in the "MF" surrogate were obviously greater than in the base case

ROG/NO_x Ratio	OTC Run no.	Side	Maximum Formaldehyde (ppm) Day 1		Day 2		Day 3
			Base Case vs MF Substitution				
13:1	241	B	xxxxxxx		xxxxxxx		
		MF	xxxxxxxx	+5%	xxxxxx	-10%	
	All Runs	B	xxxxxxxx		xxxxxx		
		MF	xxxxxxxx	+0%	xxxxxx	+6%	
10:1	249	B	xxxxxxxx		xxxxxxx		
		MF	xxxxxxxxx	+13%	xxxxxxxx	+10%	
	243	B	xxxxx		xxxxxx		
		MF	xxxxxx	+20%	xxxxxx	+0%	
	All Runs	B	xxxxxxx		xxxxxx		
		MF	xxxxxxxx	+14%	xxxxxxx	+22%	
7:1	221	B	xxxxx		xxxx		
		MF	xxxxx	-6%	xxxxx	+15%	
	248	B	xxxx		xxxxxx		
		MF	xxxxxx	+31%	xxxxxx	+0%	
	All Runs	B	xxxxx		xxxx		
		MF	xxxxx	+7%	xxxxx	+15%	
5:1	228	B	xx		x		
		MF	xxxx	+100%	xxx	+350%	
	225	B	xx				
		MF	xxx	+14%			
	All Runs	B	xx		xx		
		MF	xxx	+43%	xxx	+50%	

0.0 0.15 0.3 (ppm) 0.0 0.15 0.3 (ppm) 0.0 0.15 0.3 (ppm)

Figure IV-16. Comparison of formaldehyde yields observed in the simultaneous irradiation of the various pairs of surrogate mixtures carried out in the divided outdoor chamber.

ROG/NO_x Ratio	OTC Run no.	Side	Maximum Formaldehyde (ppm) Day 1		Day 2		Day 3	
			Base Case vs Methanol Substitution					
13:1	224	B	xxxxxxxx		xxxxx			
		M	xxxxxxxxx	+17%	xxxxxx	+36%		
10:1	237	B	xxxxxxx		xxxxxx			
		M	xxxxxxxxx	+18%	xxxxxxxxx	+37%		
	All Runs	B	xxxxxxx		xxxxxx			
		M	xxxxxxxx	+19%	xxxxxxxx	+28%		
7:1	242	B	xxxx		xxxx			
		M	xxxx	-8%	xxxxx	+8%		
	All Runs	B	xxxxx		xxxx			
		M	xxxx	-20%	xxxx	+0%		
5:1	240	B	xxx		xx		xx	
		M	xx	-13%	xxx	+29%	xxx	+50%

0.0 0.15 0.3 (ppm) 0.0 0.15 0.3 (ppm) 0.0 0.15 0.3 (ppm)

Figure IV-16 (continued) - 2

ROG/NO_x Ratio	OTC Run no.	Side	Maximum Formaldehyde (ppm) Day 1		Day 2		Day 3
			MF Substitution vs Methanol Substitution				
10:1	222	MF	xxxxxxxx		xxxxxxx		
		M	xxxxxxxxx	+4%	xxxxxxx	+0%	
	All Runs	MF	xxxxxxxx		xxxxxxx		
		M	xxxxxxxxx	+8%	xxxxxxxx	+5%	
7:1	219	MF	xxxxx		xxxx		
		M	xxxx	-19%	xxxxx	+8%	
	239	MF	xxxxxx		xxxxx		
		M	xxxx	-24%	xxxx	-19%	
	All Runs	MF	xxxxx		xxxxx		
		M	xxxx	-25%	xxxx	-13%	
			Base Case vs Blank Substitution				
10:1	223	B	xxxxxxxxx		xxxxx		
		BL	xxxxxxx	-23%	xxx	-29%	
	All Runs	B	xxxxxxx		xxxxxx		
		BL	xxxxx	-32%	xxxx	-28%	
7:1	230	B	xxxx		xxxx		
		BL	xx	-46%	xxx	-27%	
	All Runs	B	xxxxx		xxxx		
		BL	xx	-53%	xx	-54%	

0.0 0.15 0.3 (ppm) 0.0 0.15 0.3 (ppm) 0.0 0.15 0.3 (ppm)

Figure IV-16 (continued) - 3

ROG/NO_x Ratio	OTC Run no.	Side	Maximum Formaldehyde (ppm) Day 1		Day 2		Day 3
			MF Substitution vs Blank Substitution				
10:1	238	MF	xxxxxxxx				
		BL	xxxxx	-39%			
	All Runs	MF	xxxxxxxx		xxxxxxx		
		BL	xxxxx	-38%	xxxx	-41%	
7:1	All Runs	MF	xxxxx		xxxxx		
		BL	xx	-56%	xx	-60%	
			Methanol Substitution vs Blank Substitution				
10:1	All Runs	M	xxxxxxxxx		xxxxxxxx		
		BL	xxxxx	-42%	xxxx	-43%	
7:1	229	M	xxxx		xxxx		
		BL	xx	-45%	xx	-45%	
	All Runs	M	xxxx		xxxx		
		BL	xx	-42%	xx	-54%	

0.0 0.15 0.3 (ppm) 0.0 0.15 0.3 (ppm) 0.0 0.15 0.3 (ppm)

Figure IV-16 (concluded) - 4

Table IV-11. Averages of the Day 1 and Day 2 Formaldehyde Yields (in pphm) Observed in the Outdoor Chamber Irradiations of the Various Surrogate-NO_x-Air Mixtures

Surrogate	Day	Nominal ROG/NO_x Ratio			
		13:1	10:1	7:1	5:1
Base Case	1	23 ± 1	22 ± 5	15 ± 3[a]	7 ± 1
	2	18 ± 5	18 ± 3	13 ± 3	6 ± 3
MF Substitution	1	23	24 ± 4	16 ± 1	10 ± 2
	2	19	22 ± 3	15 ± 2	9
M Substitution	1	27	26	12 ± 1	7
	2	19	23 ± 4	13 ± 1	9
Blank Substitution[b]	1		15 ± 3[a]	7 ± 1	
	2		13 ± 3	6 ± 3	

[a]Anomalously low yields observed in run OTC-226 not counted in average.
[b]Same group of runs as the base case experiments at the next highest ROG/NO_x ratio.

or the methanol-only substitution surrogates, the differences tended to decrease with time as the initially present formaldehyde in the "MF" surrogate reacted, and as formaldehyde was formed from the reactions of the other surrogate components. (The large effect of "MF" substitution at the 5:1 ROG/NO_x ratio must be considered to be uncertain, since the formaldehyde monitoring technique employed could not yield precise data at the relatively low concentrations observed in the 5:1 ROG/NO_x experiments.) The ROG/NO_x ratio also appears to have an effect on the relative amounts of formaldehyde formed in the methanol-only substitution experiments compared to the base case, since at the higher ROG/NO_x ratios methanol substitution appears to form more formaldehyde while at the lower ratios it forms less initially, but eventually the formaldehyde levels approach or exceed those observed in the base case experiments. In addition, in the experiments in which methanol-only substitution is compared with methanol + formaldehyde substitution, the differences in the formaldehyde levels appear to be greater at the lower ROG/NO_x ratio, with the

difference becoming less on day 2 than on day 1. This is consistent with the ROG/NO_x dependencies observed in the base case vs "MF" and the base case vs methanol substitution experiments. However, in view of the scatter of the data, the possibility that these apparent dependencies on the ROG/NO_x ratio may be coincidental cannot be ruled out.

It should be noted that the effects of methanol substitution and even methanol + formaldehyde substitution are relatively small compared to the effects of blank substitution. In particular, the greatest differences in the formaldehyde yields were consistently observed in the base case, "MF", or methanol substitution vs blank substitution experiments; and, as shown in Table IV-11, the averages of the formaldehyde levels in the replicate blank substitution experiments are significantly lower than the averages for the other surrogates at the same nominal ROG/NO_x ratios. It is also interesting to note that the nominal initial ROG levels in the runs carried out at the 13:1 and the 10:1 ROG/NO_x ratios (excluding blank substitution runs) are the same, and that the formaldehyde levels formed in these groups of experiments are comparable, despite the differences in the NO_x levels. Thus, at least for the surrogates employed in this study, it is the total amount of ROG which is present which is the dominant factor influencing formaldehyde yields, rather than the surrogate composition or the NO_x level employed.

C. Results of Model Simulations

In order to determine whether the results of the experiments conducted in this program are consistent with current chemical mechanisms for photochemical smog formation, computer model simulations of most of the multi-day surrogate-NO_x-air irradiations were carried out. The chemical mechanism and chamber effects model employed was that recently developed and tested at SAPRC under EPA-funded Contract No. 68-02-4104 to provide an updated chemical mechanism to be used in EKMA models (Carter et al. 1986). This chemical mechanism is an update and extension of the previously published models of Atkinson et al. (1982) and Lurmann et al. (1986), and contains the detailed explicit reactions of all of the components of the base case surrogate and their major known oxidation products. The chamber effects model included representations of the major chamber effects such as chamber radical sources, dilution, NO_x offgassing,

ozone decay, N_2O_5 hydrolysis, and other heterogeneous or chamber dependent processes. Methods for calculating photolysis rates for the light sources employed in the three SAPRC environmental chambers, including the two employed in this program, and for the outdoor chamber at the University of North Carolina (UNC) (Jeffries et al. 1982, 1985a,b) were also incorporated into this model. This chemical mechanism and chamber effects model has been tested against the results of over 400 environmental chamber experiments carried out at the SAPRC and the UNC. This mechanism and chamber effects is documented in detail by Carter et al. (1986), and the reactions, rate constants, and chamber effects parameters employed in the model simulations carried out for this program are summarized in Appendix B.

Although the mechanism developed and tested for the EPA did not include the reactions of methanol, its atmospheric chemistry of methanol is believed to be straightforward, being represented in the model by adding the reaction

$$OH + CH_3OH \rightarrow HO_2\cdot + HCHO$$

with a rate constant of (Atkinson 1986)

$$k = 1.34 \times 10^{-11}\ e^{-805/T}\ cm^3\ molecule^{-1}\ sec^{-1}.$$

The relevant data concerning the kinetics and the mechanism of this reaction, which is not considered to be a significant source of uncertainty in the model, is discussed in detail by Atkinson (1986), and is not reiterated here.

The results of the model simulations of these surrogate-NO_x-air runs are shown together with the experimental results in the concentration-time plots given in Appendix A. These show the performance of the model in simulating the experimentally observed concentration-time profiles for ozone, NO, NO_2, PAN, formaldehyde, methanol, and the base case surrogate components. The experimental and calculated maximum yields of ozone, PAN, and formaldehyde are summarized in Tables IV-12 and IV-13 for the indoor and the outdoor chamber runs, respectively. In addition, to more clearly indicate the performance of the model in predicting the relative effects

Table IV-12. Comparison of Experimental and Calculated Maximum Yields of Ozone, Formaldehyde, and PAN for the Surrogate-NO_x-Air Irradiations Carried Out in the Indoor Chamber

ITC Run no.	Run Type	Maximum Ozone (ppm) Day1	Day2	Day 3	Maximum HCHO (ppm) Day1	Day2	Day 3	Maximum PAN (ppb) Day1	Day2	Day3
865	15-B	0.63	0.37	-	0.21	0.12	-	>83	36	-
		(0.58	0.33)	-	(0.17	0.06)	-	(79	27)	-
891	15-B	0.60	0.34	-	0.07	0.05	-	134	36	-
		(0.58	0.33)	-	(0.15	0.06)	-	(79	29)	-
867	15-MF	0.63	0.36	-	0.22	0.10	-	>54	23	-
		(0.61	0.35)	-	(0.22	0.06)	-	(59	22)	-
888	15-M	0.58	0.35	-	0.15	0.11	-	97	46	-
		(0.58	0.35)	-	(0.13	0.06)	-	(55	24)	-
868	15-BL	0.52	0.29	-	0.11	0.05	-	>34	19	-
		(0.52	0.34)	-	(0.09	0.05)	-	(52	27)	-
871	6-B	0.38	0.31	-	0.05	0.06	-	>10	22	-
		(0.31	0.29)	-	(0.07	0.03)	-	(28	21)	-
872	6-MF	0.21	0.23d	-	0.11	0.09	-	>5	12	-
		(0.26	0.24)	-	(0.11	0.03)	-	(16	14)	-
877	6-MF	0.25	0.29	-	0.11	0.07	-	24	26	-
		(0.27	0.29)	-	(0.10	0.03)	-	(18	14)	-
874	6-M	0.19	0.28	-	0.08	0.08	-	>2	10	-
		(0.18	0.23)	-	(0.05	0.03)	-	(13	12)	-
873	6-BL	0.16	0.26	-	0.03	0.03	-	>2	11	-
		(0.12	0.26)	-	(0.04	0.02)	-	(9	13)	-
880	3-B	0.03	0.15	0.31	0.01[a]	0.01[a]	0.01[a]	2	15	25
		(0.05	0.13	0.23)	(0.06	0.03	0.01)	(3	8	12)
881	3-MF	0.01	0.08	0.31	0.09	0.09	0.07	0	4	24
		(0.03	0.07	0.20)	(0.09	0.03	0.01)	(1	3	6)
886	3-M	0.01	0.07	0.29	0.07	0.07	0.04	0	5	19
		(0.02	0.06	0.15)	(0.04	0.03	0.01)	(1	2	3)
885	3-BL	0.01	0.04	0.13	0.01[a]	0.02[a]	0.01[a]	0	1	8
		(0.03	0.06	0.15)	(0.04	0.02	0.01)	(1	2	5)

[a]Formaldehyde data appear to be anomalously low.

Table IV-13. Comparison of Experimental and Calculated Maximum Yields of Ozone, Formaldehyde, and PAN for the Surrogate-NO_x-Air Irradiations Carried Out in the Outdoor Chamber

OTC Run no.	Run Type	Maximum Ozone (ppm) Day1	Day2+	Maximum HCHO (ppm) Day1	Day2+	Maximum PAN (ppb) Day1	Day2+
241A	13-B	0.67	0.48	0.22	0.21	64	13
		(0.71	0.62)	(0.19	0.19)	(81	47)
241B	13-MF	0.67	0.47	0.23	0.19	47	11
		(0.69	0.60)	(0.19	0.15)	(64	37)
224A	13-M	0.78	0.49	0.27	0.19	46	3
		(0.79	0.47)	(0.19	0.19)	(59	5)
224B	13-B	0.81	0.53	0.23	0.14	62	3
		(0.85	0.52)	(0.22	0.22)	(82	5)
215A	10-B	0.83	0.49	a	a	125	17
		(0.86	0.65)	(0.23	0.21)	(112	51)
215B	10-MF	0.87	0.55	a	a	123	10
		(0.96	0.68)	(0.30	0.20)	(95	37)
249A	10-B	0.35	0.23	0.24	0.21	65	83
		(0.33	0.20)	(0.21	0.20)	(70	70)
249B	10-MF	0.33	0.25	0.27	0.23	45	62
		(0.37	0.24)	(0.23	0.21)	(55	52)
243A	10-B	0.14	0.53	0.15	0.18	21	50
		(0.21	0.27)	(0.21	0.21)	(47	68)
243B	10-MF	0.15	0.49	0.18	0.18	21	37
		(0.18	0.31)	(0.19	0.18)	(34	56)
217A	10-M	0.48	0.37	-	-	68	11
		(0.61	0.56)	(0.18	0.17)	(65	37)
217B	10-B	0.83	-	-	-	121	-
		(0.92	-)	(0.20	-)	(116	-)

(continued)

Table IV-13 (continued) - 2

OTC Run no.	Run Type	Maximum Ozone (ppm) Day1	Day2+	Maximum HCHO (ppm) Day1	Day2+	Maximum PAN (ppb) Day1	Day2+
237A	10-B	0.81	0.50	0.22	0.19	64	10
		(0.82	0.67)	(0.22	0.22)	(93	46)
237B	10-M	0.76	0.44	0.26	0.26	46	10
		(0.70	0.62)	(0.21	0.20)	(76	42)
222A	10-M	0.91	0.58	0.26	0.20	30	2
		(0.95	0.60)	(0.17	0.15)	(52	3)
222B	10-MF	0.94	0.62	0.25	0.20	31	2
		(1.07	0.74	(0.23	0.14)	(48	2)
223A	10-B	0.95	0.62	0.26	0.14	54	3
		(0.86	0.52)	(0.24	0.24)	(68	19)
223B	10-BL	0.77	0.44	0.20	0.10	51	4
		(0.71	0.38)	(0.19	0.19)	(56	2)
238A	10-BL	0.41	0.39	0.14	-	47	27
		(0.39	0.46)	(0.15	0.15)	(61	52)
238B	10-MF	0.70	0.43	0.23	-	53	17
		(0.69	0.57)	(0.21	0.18)	(76	50)
221A	7-MF	0.24	0.33	0.15	0.15	36	25
		(0.28	0.51)	(0.11	0.08)	(40	34)
221B	7-B	0.39	0.39	0.16	0.13	50	26
		(0.34	0.58)	(0.13	0.11)	(57	47)
248A	7-B	0.06	0.41	0.13	0.17	12	51
		(0.18	0.44)	(0.12	0.13)	(33	45)
248B	7-MF	0.08	0.43	0.17	0.17	13	50
		(0.21	0.37)	(0.13	0.12)	(32	33)

(continued)

Table IV-13 (concluded) - 3

OTC Run no.	Run Type	Maximum Ozone (ppm) Day1	Maximum Ozone (ppm) Day2+	Maximum HCHO (ppm) Day1	Maximum HCHO (ppm) Day2+	Maximum PAN (ppb) Day1	Maximum PAN (ppb) Day2+
242A	7-M	0.18	0.35	0.12	0.14	20	26
		(0.17	0.37)	(0.10	0.09)	(23	33)
242B	7-B	0.64	0.34	0.13	0.13	38	18
		(0.62	0.35)	(0.16	0.16)	(61	29)
239A	7-MF	0.34	0.42	0.17	0.13	17	17
		(0.39	0.49)	(0.16	0.12)	(42	32)
239B	7-M	0.23	0.47	0.13	0.13	17	26
		(0.18	0.68)	(0.13	0.13)	(24	26)
230A	7-B	0.49	0.31	0.13	0.11	38	4
		(0.83	0.50)	(0.20	0.19)	(63	11)
230B	7-BL	0.27	0.32	0.08	0.08	24	14
		(0.55	0.43)	(0.14	0.14)	(43	18)
229A	7-M	0.25	0.54	0.11	0.11	27	19
		(0.47	0.44)	(0.14	0.14)	(45	31)
229B	7-BL	0.16	0.57	0.06	0.06	23	19
		(0.40	0.42)	(0.12	0.11)	(44	34)
228A	5-B	0.25	0.44	0.06	0.02	34	25
		(0.42	0.38)	(0.12	0.08)	(41	21)
228B	5-MF	0.30	0.40	0.12	0.09	25	17
		(0.43	0.37)	(0.13	0.07)	(33	14)
240A	5-M	0.03	0.11	0.07	0.09	1	12
			0.34		0.09		20
		(0.04	0.12	(0.07	0.07	(1	12
			0.31)		0.07)		21)
240B	5-B	0.22	0.33	0.08	0.07	29	33
			0.29		0.06		25
		(0.13	0.31	(0.10	0.10	(15	38
			0.27)		0.08)		24)

[a]No data.

of substitution in the various outdoor chamber experiments where two different surrogates were simultaneously irradiated, Table IV-14 summarizes the experimental and calculated differences in the ozone, PAN, and formaldehyde yields formed from the two surrogates irradiated in each experiment.

In assessing the performance of the model in simulating these data, the following points should be noted:

- As indicated in Section III-C-3, the technique for monitoring NO_2 suffers from positive interferences by PAN, other organic nitrates, and, to variable extents, nitric acid. As a result, except for the initial periods of the experiments, the experimental "NO_2" data will be higher than the actual NO_2 concentrations, with the differences reflecting the levels of the interfering species present and the amounts of nitric acid which made it through the sample line to the monitoring instrument and hence the experimental "NO_2" data would always be higher than the model simulations.

- Some of the base case surrogate components were monitored by two different GC instruments (see Section III-1), and in some cases the results did not agree well. These appear in the plots as separate curves for the experimental measurements with the same plot symbol employed. In some cases, the data from one of the instruments was judged to be less reliable than data from the other, and the initial concentrations used in the model simulations were determined from the data from the apparently more reliable instrument. However, the plots show the data from all the instruments employed. The comments in the detailed computer data sets described in Appendix C indicate which instruments are considered to have less reliable data, or to have calibration uncertainties at the time a run was carried out. If both instruments monitoring a particular compound are considered to be equally reliable, the initial concentration employed in the calculations were determined by averaging the data from the two instruments.

- For some runs, the experimental measurements of the initial concentrations of some of the surrogate components were missing or judged to be unreliable (based on known experimental problems), and the initial concentrations were estimated based on relative concentrations observed in other experiments. Since the plots in Appendix A for a given measured specie include all the experimental data for that specie on the data sets,

Table IV-14. Comparison of Experimental and Calculated Percentage Differences in Daily Maximum Ozone, PAN, and Formaldehyde Yields in the Outdoor Chamber Experiments

ROG/NO_x Ratio	OTC Run no.	Ozone Day 1	Ozone Day 2	PAN Day 1	PAN Day 2	Formaldehyde Day 1	Formaldehyde Day 2
Base vs MF							
13:1	241	-0	-2	-27	-15	+5	-10
		(-3	-3)	(-21	-21)	(+0	-21)
10:1	215	+5	+12	-2	a	b	b
		(+12	+5)	(-15	-41)	(+30	-5)
	249	-6	+52	-31	-25	+13	+10
		(+12	+20)	(-21	-26)	(+10	+5)
	243	a	-8	a	-26	+20	+0
		(a	+15)	(-28	-18)	(-10	-14)
7:1	221	-38	-15	-28	-4	-6	+15
		(-18	-12)	(-30	-28)	-15	-27)
	248	a	+5	a	-2	+31	+0
		(+17	-16)	(-3	-27)	(+8	-8)
5:1	228	+20	-9	-26	-32	+100	+350
		(+2	-3)	(-20	-33)	(+8	-13)
Base vs Methanol							
13:1	224	-4	-11	-26	a	+17	+36
		(-7	-10)	(-28	+0)	(-14	-14)
10:1	217	-42	b	-44	b	b	b
		(-34	-)	(-44	-)	(-10	-)
	237	-6	-12	-28	+0	+18	+37
		(-15	-7)	(-18	-9)	(-5	-9)
7:1	242	-72	+3	-47	+44	-8	+8
		(-73	+6)	(-62	+14)	(-38	-44)
5:1	240	a	-67	a	-64	-13	+29
			+17		+20		-50
		(a	-61	a	-45	-30	-30
			+15)		-13)		-13)

(continued)

Table IV-14 (concluded) - 2

ROG/NO_x Ratio	OTC Run no.	Ozone Day 1	Ozone Day 2	PAN Day 1	PAN Day 2	Formaldehyde Day 1	Formaldehyde Day 2
MF vs Methanol							
10:1	222	-3	-24	-3	a	+4	+0
		(-11	-19)	(+8	a)	(-26	+7)
7:1	239	-32	+12	+0	+53	-24	+0
		(-54	+39)	(-43	-19)	(-19	+8)
Base vs Blank							
10:1	223	-19	-29	-39	a	-23	-29
		(-17	-27)	(-18	a)	(-21	-21)
7:1	230	-45	+3	-27	a	-38	-27
		(-34	-14)	(-32	a)	(-30	-26)
MF vs Blank							
10:1	238	-41	-9	-11	+59	-39	b
		(-43	-19)	(-20	+4)	(-29	-17)
Methanol vs Blank							
7:1	229	-36	+6	-15	-0	-45	-45
		(-15	-5)	(-2	+10)	(-14	-21)

[a]Yield too low for percentage difference to give a meaningful comparison.
[b]No data or data rejected.
[c]Day 3 difference given.

in some cases where the data were judged to be unreliable it will appear that the model did not use the appropriate initial concentration. An example of this concerns the isooctane data for runs ITC-871 through ITC-874. In cases like this, poor fits of the model simulation to the experiment reflect known problems with the experimental data and not with the model.

• As indicated above and in Section III-C-2, the experimental formaldehyde data tended to be scattered when monitored at the levels

employed in the surrogate-NO_x-air experiments, and this is evident in the data plots. In addition, as indicated above, formaldehyde data in runs ITC-873, 880, and 885 appeared to be anomalously low and are probably not valid. This should be taken into account in assessing the model performance in predicting formaldehyde levels. In general, the formaldehyde data in the outdoor chamber runs appear to be of higher quality than the indoor chamber runs (i.e., less scattered and fewer cases of anomalous measurements), although the reason for this is not known.

In general, the model performed reasonably well in simulating the results of the surrogate-NO_x-air experiments carried out in both chambers, especially after the known experimental uncertainties are taken into account. The following points regarding the performance of this model in simulating these data should be noted:

- In order to fit the consumption rate for n-butane, methanol, and other relatively slowly reacting species in the indoor chamber run, it was necessary to assume the chamber contents were being diluted at a rate of approximately 2% per hour. Assuming dilution also results in generally better fits to observed ozone yields. This contrasts with the results of the model simulations of the previous series of ITC surrogate-NO_x-air runs (Carter et al. 1985, 1986), as well as the outdoor chamber experiments carried out in this program, where no such dilution had to be assumed. This suggests that there may have been a small leak in the Teflon reaction bag employed in the ITC during this program.

- The day 1 and day 2 ozone yields were well simulated in all of the indoor chamber runs except for the 3-BL run ITC-885, where the relatively low day 2 ozone yield was underpredicted as were the day 3 ozone yields in the other three ITC runs carried out at the 3:1 ROG/NO_x ratio. However, the model correctly predicted the day 3 ozone yield observed in ITC-885.

- The fits of the model simulations to the ozone data in the outdoor chamber experiments were in general not as good as the simulations of the indoor chamber experiments, though for most experiments the fits to the day 1 ozone yields were satisfactory. The major exceptions to this were runs OTC-229 and OTC-230, where the model significantly overpredicted the amount of ozone formed on both sides, and run OTC-226, where the day 1 ozone yield was underpredicted. The model had a tendency to overpredict the amount of ozone formed on day 2 in many of the experiments, although

in most cases the discrepancies observed were not large. As shown in Table IV-14, the model successfully predicted the relative effects of methanol substitution on day 1 and day 2 ozone yields for most of the OTC runs, even those where the absolute yields were not well simulated. In general, simulations of outdoor chamber experiments are expected to be more difficult than simulations of indoor chamber runs because of the greater variability of experimental conditions and the greater uncertainties in the light intensity parameters (Carter et al. 1986).

- For runs ITC-865 and ITC-867, NO was added on the third day, thus allowing subsequent formation of ozone to continue. (The results following the subsequent addition of NO are not shown in the summary tables in this section.) In both of these experiments, the amounts of ozone formed following this addition of NO were well simulated by the model (as shown in Figures A-14 and A-16).

- In general, the performance of the model in simulating the PAN data was more variable than was the case for ozone. In the indoor chamber experiments, two different GC instruments were used to monitor PAN, one with a manual sampling system and one with an automated system. The model tended to simulate reasonably well the data from the manual instrument, but underpredicted the PAN yields (typically by approximately 40%), measured with the automated instrument. However, in the outdoor experiments, where all PAN data were obtained with the automated GC instrument, the model tended to overpredict the PAN concentrations in some runs, to fit PAN in others, and significantly underpredict PAN yields in a few other runs. These discrepancies may be due to calibration uncertainties, and may not necessarily indicate problems with the chemical model. Thus the model was reasonably successful in predicting the the shapes of the PAN concentration-time profiles (with the exception of those runs where ozone was poorly predicted), and the relative effects of substitution on PAN yields in the outdoor experiments (see Table IV-14) and in those indoor experiments where comparable monitoring techniques were employed.

- An interesting observation with regard to the PAN concentration-time profiles is that in some experiments significant nighttime formation of PAN was observed, and this was predicted by the model simulations. Examples of nighttime PAN formation involve runs ITC-877 (Figure A-21), OTC-221 (A-40), OTC-242A (A-42), and OTC-228 (A-48). In general this occurred between day 1 and day 2 in runs where significant ozone formation

occurred on both days. Test calculations indicated that this effect can be attributed to the high nighttime levels of NO_3 radicals formed in those experiments where significant qualities of both ozone and NO_2 were present at the end of the previous day; calculations where the reaction between NO_3 radicals and acetaldehyde was removed did not predict this nighttime PAN formation. This indicates the importance of NO_3 radical chemistry in multi-day chamber runs.

- For most of the outdoor chamber experiments, the model appeared to simulate the experimental formaldehyde data to within the relatively large experimental uncertainties. However, as shown in Table IV-14, the model predicted that methanol + formaldehyde substitution has less of a tendency to enhance maximum formaldehyde levels (relative to the base case) than indicated by the experimental data, and the model predicted that methanol-only substitution leads to a more consistent reduction in maximum formaldehyde levels than indicated by the base case vs methanol-only substitution experiments. However, in both cases the effects of substitution on experimental or predicted formaldehyde maxima were relatively small, being on the order of the uncertainties and variabilities of the experimental data.

- As noted above, the formaldehyde data from the indoor chamber experiments appeared to be of lower quality than those from the outdoor experiments, and the performance of the model in simulating the ITC formaldehyde data was correspondingly worse. Several indoor chamber runs appeared to have anomalously low formaldehyde data, and the model indeed predicted significantly higher formaldehyde yields in those runs. There were also several indoor chamber experiments where the model predicted significantly lower formaldehyde concentrations than were experimentally observed. Because of the apparent problems with the ITC formaldehyde data, these data are probably not useful for model testing purposes.

- As shown in the figures in Appendix A, the model simulates reasonably well the rates of decay of methanol and the constituents of the base case surrogate observed in most experiments, though as indicated above it was necessary to assume that non-negligible dilution was occurring in the indoor chamber experiments in order to achieve these acceptable fits. Most of the cases where poor fits of model calculation to the experimental measurements of these species can be attributed to known analytical problems with the GC analyses or calibrations.

V. CONCLUSIONS

The indoor and outdoor chamber experiments carried out in this program provide a data base concerning the air quality effects, for both single-day and multi-day episodes, which may occur if a significant number of conventionally-fueled motor vehicles were replaced by vehicles using neat methanol fuel. Such a large scale conversion of vehicles in the CSCAB to methanol could result in a number of changes in emissions, but the most obvious change would be that a significant fraction of the components of current organic emissions would be replaced with methanol or methanol + formaldehyde, and it is the effects of this change that the experiments carried out in this program were designed to address. In particular, three highly idealized substitution scenarios were examined in this program. In the first of these scenarios, approximately one-third of the "base case" organic mixture representing current ROG emissions was replaced by an equal amount (on a mole carbon basis) of methanol. In the second scenario, one third of the base case emissions were replaced by 90% methanol + 10% formaldehyde, and in the third scenario, designed to compare the effects of substitution to the effects of simple reduction of ROG emissions, the base case emissions were reduced by one-third. Although the three scenarios were based on the assumption that substitution to methanol fuel will not change the NO_x or total ROG emissions, the base case and substitution experiments were carried out at several different organic/NO_x ratio, to determine the dependence of substitution effects on the organic/NO_x ratios.

The specific aspects of air quality for which data were obtained concerned the effects of substitution on the atmospheric levels of ozone, formaldehyde, PAN, NO_x, the individual hydrocarbons used to represent current organic emissions, other oxidation products such as acetaldehyde, acetone, and organic nitrates, and methanol itself. Thus the results of these experiments can be used to test chemical model predictions concerning the effects of methanol fuel substitution on atmospheric levels of all of these species. The discussion in this report has concentrated primarily on the effects of methanol substitution on the atmospheric levels of ozone, PAN, and formaldehyde, since ozone and PAN (and other PAN-like species) are secondary pollutants of particular concern in the

California South Coast Air Basin and there is a concern that methanol substitution may have an adverse impact on the atmospheric levels of formaldehyde.

The conclusions derived from these data concerning the qualitative effects of methanol substitution on atmospheric levels of ozone species are summarized below, followed by a discussion of the factors which must be taken into account in interpreting these results and in calculating the effects of specific methanol substitution scenarios on air quality in the CSCAB and in other airsheds.

Effects of Substitution on Ozone Formation. The results of these experiments indicate that the benefits of methanol substitution on atmospheric levels of ozone will depend critically on the amount of formaldehyde co-emitted with methanol. If little or no formaldehyde is emitted from methanol-fueled vehicles, then methanol substitution can result in a reduction in atmospheric ozone levels, although the amount of reduction depends on such factors as the ROG/NO_x ratio, temperature and lighting conditions, and the number of days of irradiation in the multi-day experiments. However, if significant quantities of formaldehyde are co-emitted with methanol, then our experiments indicate that the benefits of substitution on ozone levels will be significantly less, if not eliminated entirely. In particular, if the base case surrogate employed in this study is reasonably representative of current ROG emissions (see below), then these data indicate that it is necessary that the formaldehyde content in emissions from methanol-fueled vehicles be less than 10% in order to achieve a reduction in ambient ozone levels, assuming no significant changes in the total amounts of ROG or NO_x emitted.

The results of these experiments also indicate that the benefits of methanol substitution on ozone will in general decrease with increasing ROG/NO_x ratios, and also will decrease with the number of days the pollutants are irradiated. In particular, although methanol substitution (with no added formaldehyde) resulted in reduced day 1 ozone levels at the low or moderate ROG/NO_x ratios, little or no improvement in final ozone levels was observed at the highest ROG/NO_x ratios, or after two or three days of irradiation at lower ROG/NO_x ratios. The benefits of methanol substitution on ozone yields at the lower ROG/NO_x ratios and with limited irradiation times can be attributed to the fact that substitution of the

base case organics by methanol reduces the rate of ozone formation, the main factor in determining how much ozone is formed under those particular conditions. At higher ROG/NO_x ratios, or if the irradiation proceeds for a sufficiently long period of time, then the amount of ozone formed is not determined by the rate of ozone formation, but rather by the maximum ozone forming potential of the ROG and NO_x mixture employed. The fact that methanol substitution does not reduce the maximum ozone yields under conditions of high ROG/NO_x ratios or of long irradiation times shows that the ultimate ozone forming potential of methanol is very similar to that of the base case surrogate mixture employed in this study. However, provided that formaldehyde co-emissions are kept sufficiently low (i.e., less than 10% for the conditions employed in our experiments), these data do not indicate any conditions where methanol substitution will have significant adverse impacts on ozone levels; such substitution would either be beneficial or have no net effect, depending on the conditions. Airshed model calculations are clearly required to determine the exact magnitude of ozone reduction for specific substitution scenarios and meteorological conditions.

Effects of Substitution on PAN. The results of the experiments carried out in this program indicate that methanol substitution should have a beneficial effect on PAN levels under essentially all conditions. Although as with ozone the exact magnitude of the improvement varies considerably with conditions. In contrast with the results for effects on ozone, the improvement in PAN levels caused by substitution does not appear to be significantly affected by formaldehyde co-emissions. In addition, and also in contrast with the effects on ozone where the benefits of methanol substitution appeared to decrease with the number of days in multi-day irradiations, most of these experiments suggest that the benefits of substitution on reducing PAN may increase with time, or at least will not consistently decrease. Thus the benefits of methanol substitution in reducing PAN levels appears to be more general and applicable under a wide variety of conditions than the benefits on ozone reduction.

The clear-cut benefit of methanol or even methanol + formaldehyde substitution on PAN levels is not unexpected, since PAN is formed only from the reactions of the components of the base case surrogate, and not

from methanol or formaldehyde. Thus, if other factors were equal, replacing a certain fraction of base case emissions with methanol or methanol + formaldehyde should result in a corresponding reduction in PAN levels. However, since PAN can only be formed in significant quantities in the absence of NO (since PAN is in equilibrium with acylperoxy radicals which are destroyed by reaction with NO), its yields are also determined by factors which affect the rates of NO consumption. This additional dependence is the reason that the actual magnitude of PAN reduction caused by methanol or methanol + formaldehyde substitution was found to vary significantly depending on experimental conditions, such as temperature, light intensity, ROG/NO_x ratio. Thus, as with ozone, model calculations would be required to predict the exact magnitude of reductions of PAN levels caused by specific fuel conversion scenarios in specific airsheds.

Effects of Methanol Substitution on Atmospheric Formaldehyde Levels. Since formaldehyde is expected to be co-emitted with methanol, and is also its major atmospheric photooxidation product, this is one aspect of air quality where methanol substitution is expected to have an adverse impact. The worst impact in this regard is expected to be the possibility of unacceptably high levels of formaldehyde in the immediate vicinity of methanol vehicle emissions under poor mixing conditions (such as garages, tunnels, street-canyons, etc.); a problem not addressed in this program. However, methanol substitution is also expected to have an impact on formaldehyde levels in the bulk atmosphere away from the immediate emissions sources under photochemically reactive conditions, and the data obtained in this program provides useful information in this regard.

The results of these experiments indicate that methanol substitution will tend to increase atmospheric formaldehyde levels, but that the increases are relatively moderate compared to the amounts of formaldehyde already formed in the photochemical reactions of the base case organics. Substitution by methanol alone appears to have a variable effect on maximum formaldehyde levels on day 1, and appears to cause a consistent increase in these levels on day 2. This is expected since methanol is a more efficient photochemical source of formaldehyde than the base case organics, but it takes longer for it to react and thus form formaldehyde. A 33% substitution of the base case surrogate in these experiments

resulted in an average increase of approximately 20% in day 2 formaldehyde levels, so it can be seen that the formaldehyde formed from the reactions of the base case organics is still making the major contribution to the overall formaldehyde yields. Of course, as indicated below, the exact amount of increase in formaldehyde levels caused by substitution will depend on the formaldehyde formation efficiency of the base case organics, and applicability of the quantitative results obtained in these experiments depends on the representativeness of the 8-component surrogate we employed relative to the actual base case emissions.

Substitution by methanol + formaldehyde resulted in higher initial formaldehyde levels (as expected since it is directly injected). But under conditions favorable for photochemical reactions the differences between methanol + formaldehyde substitution and substitution by methanol alone become much less by the end of day 1, and the added formaldehyde has essentially no effect on day 2 formaldehyde levels. This is expected since the initially-present formaldehyde is photochemically consumed at a relatively rapid rate, and by the end of day 1 or by day 2 the directly injected formaldehyde is dominated by the formaldehyde which is photochemically generated. The directly emitted formaldehyde is expected to be relatively more important in affecting atmospheric formaldehyde levels under conditions less favorable to photochemical reaction (e.g. overcast, etc.), where the consumption of the initial formaldehyde, and its formation from other emitted species, would be much slower. The experiments carried out in this program are primarily relevant to conditions of relatively high photochemical reactivity, and this should be taken into account in interpreting these results.

Interpretation and Use of the Data Obtained in This Program. The experiments carried out in this program were designed to provide data regarding effects of methanol substitution under highly idealized scenarios for the purpose of determining relative effects and to provide data suitable for testing of photochemical models. Thus the following caveats need to be taken into account when using these data to estimate the air quality impacts of specific methanol fuel substitution scenarios in specific urban airsheds, such as the CSCAB:

- As indicated above, these experiments examined the effects only of changing the composition of reactive ROG emissions, and not of changes in

total amounts of ROG or NO_x which are emitted. A massive conversion of motor vehicles to methanol fuel will almost certainly have some impact on the amounts of ROG and NO_x emitted, though the magnitude (and even sign) of these changes are difficult to predict. These scenarios also do not take into account possible future changes in the composition of emissions from conventionally-fueled vehicles or from other sources, which are also difficult to predict.

- The magnitudes of all the substitution effects examined in this program depend critically on the composition and reactivity of the base case organics. For example, if the actual present organic emissions into the CSCAB are, as a whole, less reactive with regard to ozone or PAN formation than the 8-component mixture of organics used in this study to represent these emissions, then the actual benefits of methanol substitution would be less than indicated by the results of these experiments. Conversely if the actual emissions are more reactive than the surrogate we employed then the actual benefits of methanol substitution would be greater than indicated by our experiments. Likewise, if the formaldehyde-forming potential of the surrogate employed in these experiments is greater than that of the actual organics emitted, then the relative impacts of methanol substitution on atmospheric formaldehyde levels may be greater than indicated by these experiments. Indeed, in view of the fact that lower molecular weight compounds tend to be used to represent the reactions of chemically analogous higher molecular weight compounds in designing simplified representations of emitted organics, our "base case" surrogate may well overestimate the formaldehyde formation potential of currently emitted organics, and thus underestimate the impacts of methanol substitution on atmospheric formaldehyde levels. On the other hand, if the amount of current formaldehyde emissions are greater than assumed when this surrogate was designed, then the impacts of methanol or methanol + formaldehyde substitution on formaldehyde may be less than indicated by the results of these experiments.

- Methyl nitrite has also been observed to be formed in the exhaust of methanol-fueled vehicles (Ito et al. 1982, Jonsson and Bertilsson, 1982), but the effect of emissions of this compound have not been examined in this study. Methyl nitrite is a highly photoreactive compound, and if emitted in sufficient quantities, it would tend to decrease the ozone

benefits of methanol fuel substitution. However, the observation of methyl nitrite may well be due to sampling artifacts, since its formation from methanol in the presence of NO_x is expected to be heterogeneous, and in any case its levels in methanol exhaust are expected to be minor compared to formaldehyde. Whitten and Hogo (1983) estimate that 1% is a realistic upper limit for methyl nitrite in methanol exhaust, and at that level they calculate its impact on ozone formation to be minor.

- As indicated above, the data obtained in this study are relevant only for air quality impacts in the well-mixed atmosphere, and under conditions favorable for photochemical reaction. Thus, these results do not provide any information concerning the effects of conversion to methanol fuel on air quality in areas immediately adjacent to emissions sources or under poor mixing conditions, or under extremely overcast conditions when photochemical reactions are of relatively minor importance.

Because of the above considerations, and the other factors which need to be considered in assessing the situation in real airsheds but which cannot be duplicated in environmental chamber experiments, it is clear that airshed model calculations are necessary in order to obtain quantitative assessments of impacts of specific methanol fuel conversion scenarios. However, in order for such calculations to yield meaningful and scientifically valid results, it is critical not only that accurate input data be employed, particularly with regard to such factors as amounts of formaldehyde co-emitted from methanol vehicles and the reactivity of the base case emissions, but also that the airshed model employ a chemically accurate and suitably tested photochemical mechanism. The importance of utilizing a validated chemical mechanism is particularly significant in this case, since calculations of effects of methanol fuel substitution amount, to a major extent, to examining effects of changing chemical composition, as opposed to total amounts of pollutants emitted.

The experiments carried out in this program are designed to provide a data base suitable for testing mechanisms to be used in airshed calculations aimed at assessing quantitative effects of methanol fuel substitution. In particular, the experiments were carried out under a variety of conditions, with the ROG/NO_x ratio, temperature, light intensity, and even the chamber employed varied. In addition, the experiments were carried

out in conjunction with the appropriate array of characterization and control runs, which are required for maximum utility of these data for the purpose of model testing.

The model calculations carried out in this program indicate that the predictions of a recently-developed detailed chemical mechanism are in general reasonably consistent with the results of these experiments. This detailed mechanism has also been recently tested against a wide variety of other environmental chamber experiments (Carter et al. 1986), and thus we consider it to be sufficiently well validated for use in airshed model calculations for the purpose of assessing atmospheric impacts of methanol fuel conversion for specific substitution scenarios. (It should be pointed out, however, that the detailed mechanism employed [see Appendix B] is much too large to be used in current detailed airshed models, and thus future work in this area is required.) The detailed mechanism employed is not without significant areas of uncertainty (Carter et al. 1986), but we suspect that impacts of these uncertainties in the detailed mechanism are probably less than the impacts of the uncertainties in the current or projected emissions data. However, a comprehensive sensitivity study of the various factors involved in assessing substitution effects have not been carried out, and these are clearly required before reliable and quantitative assessments of the effects of methanol fuel substitution on air quality can be made.

VI. REFERENCES

Atkinson, R., Lloyd, A. C. and Winges, L. (1982): Atmos. Environ., 16, 1341.

Atkinson, R. and Lloyd, A. C. (1984): J. Phys. Chem. Ref. Data, 13, 315.

Atkinson, R. (1986): Chem. Rev., 86, 69-201.

Brinkman, N. D. (1979): Energy Res., 3, 243.

California Energy Commission (1981): Senate Bill 620: Alcohol fleet test program, Staff Report, December.

California Energy Commission (1982): California's Alcohol Fleet Test Program, 1982 Progress Report for Senate Bill 620, Report No. P-500-82-056, December.

Carter, W. P. L., Ripley, P. S., Smith, C. G. and Pitts, J. N., Jr. (1981): Atmospheric chemistry of hydrocarbon fuels: Vol. I, Experiments, results and discussion. Final Report, ESL-TR-81-53, November.

Carter, W. P. L., Atkinson, R., Winer, A. M. and Pitts, J. N., Jr. (1982): Int. J. Chem. Kinet., 14, 1071.

Carter, W. P. L., Winer, A. M., Atkinson, R., Dodd, M. C. and Aschmann, S. A. (1984): Atmospheric photochemical modeling of turbine engine fuels. Phase I. Experimental studies. Volume I of II. Results and Discussion. Final Report to the U. S. Air Force, ESL-TR-84-32, September.

Carter, W. P. L., Dodd, M. C., Long, W. D. and Atkinson, R. (1985): Outdoor chamber study to test multi-day effects. Volume I: results and discussion. Final Report, EPA-600/3-84-115, March.

Carter, W. P. L., Lurmann, F. W., Atkinson, R. and Lloyd, A. C. (1986): Development and testing of a surrogate species chemical reaction mechanism. Final Report, U. S. Environmental Protection Agency Contract No. 68-02-4104, Atmospheric Chemistry and Physics Division, Atmospheric Sciences Research Laboratory, Research Triangle Park, NC 27711.

Darnall, K. R., Atkinson, R., Winer, A. M. and Pitts, J. N., Jr. (1981): JAPCA, 31, 262.

DeLorenzo, M. (1982): "Bank is bullish on methanol fuel." Automotive News, June 7.

Doyle, G. J., Bekowies, P. J., Winer, A. M. and Pitts, J. N., Jr. (1977): Environ. Sci. Technol., 11, 45.

Ito, K. et al. (1981): Methylnitrite formation in exhaust gases emitted from a methanol fuel S.I. engine. In: Proc., Fifth International Alcohol Fuel Technology Symposium, May 13-18, Auckland, New Zealand.

Jeffries, H. E., Kamens, R. M., Sexton, K. G. and Gerhardt, A. A. (1982): Outdoor chamber experiments to test photochemical models. Final Report, EPA-600/3-82-016A, April.

Jeffries, H. E., Sexton, K. G., Kamens, R. M. and Holleman, M. S. (1985a): Outdoor smog chamber experiments to test photochemical models: Phase II. Final Report, U. S. Environmental Protection Agency Cooperative Agreement No. 808881, Atmospheric Chemistry and Physics Division, Atmospheric Sciences Research Laboratory, Research Triangle Park, NC 27711.

Jeffries, H. E., Sexton, K. G., Morris, T. P., Jackson, H., Goodman, R. G., Kamens, R. M. and Holleman, M. S. (1985b): Outdoor smog chamber experiments using automobile exhaust. Final Report, U. S. Environmental Protection Agency Cooperative Agreement No. 809391, Atmospheric Chemistry and Physics Division, Atmospheric Sciences Research Laboratory, Research Triangle Park, NC 27711.

Jonsson, A. and Bertilsson, B. M. (1982): Environ. Sci. Technol., 16, 106.

Joseph, D. W. and Spicer, C. W. (1978): Analyt. Chem., 50, 1400.

O'Toole, R., Dutzi, E., Gershman, R., Heft, R., Kalema, W. and Maynard, D. (1983): California methanol assessment, Vol. 2. Technical Report, JPL Publication 83-18.

Pefley, R. K., Pullman, J. B. and Whitten, G. Z. (1984): The impact of alcohol fuels on urban air pollution: methanol photochemistry study. Final Report, U. S. Department of Energy, Office of Vehicle and Engine R&D, Washington DC 20583.

Pitts, J. N., Jr., Carter, W. P. L., Darnall, K., Winer, A. M. and Atkinson, R. (1979): Mechanisms of photochemical reactions in urban air. Final Report, U. S. Environmental Protection Agency, EPA-600/3-79-110, November.

Pitts, J. N., Jr., Winer, A. M., Carter, W. P. L., Atkinson, R. and Tuazon, E. C. Tuazon (1981): Chemical consequences of air quality standards and control implementation programs. Final Report to California Air Resources Board Contract No. A8-145-31, March.

Pitts, J. N., Jr., Atkinson, R., Carter, W. P. L., Winer, A. M. and Tuazon, E. C. (1983): Chemical consequences of air quality standards and of control implementation programs. Final Report to California Air Resources Board Contract No. A1-030-32, April.

Stephens, E. R., Burleson, F. R. and Cardiff, E. A. (1965): JAPCA, 15, 87.

Stephens, E. R. and Price, M. A. (1973): J. Chem. Educ., 50, 351.

Whitten, G. Z. and Hogo, H. (1983): Impact of methanol on smog: A preliminary estimate. Final Report, SAI Publication No. 83044, February.

Winer, A. M., Peters, J. M., Smith, J. P. and Pitts, J. N., Jr. (1974): Environ. Sci. Technol., 8, 1118.

Zafonte, L., Rieger, P. L. and Holmes, J. R. (1977): Environ. Sci. Technol., 11, 483.